Imiquimod based transcutaneous immunization – insights and novel concepts

Dissertation zur Erlangung des Grades eines `Doktor rerum naturalium (Dr. rer. nat.)'
der Fachbereiche:
- 08 - Physik, Mathematik und Informatik
- 09 - Chemie, Pharmazie und Geowissenschaften,
- 10 – Biologie,
- Universitätsmedizin

der Johannes Gutenberg-Universität.

Karsten Gogoll,

geb. in Darmstadt

Max Planck Graduate Center

Mainz, 2014

1. Gutachter:

2. Gutachter:

Tag der mündlichen Prüfung: 28.11.2014

I hereby declare that I wrote the dissertation submitted without any unauthorized external assistance and used only sources acknowledged in the work. All textual passages which are appropriated verbatim or paraphrased from published and unpublished texts as well as all information obtained from oral sources are duly indicated and listed in accordance with bibliographical rules. In carrying out this research, I complied with the rules of standard scientific practice as formulated in the statutes of Johannes Gutenberg University Mainz to insure standard scientific practice.

“Origin of man now proved. Metaphysics must flourish. He who understand baboon would do more towards metaphysics than Locke”

Charles Darwin, The Red Notebook of Charles Darwin

Table of content

1. Abbreviations

AATT:	Alumn-adsorbed tetanus toxoid
AK:	Actinic keratosis
APC:	Antigen presenting cell
API:	Active pharmaceutical ingredient
bARE:	Bacterial ADP-ribosylating exotoxin
CD:	Cluster of differentiation
CD 4^+:	T helper cells (T_H cells)
CD 8^+:	Cytotoxic T-cells, T killer cells (see also CTL)
CO_2:	Carbon dioxide
CoA:	Certificate of analysis
CT:	Cholera toxin
CT-B:	Beta subunit of cholera toxin
CTL:	Cytotoxic T-cells ($CD8^+$)
Da:	Dalton
DAC:	Deutscher Arzneimittel-Codex
DC:	Dendritic cell
DLS:	Dynamic light scattering
DMSO:	Dimethylsulfoxide
DNA:	Deoxyribonucleic acid
DSC:	Differential scanning calorimetry
dsRNA:	Double strained ribonucleinic acid

Abbreviations

ER:	Endoplasmatic reticulum
FSME:	Early summer meningoencephalitis
FT:	Follicular transport
h:	Hour
HBsAG:	Surface antigen of the hepatitis B virus
HIB:	Haemophilus influenzae type b virus
HIV:	Human immunodeficiency virus
HPV:	Human papilloma virus
i.d.	Intra dermal
IG:	Immunoglobulin (antibody)
IL:	Interleukin
i.m.:	Intra muscular
i.n.:	Intra nasal
IPV:	Inactivated poliovirus vaccine
IUPAC:	International Union of Pure and Applied Chemistry
i.v.:	Intra venous
LC:	Langerhans cell
LT:	Heat labile toxin
LUV:	Large uni-lamellar vesicles
MHC:	Major histocompatibility complex
min:	Minute
MLV:	Multi-lamellar large vesicles
MN:	Micro needle

Abbreviations

MSP-1:	Plasmodium falciparum-merozoite surface protein 1
MW cutoff:	Molecular weight cutoff
NK:	Natural killer cell
nm:	Nanometer
O/W:	Emulsion type oil in water
p.a.:	Pro analysis grade
PAMP:	Pathogen associated molecular pattern
PDI:	Polydispersity index
PE:	Penetration enhancer
Ph. Eur.:	European Pharmacopoeia
p.o.	Per oral
PRR:	Pathogen recognition receptor
PVP:	Polyvinylpyrrolidone
RNA:	Ribonucleic acid
RP:	Reversed phase
rpm:	Rotations per minute
sBCC:	Superficial basal cell carcinoma
SC:	Stratum corneum
SLN:	Solid lipid nanoparticles
SN:	Imiquimod nanoparticle based solid nanoemulsion
ssRNA:	Single strained ribonucleinic acid
STIKO:	Ständige Impfkommission des Robert Koch Institutes
SUPAC:	Scale up and post approval changes

Abbreviations

SUV: Small uni-lamellar vesicles

TCI: Transcutaneous immunization

TFP: Trans-follicular penetration

TH: T-helper cell ($CD4^+$)

TLR: Toll like receptor

Treg: Regulatory T-cells

TT: Tetanus toxoid

TTS: Transdermal therapeutic systems

W/O: Emulsion type water in oil

2. Aim of the thesis

2.1. General objectives

The objective of this work is the development of a tumor specific immunity by an optimized transcutaneous immunization method.

Since imiquimod based dermal treatment has highlighted the opportunity of tumor rejection in a C57BL/6 mouse model, particularly if UV-B radiation is concomitantly applied, transcutaneous immunization based on imiquimod became of special interest. On the basis that imiquimod, dermally applied, facilitates a substantial but not sustained anti tumor activity by activating cytotoxic T-cells, the question arose whether pharmaceutical efforts towards imiquimod may generate a prolonged tumor protection.

This work aims at gaining further insight into transcutaneous immunization. Attempts on formulation development focused on creating highly efficient formulations in terms of bridging cancer research and pharmaceutical technology. Commercially available formulations were investigated with respect to both, *in vitro* characteristics but also *in vivo* activity. The elementary findings of pharmaceutical differences with their respective *in vivo* consequences represented a valuable tool in order to draw conclusion on the development of novel formulations concepts. The unique opportunity of receiving direct *in vivo* results driven by a C57BL/6 mouse model enabled both, a straightforward formulation development but also threw up some interesting results and new insights into transcutaneous immunization.

2.2. Application of *in vitro* methods in order to predict *in vivo* effects

In order to assess transcutaneous immunization effectiveness, different methods are available and individually used. These methods (e.g. cytotoxicity test or Interferon gamma detection) are associated with elaborate preparations. Hence, this work aims

at a possibility to predict transcutaneous immunization performance in a laboratory scale.

2.3. Development and manufacturing of novel imiquimod based formulation concepts

In the context of this work the task was set of examining the extent as to which differences in quality and pharmaceutical characteristics impact on the performance of miscellaneous 5% imiquimod containing creams. Results obtained within this comparison laid the foundation of semi-solid formulation development. A novel concept on the basis of a freeze dried solid nano emulsion for transcutaneous immunization was created. Based on adjustments of a defined parenteral nanoemulsion formula, this concept was developed further in order to benefit from freeze drying related advantages but also maintain spreadable properties in order to enable dermal administration. This dermal formulation concept offers the possibility to determine the extent to which the use of imiquimod submicron particles in combination with versatile pharmaceutical oil components impacts on immunization performance.

A further concept describes a conventional semi-solid formulation offering an easy and convenient handling. Gained knowledge from both, freeze dried formulations but also from the comparison of different commercially available creams acted as a valuable tool in order to design this concept. Based on an aqueous gel, an emulsion gel was created. In order to ensure a prolonged residue period at the site of application, a retarding effect seemed to be meaningful. The emulsion gel concept is thus based on jojoba wax in order to fulfill the purpose of a prolonged retention period.

3. Introduction

3.1. The human immune system

3.1.1. Innate and acquired immune system

As a result of ubiquitously existing germs there was a development of protective measures in order to eradicate pathogens (e.g. viruses, bacteria, helminthes, degenerated cells and fungal diseases). Our immune system in general consists of both, an innate and an acquired (or adaptive) part with a respective humoral and cellular answer. A vital requirement to protect the human body against pathogenic germs is the distinction between friend and enemy.

Indeed, the innate immune system represents the first line of defense [1], but it does not act specifically on a single antigen. It does not only produce quick and potent responses to common invaders but it also activates and controls the acquired immune response.

In some cases the innate immune system does not sufficiently eliminate pathogens. Consequently, the antigen specific acquired immune system is activated to facilitate a complete elimination of pathogens. Lymphocytes such as B-cells, T-cells, and natural killer cells (NK) are crucially involved in recognition and eradication of extracellular but also intracellular pathogens. Following antigen contact, activated B-cells reproduce, then mature into plasma cells and finally secrete high amounts of antigen specific antibodies. In contrast to the B-cell related humoral answer, T-cells are highly specialized in recognition and eradication of virus infected cells but also cancer cells, representing the cellular answer.

3.1.2. Major histocompatibility complex

Major histocompatibility complex (MHC) represents a comprehensive gene locus located on chromosome 6. Each nucleated cell owns this receptor complex in order to present intracellular proteins (but not lipids, carbonhydrates, or nucleonic acids) on the cell surface. This mechanism is most relevant for the recognition of viruses or

intracellular bacteria. MHC molecules present various proteins hereby acting with a broad specificity instead of a high affinity. Otherwise, a low rate of dissociation facilitates the antigen presentation to the respective T-cells. In general, one can differentiate between MHC I and MHC II.

3.1.2.1. Major histocompatibility complex I

Purpose of the MHC I receptor is the presentation of intracellular antigens on the cellular surface enabling NKs but also CTLs to recognize and eliminate infected cells. MHC I hereby acts comparable to a member card of each nucleated cell. Targets presented by the MHC I receptor include regular products from protein biosynthesis as well as tumor related proteins. Cytosolic antigens such as viral DNA or unfolded proteins of intracellular bacteria are ubiquitylated and subsequently degraded by the proteasome. The resulting fragments then are transported into the ER by the TAP transporter. Within the ER, novel MHC I molecules are synthesized in order to bind on peptide fragments. Finally, the MHC I peptide complex is transported to the cell surface (figure 1a). Another characteristic for virus infected cells is their lack of MHC I molecules. Consequently, NKs eliminate infected cells by releasing cytotoxic granula.

3.1.2.2 Major histocompatibility complex II

Occasionally, MHC II receptors are primarily located on the surface of antigen presenting cells (APCs) including dendritic cells (DC), macrophages, and B-cells. Following antigen uptake, internalized pathogens are degraded within lysosomes. MHC II molecules, consecutively synthesized within the ER, are transported via vesicles. The resulting cleavage products of proteolytic enzymes and MHC II molecules are linked after CLIP removal and subsequently transported to the cell surface to facilitate the antigen presentation to $CD4^+$ cells (figure 1b).

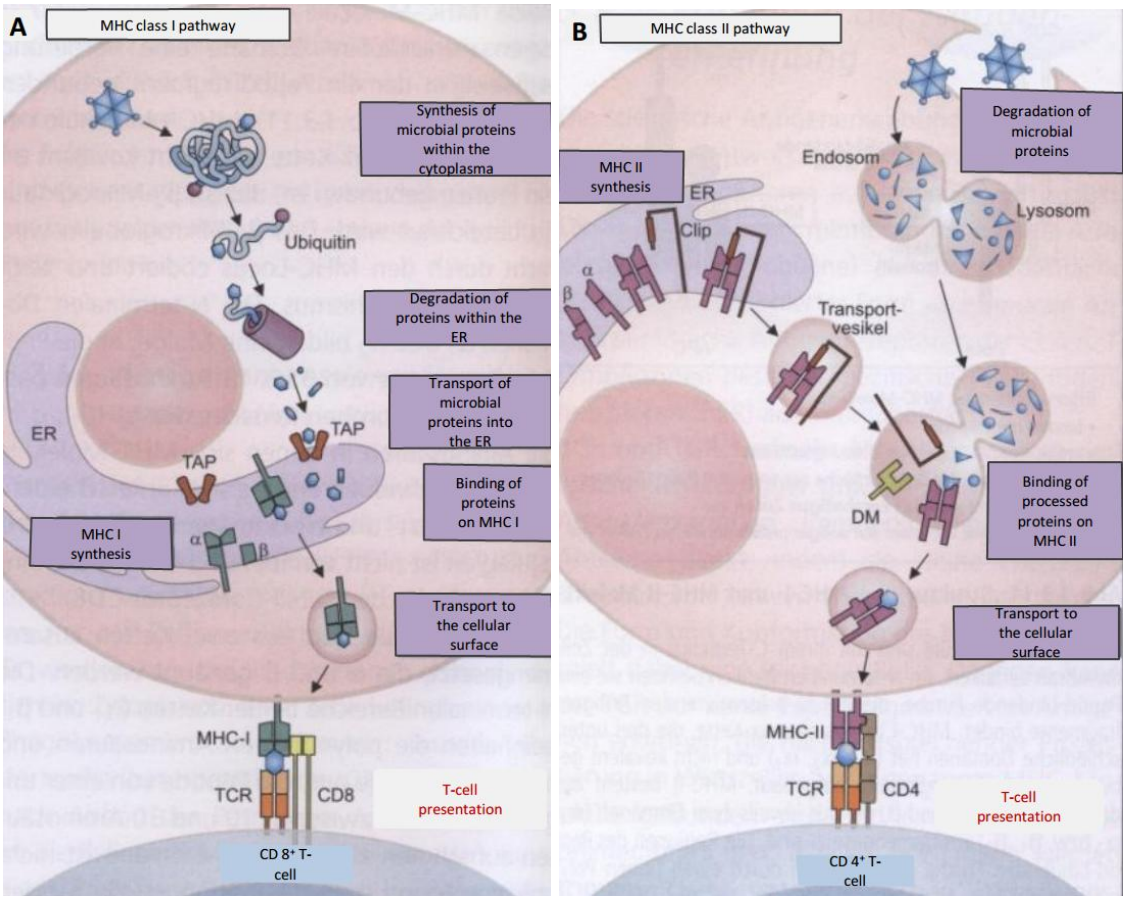

Figure 1a: MHC I antigen complex of a virus infected cell is recognized by the T-cell receptor that expresses the CD8 co-receptor. Graphical representation according to Vollmar [2].

Figure 1b: MHC II antigen complex of an APC with a phagocyted antigen recognized by a T-cell recptor expressing CD4 co-receptor. Graphical representation according to Vollmar [2].

3.1.3. Antigen presenting cells

Generally, each cell constantly displaying proteins via MHC I receptor acts as an antigen presenting cell. However, within this work the term antigen presenting cell is used for so called professional APC including dendritic cells (DC), macrophages, and B-cells. The most important role of APCs consists in both, capturing and processing antigens but also to contact and activate naive T-cells. In addition, macrophages and B-cells may also act as APCs whereas the effectiveness does not match DC performances [2]. Langerhans cells (LC), a DC subpopulation, not to be confused with cells from the islets of the pancreas, are most prominent within the epidermis of the skin but also mucous membranes of the mouth, foreskin and vagina [3].

In short, matured APCs own two characteristics: expressing MHC II molecules on the surface but also secreting essential co-stimulatory molecules to activate naive T-cells.

3.1.4. Toll like receptor

Pathogen recognition by phagocytes but also the complement system is facilitated by a broad variety of PRRs (pathogen recognition receptors). PRRs aim at specific pathogen associated molecular pattern (PAMP) for instance double strained RNA (dsRNA), exclusively occurring in viruses. Changes within a cluster of PAMPs would entail a lethal risk to microorganisms thus a limited number of PRRs facilitates the recognition of PAMPs in a wide variety.

Toll like receptors (TLRs) located at the cellular surface or within the endosomal membranes, sense the presence of PAMPs. TLR as the most relevant subunit of PRRs represent a structure of crucial importance to the immune system. Within mammalians, eleven different TLRs are identified so far (table 1). TLR activation triggers cascades following an acute inflammatory reaction induced by a plethora of molecules (e.g. antibacterial proteins, inflammatory cytokines, chemokines, adhesion molecules, and NO-synthase). Furthermore, TLR activation allows a seamless handover between the innate and the acquired immune system. Immature DCs for instance may ingest pathogens by PRR, hereby acting as a part of the innate immune response. Activated by signals of the TLR system, DCs migrate into local lymphatic tissue in order to mature to highly specialized APCs with an increased expression rate of MHC II molecules. Simultaneously, APCs secrete costimulatory proteins but also adhesion molecules in order to interact with naive T-cells.

Table 1: List of several relevant agonists and PAMPs for each TLR [2, 4]

TLR	Ligands
1	Triacyl lipopeptides
2	Peptidoglycans and lipoteichonic acid of grampositive bacteria, lipoarabinomannanes of Mykobacteria, lipoproteines of grampositive bacteria, Pam_3cys and cymosan from yeasts. TLR 2 cooperates with TLR-1 and TLR-6. Only expressed on APC and endothelial cells
3	Viral double-stranded RNA. Almost exclusively on DCs
4	Lipopolysaccharides of gram negative bacteria, fusion protein of respiratory syncytial virus
5	Flagellin at basolateral side of intestinal mucosa
6	Functional realation with TLR-2
7	Endosomal or lysosomal related single stranded RNA, Imidazoquinolines (**Imiquimod,** Resiquimod)
8	Endosomal or lysosomal related single stranded RNA, Imidazoquinolines (Resiquimod)
9	Unmethylated CpG-motives of bacterial but also viral DNA
10	Yet unclear, close relation to TLR-1 and TLR-6
11	Profilin, not precisely known

3.1.5. T-cells

Besides APCs, T-lymphocytes play a fundamental role in the acquired immune system. T-cell populations include cytotoxic $CD8^+$ T-killer cells (CTL) and $CD4^+$ T-helper (T_H) cells. More into detail, T_H cells can be further classified into T_H1, T_H2, and T_H17 cells, thereby affecting the type of immune reaction in a pathogen dependant manner. In addition, regulatory T-cells (T_{reg}) are involved in down regulating processes thus avoiding an overreaction of the immune response.

3.1.5.1. Cytotoxic T-cells

Cytotoxic T-cells combat cancer cells but also virus infected cells in order to eradicate the source of infection. Therefore, they patrol the blood, lymph nodes and organs. As described previously, virus infected cells present cellular proteins via the MHC I pathway. CD8, a T-cell receptor related glycoprotein interacts with the MHC I antigen complex on the cell surface. As a consequence of activation, CTLs secrete perforin, a protein, in order to perforate virus infected cell membranes. Moreover, granozymes penetrate these pores, consequently inducing apoptosis by activation of caspsis (figure 2). Additionally, CTLs secrete IFNγ in order to stimulate macrophages to additionally support the eradication of apoptotic cells.

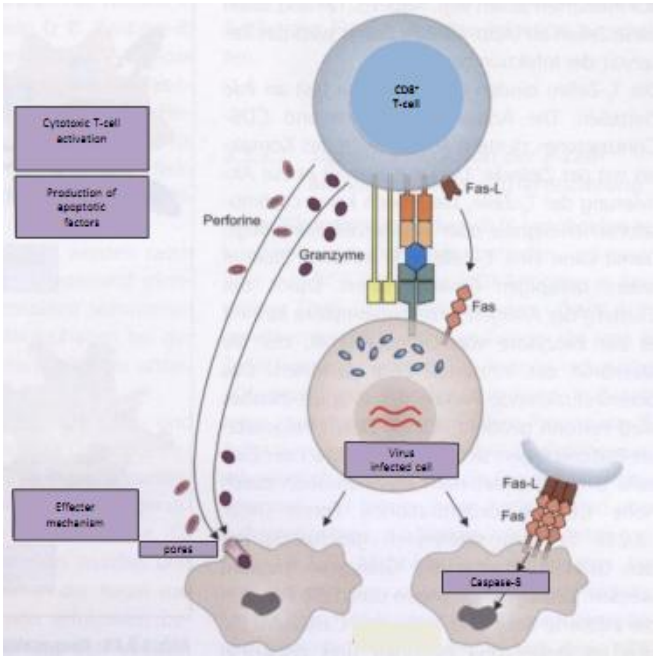

Figure 2: Mechanism of an activated cytotoxic T-cell towards infected cells. Graphical representation according to Vollmar [2].

3.1.5.2. T-helper cells

Stimulated $CD4^+$ cells transmit signals in order to amplify the immune response. Depending on antigen pattern, DC related cytokines affect the extent as to which a T_H1 or T_H2 reaction is triggered.

Since T_H1 cells produce cytokines, in particular IFNγ, in order to support both, inflammatory reactions but also the cellular immune response. IFNγ specifically activates macrophages but also monocytes by a concomitant inhibition of T_H2 cells.

Additionally, IFNγ effects an up regulation of MHC I and MHC II expression. Taken into account, T_H1 cells focus on the elimination of virus infected cells but also degenerated cells (figure 3).

T_H2 cells secrete cytokines in order to generate a B-cell response on bacteria and extracellular pathogens. Therefore T_H2 produce IL-4, IL-5 but also IL-10 that simultaneously inhibits T_H1 cells.

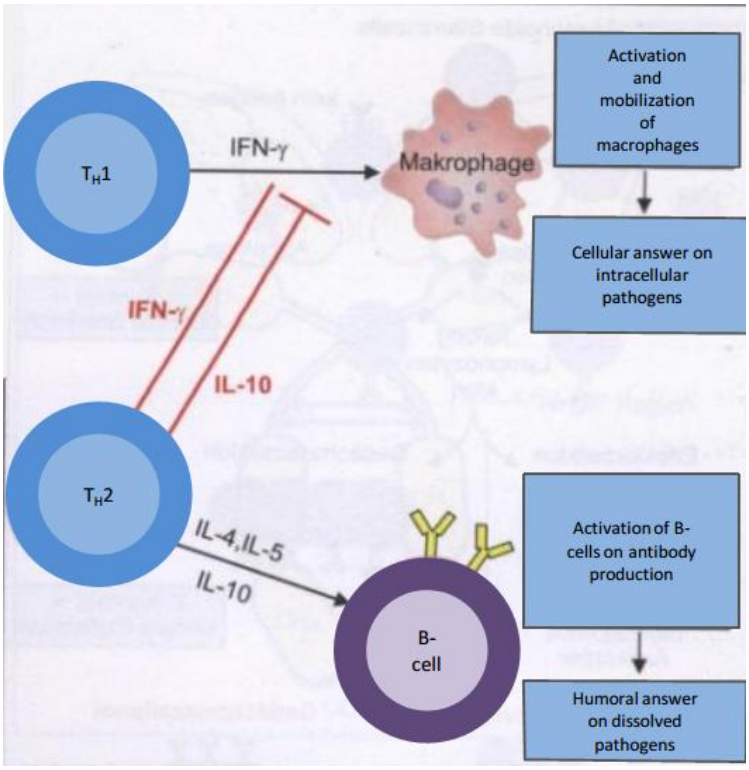

Figure 3: Mechanism of activation and mutual inhibition of T_H1 and T_H2 $CD4^+$ cells. Graphical representation according to Vollmar [2].

3.2. Active vaccination

Vaccination as a groundbreaking invention has had a tremendous impact in medical science and human welfare. Generally, one can distinguish between live attenuated and inactivated death vaccines. Since vaccines are applied to healthy patients, the

human immune system is sufficiently trained for a real emergency. Vaccination as a preventive measure requires a healthy vaccinee in order to facilitate a comprehensive immune reaction towards the applied antigen. Within this work the term vaccination implies the process of an active vaccination.

Most frequently, active immunizations are performed in order to induce a specific antibody but also T-cell induction. In order to facilitate a long term protection, vaccination aims towards the induction of B- but also T-memory cells thus providing an immunological memory against pathogens or pathogen associated toxoids.

3.2.1. Live vaccines

Live vaccines contain a specified amount of less virulent (attenuated) viruses. Attenuated vaccines provide the most efficient formation of antibodies and specific immune cells as this combination often provides particularly effective and enduring protection against the disease in question. Concededly, one cannot exclude that attenuated viruses regain their virulent characteristics. Live attenuated vaccines include polio-, measles-, mumps-, rubella-, varizella-, rota-, influenza-, and yellow fever viruses. Although commonly used to prevent virus induced diseases, there is also an attenuated bacterial vaccine against typhus.

3.2.2. Inactivated vaccines

As a further active vaccination concept, inactivated bacteria or viruses are termed inactivated or death vaccines. These include polio- (inactivated viruses IPV since 1998), rabies-, hepatitis A-, early summer meningoencephalitis- (FSME), whooping cough-, and cholera vaccines. Inactivated vaccines have in common that they are manufactured on the basis of virulent strains. The primary function of inactivating pathogens is achieved by heat treatment or the use of chemicals such as formaldehyde. Inactivated vaccines provide a reduced risk to the patient however this implies a total pathogen inactivation. Since inactivated pathogens neither replicate nor grow, dead vaccines are less immunogenic compared with attenuated vaccines.

3.2.3. Subunit-, gap-, and polysaccharide vaccines

Subunit-, gap-, and polysaccharide based vaccines represent a subset of inactivated vaccines. Since this vaccine type comprises of one or more selected antigens, gap vaccines are more homogenous but also less virulent as both, attenuated but also inactivated vaccine types. On the other hand, they bare a reduced risk of side effects. To date, single antigen vaccines contain bacterial or viral proteins or bacterial capsule related polysaccharides. On the basis of pathogen splitting the resulting fragments are termed as gap vaccines. In contrast hereto, subunit based vaccines are composed of highly purified surface proteins. In case of non protein based vaccines fragments of bacterial capsules serve as immunogenic unit.

3.3. Human skin

3.3.1. Structure of the skin

Due to a relatively large and easily accessible surface, skin disorders appear to be predestinated for a local treatment based on semi-solid dosage forms (e.g. ointments, cremes, gels, pastes, cutaneous plasters and drug loaded plasters). Already in the ancient world, administration of ointments and fragrant oils has been cherished in human history. Except local effects, systemic side effects or burden may occur due to dermal administration of active substances. Flight ointments (Flugsalben), widely used since the early modern during the fifteenth and sixteenth century provide a good example for systemic adverse effects. Individuals accused of witchcraft were, after rubbing their bodies with the ointment, flying where they wished, past beautiful cities and woods and streams [5]. The physician of Pope Julius III applied an ointment from an arrested sorcerer onto a woman’s body who suffered from nervous disorders. After a 36h period of sleeping she described various strange but pleasant hallucinations [6]. Considered ingredients of flight ointments were soot, fat of slain infants, and bat’s blood [7]. However, from a pharmaceutical point of view, lipophilic alkaloids derived from monkshood and deadly nightshade may be

considered as responsible active ingredients. In 1979, scopolamine, an active substance that is closely related to the above mentioned alkaloids, was approved by the FDA as a drug loaded three day transdermal system in order to treat motion sickness [8].

With an average surface of $2m^2$ in adults, skin is the largest organ in humans. Skin establishes a physical protective barrier between ourselves and our environment. Furthermore, skin facilitates the evaporation of water in a physiological manner by simultaneously preventing the body from desiccation. Finally, as a part of the innate immune system its barrier function prevents the human body against invaders. In order to maintain body temperature, skin may influence on blood flow by constriction or dilatation of blood vessels. Additionally, skin as a sensory organ mediates numerous pressure- temperature- and pain stimuli [9].

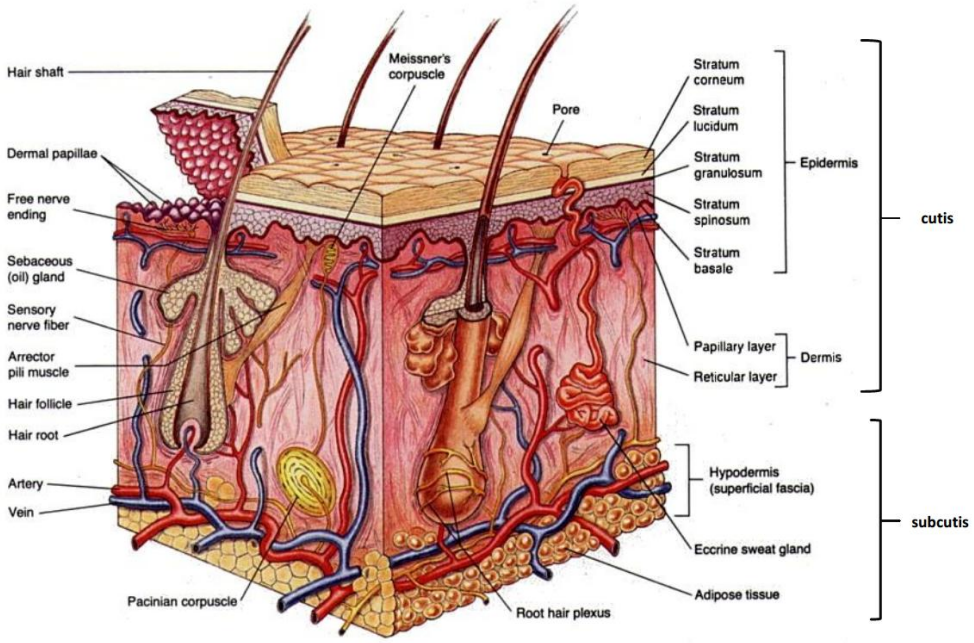

Figure 4: Schematic illustration of a skin cross section according to raksti.daba.lv [10].

Mammalian skin is composed of the epidermis and the underlying dermis, summarized as cutis. The underlying subcutis with connective tissue is traversed by blood vessels and nerves (figure 4). More in detail, the epidermis consists of following five different layers:

- Stratum corneum, representing the outermost skin layer with a 10-20µm thickness. Due to its brick and mortar format it represents an effective but also fragile barrier to the hostile microbial world [11].
- Stratum lucidum, a uniform looking layer located on the palms of hands and soles of feet.
- Stratum granulosum where cells convert into lifeless keratinocytes.
- Stratum spinosum where stepwise keratinization process starts.
- Stratum basale, a monolayer of cells responsible for cell division.

3.3.2. Drug flux across the skin

Skin as the human integument generally represents an obstacle to dermally applied substances. Furthermore, penetration of active substances across the skin requires certain conditions concerning molecular pattern. These include small molecular size but also defined lipophilic properties. The 500 Da (Dalton) rule indicates that the molecular weight of a compound must be beneath 500 Da in order to overcome the SC. This rule is confirmed on the basis that virtually all common contact allergens are under 500 Da of weight whereas larger molecules are not known as contact sensitizers. In addition, the most commonly used pharmaceutical actives for topical use are all beneath 500 Da. Likewise, all known drugs used in TTS devices are beneath 500 Da [12].

Although several types of skin cells own specific transporters, for instance for amino acid absorption, they play a subordinate role. Consequently, skin related absorption of active substances acts as a passive diffusion process described by the diffusion equation according to Fick's First law:

$$J = \frac{D * K}{\delta} \Delta c_s = K_p * \Delta c_s$$

J = flux of solute or penetrant

D = solute diffusion constant in the SC

K = SC : vehicle partition coefficient for the solute

δ = thickness of SC

Δc_s = external concentration difference across the SC

K_p = permeability constant

$1/K_p$ = diffusional resistance

As it is obvious by Fick's diffusion law, drug flux depends on both, penetrant but also vehicle. In case of a small extent of partition within the horny layer, a high absorption of both, vehicle but also active substance occurs. In case of a high extent of partition the percutaneous absorption depends less strongly on the vehicle [13].

3.3.3. Possible transport mechanism across the skin

As outermost barrier, skin and in particular the SC constitutes an obstacle to environmental influences but also drug flux. However, skin is not completely impermeable. In order to trigger local or systemic effects following dermal administration, active substances have to overcome the SC barrier which represents a horizontal obstacle. The SC is described as a composite of corneocytes and the secreted contents of the lamellar bodies that give it a brick-and-mortar organization [14]. This arrangement creates a tortuous obstacle through which substances have to traverse in order to cross the SC [15]. To date, three possible penetration routes across the skin are proposed including intercellular penetration pathway surrounding the corneocytes, follicular penetration pathway into hair follicles, and transcellular penetration pathway (figure 5). In order to sufficiently traverse the SC, lipophilic actives offering a certain amount of solubility seem to be advantageous. In contrast hereto, nor fats neither fatty oils but also distinctly hydrophilic actives permeate the skin to a noticeable extent [16].

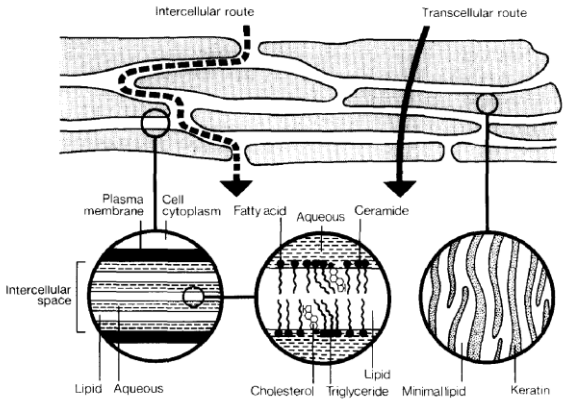

Figure 5: Schematic illustration of the transcellular and the intercellular transport route across the human skin according to Junginger [17].

Previously, it was assumed that topically applied actives penetrate via the intercellular pathway inside the lipid layers into and across the SC [18-20]. In contrast hereto, hair follicle based penetration pathways were assumed to play a subordinate role. Indeed, approximately 0.1% of the skin surface is accounted skin appendages [21]. Concededly, in contrast to the reservoir function of SC with a limited residence time of topically applied substances due to consecutive renewing process (one layer of corneocytes per day), hair follicles represent a long term reservoir [21]. It is reported that drug particles in a range of 300-400nm provide a tenfold prolonged residence time in hair follicles [20]. Depletion of topically applied substances occurs due to slow process of sebum production and hair growth. As a result of particle dependant transfollicular penetration, particle sizes in a magnitude of 320-700nm are described as most feasible to enable follicular transport. This diameter corresponds with the thickness of keratin cells of hairs, supporting the hypothesis of a geared pump mechanism within the hair follicle [20, 22]. Investigations on transfollicular transport using dye nanoparticles (figure 6a) with an average particle diameter of 320nm, in comparison with a non-particle based dye formulation, announced a prolonged duration within the hair follicle for ten days. In case of the latter one, dissolved state formulation, a residence period of only four days occurred. However, this prolonged residual time in hair follicles implied a massage during the administration of each dye formulation [23] (figure 6b).

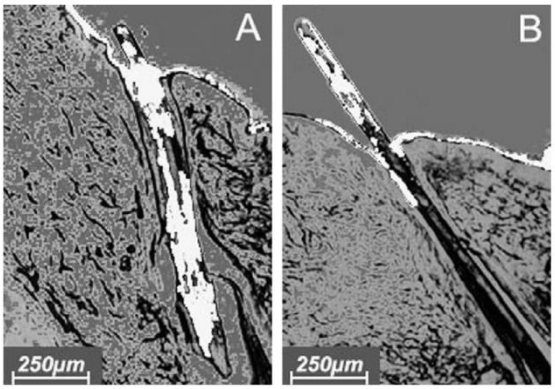

Figure 6a: Superposition of a transmission and fluorescent image, demonstrating *in vitro* drug penetration into porcine skin. Results of FT with fluorescent dye (white colored) containing formulations A with a diameter of 320nm were applied by a massage. B depicts a non-particle containing formulation [23].

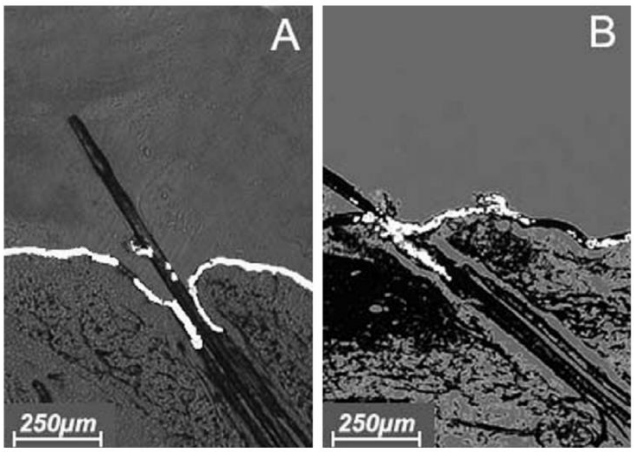

Figure 6b: Superposition of a transmission and fluorescent image, demonstrating *in vitro* drug penetration into porcine skin. Graphical representation A demonstrates the penetration depth into porcine ear skin in case of a particle containing formulations, whereas B represents a non-particle containing dye formulation. Both formulations were applied without a massage [23].

3.3.4. Skin penetration enhancement

In order to overcome the SC barrier, a broad variety of pharmaceutical excipients, widely known as penetration enhancers (PE), increase drug flux across the skin. In dermal formulation development PE represent a helpful tool since they facilitate an effective treatment of skin disorders in particular with regard to active substances with poor skin penetration. Examples of PEs include water, alcohols, sulphoxides and similar chemicals, terpenes, steroids, dioxolanes, 2-pyrrolidone and imidazole derivates, fatty acids, laurocapram (Azone®) and its derivates, oleic acid, 1,2-

propylenglycol, and urea [16, 24, 25]. Moreover, natural oil, liposomes, niosomes, ethosomes, phospholipid micelles, polymers, and surfactants clearly illustrate the great heterogeneity of potential penetration enhancers [26-29].

Besides API penetration enhancement for dermal purposes, PEs should fulfill the following requirements: non-toxicity without irritating potential, omitting any pharmacological activity to the body, work uni-directionally, and skin barrier properties should recover rapidly but also completely. Thereby, the PE should be compatible with both, inactive but also active ingredients. Finally, PEs are desired to be cosmetically acceptable with an appropriate skin feel [30]. Driven by the fact that PE interact with skin lipids, yet an ideal PE fulfilling the entirety of the above mentioned prerequisites has not been discovered.

Besides chemical PEs, physical capabilities in order to increase the bioavailability of dermally applied active substances include SC modification, hydration provided by moisturizing factors, occlusive films, and hydrophobic ointments [31].

3.3.4.1. Water

Water was reported to open up the compact SC structure thus increasing the bioavailability of most, but not all substances [32]. DSC measurements elucidated that the mechanism of water induced penetration enhancement is driven by increased fluidity of the bilayer region. As lipids provide a significant part of the skin's barrier function, any reduction in the relevant intermolecular forces will ease drug migration. This may help to explain why, for most molecules, hydration increases both, polar and non-polar permeant fluxes; all drug chemicals will be more mobile in the less tightly packed lipophilic region of the bilayer [33].

Occlusion in particular, is reported to not necessarily increase percutaneous absorption and that transdermal delivery of hydrophilic compounds may not be enhanced by occlusion. Furthermore, local skin irritation may occur [34]. The amelioration of penetrating actives can be confirmed by the fact that the water content within the outer skin membrane can approach 400% of the tissue dry weight [24].

3.3.4.2. Sulphoxides

Sulphoxides, such as DMSO act as PE by changing the conformation of SC related keratin from alpha-helical to beta sheet conformation [35]. Furthermore, as reported for concentrations above 60%, DMSO directly interacts with SC lipids. Taken together, penetration enhancement provided by DMSO affects both, changes in protein structure but also may result in alterations of SC lipid organization [35]. DMSO, an odorless, colorless, and hygroscopic enhancer is widely used as a “universal solvent” in pharmaceutical sciences, hereby acting as a powerful aprotic solvent in order to form hydrogen bonds with itself rather than water [24]. Since the human body metabolizes DMSO, the resulting dimethylsulphide causes a foul odor on breath. Additionally, DMSO in high concentrations applied over a period of several weeks may induce local skin reactions such as erythema, scaling, contact urticaria, stinging, and burning sensations [36, 37].

3.3.4.3. Laurocapram

1-dodecyl azacycloheptan-2-one, laurocapram or Azone® represents the first compound specifically designed as a skin PE [38]. Azone® is miscible with most organic solvents and represents an excellent solubilizer for a wide range of drugs. Furthermore, Azone® can be incorporated rapidly into different formulations and demonstrates a high chemical stability thereby being compatible with most excipients [39]. Azone® is a clear, amber-liquid melting at -7°C with distinct lipophilic properties [40]. It is described that a “soup-spoon” conformation of Azone® seems likely with respect to accommodate the Azone® molecule at the interface of the hydrocarbon and the polar head groups, respectively. This data suggests that Azone® acts due to the interference with the packing arrangement of intercellular lipids within the SC [41]. Dealing with safety concerns, contradictory statements are reported in the literature. On the one hand, Azone® is mentioned to be poorly absorbed by the dermal route and eliminated rapidly by the kidney [42]. In concentrations of up to 10% no irritating effects could be observed, whereas in high concentrations of 100% severe skin reactions occurred in hairless mice [43]. On the other hand, studies in mice, rats, rabbits, pigs, and monkeys demonstrated no systemic adverse effects or dermal toxicity after one month of skin exposition [44].

3.3.4.4. Short chain alcohols

Short chain alcohols such as ethanol or isopropyl alcohol are reported as the most common short chain alcohols in transdermal formulations but also transdermal patch devices [45]. Since ethanol with its history as a cosolvent and its well-established systemic toxicology and local tolerability is described as the clear choice for the first enhancer to be incorporated into transdermal drug delivery systems [46]. The effect of enhanced penetration is described by morphological changes within the SC thus forming additional free volumes. Furthermore, the solubility of actives must be in a sufficient magnitude in order to take advantage of the altered pathway [47]. In case of ibuprofen, ethanol increases the penetration across the skin primarily influenced due to enhanced solubility of the active in the membrane in a concentration dependant manner. In contrast, however, a pure ethanol solution did not enhance the skin penetration of ibuprofen [48]. Interestingly, the presence of ethanol strongly affects its ability as penetration enhancer. Recent insights revealed that Durogesic®, a transdermal therapeutic system, stopped working after three days because of ethanol exhaustion, however the patches still contained residual amounts of fentanyl [49].

3.3.4.5. Terpenes

Terpenes and essential oils are naturally occurring in flowers and plants. These non aromatic compounds comprising of carbon, hydrogen, and oxygen have commonly been used as medicines, flavorings, and fragrances. Menthol, a monoterpene, has been used in inhalation pharmaceuticals, but also, due to its mild antipuritic effect incorporated into emollient preparations [24]. Eucalyptus oil as the most potent essential oil demonstrated an increased drug permeability coefficient across excised human skin of up to 30fold [50]. As it is described in case of a 1,8-cineol pretreated skin combined with 5-fluorouracil as model API, penetration enhancement in an order of up to 100fold occurred under certain conditions [51]. Such tentative effects are in consequence strongly drug dependent. Data on the subject of terpenes acting as PE generally demonstrated that smaller terpenes tend to be more effective enhancers than larger sesquiterpenes. Furthermore, non-polar group containing terpenes such as limonene provide a better enhancement for lipophilic drugs by contrast with the

polar group containing terpenes. Conversely, less lipophilic terpenes such as 1,8-cineol seem to be more effective for lipophilic agents [24].

3.4. Transcutaneous immunization, purpose and advantages

Vaccination in general, had a tremendous impact in medical science and human welfare. However, particularly in developed countries, due to vaccination based herd immunity, severe diseases fell into oblivion, whereas the public awareness focused on rarely occurring adverse effects of vaccination. In terms of avoiding pain at application site and needle related stress, considerable efforts have been made to develop novel attempts on transcutaneous immunization.

Needles and syringes represent the most commonly used device in order to apply vaccines. Due to numerous immunizations that children routinely receive, health care organizations worldwide support novel concepts waiving the use of needle and syringes. Attempts on needle free devices aim towards needle free injections, transcutaneous immunization (figure 7) but also mucosal immunization. Over the past few years, the skin has emerged as a potential route for non-invasive vaccine delivery. Novel TCI strategies aim towards skin resident APCs which must subsequently reach the secondary lymphoid organs as the sites of the immune response. From the various field of TCI, the following sections describe both, advantages but also possibilities attempting on drug delivery by the dermal route.

Immunization via the dermal route offers considerable merits such as a reduction of costs, better compliance with immunization schedules, decreased or eliminated pain at application site, and accelerated vaccine delivery [52]. The basic idea of TCI involves improvements of safety for vaccinator, vaccines, and community.

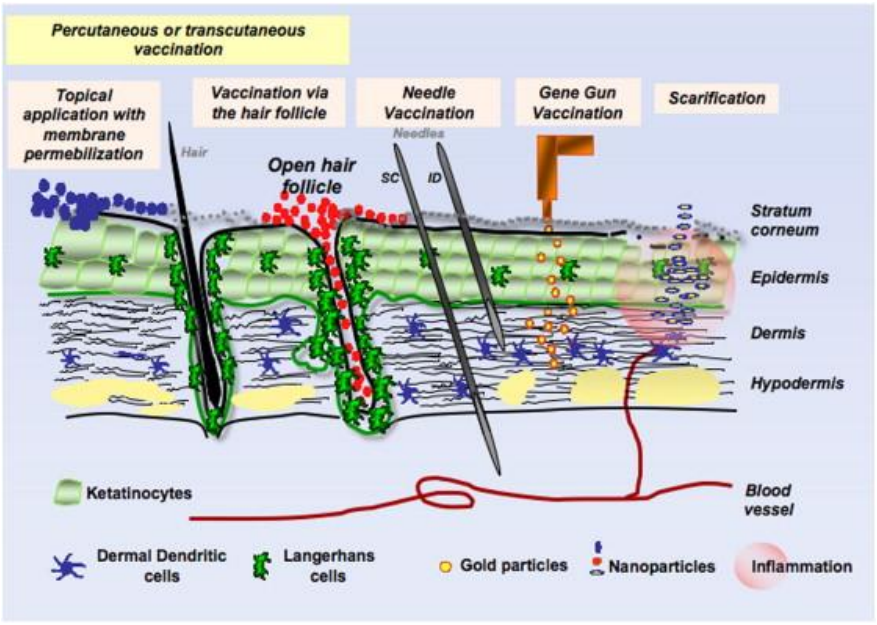

Figure 7: Schematic representation of percutaneous and transcutaneous particle based immunization route depicting needle based vaccination in comparison with transcutaneous vaccination either with or without skin barrier compromising techniques. As it becomes apparent, high amounts of LCs are located within the epidermis but also surrounding hair follicles. In contrast hereto, dermal DCs are commonly localized within the dermis. Graphical representation according to Combadière [53].

3.4.1. Safety

Traditional vaccinations via needle and syringe bear substantial risks for patients, healthcare providers, and community. This concern is particularly described for developing countries such as Ghana, Uganda, and Ivory Coast. Within these countries, multiple using of non-sterile needles between patients is a common practice [54]. Major safety concerns can be summarized as the reuse of contaminated needles and syringes without sterilization between patients, incorrect disposal of used needles and syringes in the community, and further unsafe practices such as changing needles but not syringes between patients [55, 56]. Consequently, serious hygiene shortcomings are described to contribute to hepatitis B, hepatitis C, and HIV infections in a substantial proportion [57]. It is described that at least 50% of injections are considered unsafe in 14 countries of 5 developing world regions. Furthermore, studies indicate that 20-80% of new hepatitis B infections are related to unsafe injections [58].

3.4.2. Compliance

During the first two years of life, the STIKO recommendation for 2013 requires at least 13 vaccination doses for basic immunizations. These include diphtheria, tetanus, whooping cough, poliomyelitis, Haemophilus influenza type b, hepatitis B, pneumococcae, meningococcal disease, measles, mumps, rubella, and varicella [59]. In terms of improved compliance with vaccination schedules in developed countries, TCI represents a pursuit to avoid frequently occurring needle phobia of both, children but also adults. Studies dealing with vaccination associated pain have shown that 90% of a 15-18 months and 45% of a 4-6 year of age study population suffered serious distress or worse [60] during the procedural phase of vaccination. In 8.2% of young adults an unreasonable fear of injection occurs [61]. This needle phobia contributes to a reluctant attitude towards immunization schedules particularly in developed countries.

3.4.3. Cost effective

By looking purely at the material costs per needle and syringe based vaccination the costs amount to $ 0.06 [62]. This low value however, does not take consequences of iatrogenic blood-borne pathogen transmission into account. Taken the social costs such as medical care and lost productivity related to iatrogenic blood-borne pathogen transmission into consideration, costs per needle and syringe based injection in developing countries may raise up to $ 26.77 [62]. Since vaccine delivery via needle and syringe have been compared with jet injectors and aerosol based vaccination techniques the latter ones can be seen as encouraging [62, 63].

3.4.4. No medical trained personal required

Vaccinations in a general sense may be simplified by the use of a cream or ointment based formulation. Obviously, TCI formulations enable self-application which means that in consequence no medical trained personal is required. The additional risk of needle stick related transmission of blood borne pathogens can be almost excluded, particularly within the developing world where an often occurring shortage of medical healthcare workers occurs. Moreover, in case of epidemics, pandemics or

bioterrorism a mass immunization campaign can be implemented even more rapidly [52].

3.4.5. Dose sparing

Investigations on i.d. versus i.m. administration of influenza vaccines demonstrated that one fifth of the applied dose deemed equivalent or superior immune responses in humans [64]. Investigations of immune responses on rabies and hepatitis B were in line with the above mentioned findings. Results obtained by comparing i.d. application with both, i.m. but also the s.c. route pointed out that antigens applied intradermally were suitable to trigger equal immune responses with a concomitant reduction of required antigen amounts. Local reactions occurred more frequently among recipients of the i.d. applied antigen however, adverse effects were described as mild and transient [65-70]. Although i.d. administration represents a needle and syringe related device, dermal administration evidences the viable dermis as a promising and capable target site. With regard to the obstacle function of the SC, a reduced amount of required antigens to generate equal immunization levels can thus, in principle, be considered advantageous.

3.5. Technologies of transcutaneous immunization

3.5.1. Microneedles

Modern biotechnology offers sophisticated and potent new active substances. However, limitations on bioavailability but also lacking skin permeability require novel administration concepts such as microneedles (MN) to traverse the human SC in order to deliver these actives in a transdermal but also painless manner. Studies on pain levels during the administration showed a significant pain reduction of MN techniques when compared with a 26-gage (0,45mm) hypodermic needle device [71]. Common MNs have a length of less than one millimeter. Generally, needle lengths of 25µm are suitable to sufficiently overcome the SC barrier. However, studies on needle lengths demonstrated a minimum of 550µm as necessary whereas MNs of

300µm length failed to pierce the SC and concomitantly to overcome the bulk of elastic tissue [72].

Although first proposed in the 1970s [73], suitable fabrication techniques allowing a cost-effective manufacturing of MN arrays became available since the 1990s. According to the needle type and shape, MN devices offer a plethora of geometrics. Generally, one can distinguish between solid MN, coated MN, hollow MN, dissolvable MN, and other MN types.

3.5.1.1. Solid microneedles

Solid MNs, as the most straightforward concept of microneedles (figure 8a), perforate the skin in order to facilitate transport of molecules through resulting conduits. In contrast to the above mentioned MN length requirements, studies conducted in the field of solid MN have yielded contradictory results. Solid MNs with a length of 150µm augmented the permeability of calcein as a model substance in four orders of magnitude [74]. Studies addressing the effect of solid MNs (300µm) in terms of DT but also influenza subunit vaccines demonstrated a drastic enhancement of IgG serum levels against diphtheria toxoid (DT) in BALB/c mice. In DT TCI, MN array pretreatment of the skin was essential to achieve substantial IgG and toxin-neutralizing antibody titers. The addition of cholera toxin (CT) further boosted the immune response to similar levels as observed after subcutaneous injection of $AlPO_4$-adsorbed DT (DT-alum). However, MN array pretreatment showed no effect on the immune response to plain influenza vaccine. This response was strongly improved by inclusion of CT, independent of MN treatment [75].

3.5.1.2. Coated microneedles

Coated MNs contain the antigen adsorbed at the needle surface (figure 8b). Driven by the fact that antigen concentrations within the coating solution may differ, depending on the required amount of antigen at the needle surface, coated MNs may contain precisely adjusted amounts of antigens. Since coated MNs are free of water,

this circumstance is assumed to be associated with antigen stability related advantages [76]. Although the amount of active compound on the needle surface is limited, investigations on influenza vaccines confirmed that coated MNs were suitable to trigger a sufficient immune response [76, 77].

3.5.1.3. Hollow microneedles

Hollow MNs contain an antigen or API loaded gap (figure 8c). Unlike solid MNs, as a relatively easy and straightforward approach enabling API permeation along conduits, hollow MNs enable vaccine injections to a well defined depth in the skin. Hollow MN techniques are of particular interest since hollow MN devices demonstrated to facilitate both, intradermal but also transcutaneous vaccine delivery depending on needle length [78, 79].

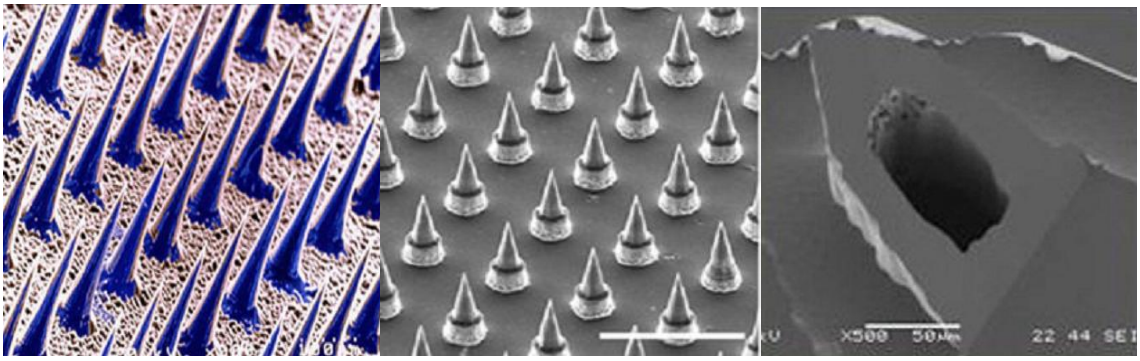

a b c

Figure 8a-c: Electron micrographs of different MN devices. Figure 8a represents a conventional silicon based solid MN device, according to Henry [74]. Figure 8b represents a coated MN device, graphical representation according to Crichton [80]. Figure 8c depicts an electron microscopic specimen of a hollow MN device according to Ding [75].

3.5.2. Injectors

Since the 1950s, needle free injections provided by jet injector devices have been studied extensively among military recruits and mass vaccination campaigns for disease control and eradication [81]. Driven by high pressure, jet injectors deliver either fluid vaccines or epidermal powder across the skin (figure 9). The required pressure through a nozzle orifice of approximately 0.20mm diameter is either

provided by CO_2 cartridges or spring-powered. Sufficient immune responses towards influenza vaccines have been demonstrated in case of Biojector® 2000 but also VitaJet® when compared with a standard needle and syringe application. Moreover, a decreased amount of antigen was required to achieve similar immune responses. Jet injector related pain levels tended to be somewhat higher compared with a needle and syringe related application. However, both, needle and syringe but also the jet injectors did not match pain levels of a venipuncture [82].

Serious safety concerns arose in the 1980s due to an incident occurring in a weight reduction clinic. Overweight patients were treated with human chorionic gonadotropin either applied by needle and syringe or a jet inceptor device. In case of the latter one, 60 of 287 patients became infected with hepatitis B. Unlike jet injector based application, none of the patients treated with needle and syringe became infected with hepatitis B [83]. This incidence of iatrogenic blood-borne pathogen transmission evidenced the potential risk of this needle free application device.

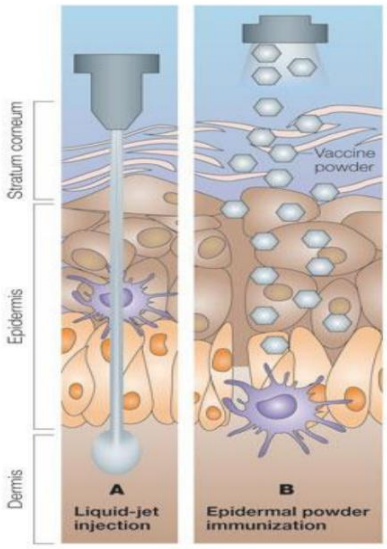

Figure 9: Graphical illustration of either liquid-jet injection (A) in comparison with epidermal powder injection (B) across the human skin according to Mitragotri [84].

3.5.3. Cholera toxin and heat labile toxin

Noninvasive dermal vaccination involves techniques including semi-solid dosage forms, solutions, and transdermal patches in order to facilitate an immunization

without disrupting or ablating the skin barrier. Obviously, a noninvasive dermal immunization represents the most desirable approach in terms of the above mentioned TCI related advantages. Large molecules such as proteins generally fail to pass the intact human SC thus representing a challenge on TCI development. Yet, only few immune stimulants such as Cholera toxin (CT), a 86kDa heterodimeric protein from bacterium *vibrio chloerae*, have demonstrated their capacity to penetrate across the human SC hence enabling a sufficient immune response. This potential immunostimulant is a member of the bacterial ADP-ribosylating exotoxin (bARE) family with the highest adjuvant potency when both, A and B units are present and functional [85]. Since it has been applied either by the p.o. or i.n. route, CT induces an antibody response against both, itself but also coadministered proteins. Hence, it has been considered as a potent mucosal adjuvant [86]. Investigations on mice immunized transcutaneously with both, tetanus fragment C and CT developed anti-tetanus toxoid antibodies and were consequently protected against systemic tetanus toxin challenge [85]. Besides CT, heat labile toxin (LT) from Escherichia coli facilitates an immune stimulating effect. This heat labile toxin is functionally, structurally, and immunologically similar to CT [87] however, investigations on recombinant B subunit of CT and LT identified the latter one as a more potent adjuvant [88]. Investigations on mice challenged i.n. with a lethal dose of CT exhibited a significant protection when previously immunized with CT by transcutaneous route [89]. With regard to the potential use for developing countries, a transcutaneous immunization of rodents with a C-terminal 42 kDa fragment of Plasmodium falciparum and CT exhibited both, IgG antibodies against the blood stage malaria antigen MSP-1 but also a protection against diarrheal diseases. These findings emphasize that the use of toxin-based adjuvants may confer simultaneous immunity against parasitic but also diarrheal diseases [90]. In summary, studies have shown that TCI induces priming but also secondary antibody responses (IgG and IgA) similar to traditional routes of immunization. Investigations aimed at T-cell response pattern of different immunostimulant agents based on CT and LT in combination with tetanus toxoid yielded in a mixed Th1/ Th2 phenotype. Either inguinal LN and spleen cells, higher levels of Th2-specific IL-5 were detected over IFNγ indicating a Th2 bias [91].

In conclusion, both, CT but also LT induce a substantial immune response via the Th2-dependant pathway. However, safety issues compromise an overall use of these

immunmostimulants by dermal but also mucosal route of administration. Investigations related to potential toxicity to the central nervous system of both, CT but also CT-B resulted in an accumulation in the olfactory nerves/ epithelium and olfactory bulbs of mice when applied intranasal in mice [92]. Elderly data assumed CT and LT as practically unsuitable for the use in humans due to high toxicity [93].

3.5.4. Liposomes

Liposomes are lipid bilayer based vesicular systems. Depending on composition and size, liposomes comprise of at least one phospholipid bilayer (figure 10). Besides egg lecithin or soy lecithin, liposomes may contain miscellaneous lipids but also surfactants in order to modify physicochemical characteristics such as pH stability or liquid crystalline state. Depending on size and homogeneity one can distinguish multilamellar vesicles (MLV), small unilamellar vesicles (SUV), and large unilamellar vesicles (LUV). Common manufacturing procedures of liposomes include the application of ultra sound but also fittings by means of extrusions using Nuclepore™ filters. Since actives may, depending on drug characteristics, be embedded either in the inner lipophile phase between phospholipid layers, at the interface of lamellar layers and aqueous gap or in case of distinctly hydrophilic actives in the aqueous interior, liposomes offer considerable merits. These include enzymatic degradation protection, drug targeting, and a prolonged systemic residue period by simultaneously reducing side effects. To date, treatments on the basis of liposomal formulated amphotericin B but also doxorubicin and daunomycin are well established [16].

In terms of dermal purposes there are special types of liposomes designed with a broad variety of excipients which contribute to overcome the human SC. Besides standard liposomes, these types are referred to as niosomes basing on non-ionic surfactants, transferosomes basing on ultradeformable lipid vesicles, and ethosomes due to an enhanced ethanolic content.

Although miscellaneous types of liposomes are described as a promising opportunity in order to achieve both, degradation protection due to drug encapsulation but also penetration enhancement of antigens and, more generally, APIs, there are also critical voices towards liposomal benefits. Data among TCI with DT loaded cationic-

but also anionic surfactant based liposomes demonstrated substantial antibody titers only if microneedle pretreatment was applied. Moreover, within this study vesicle based formulations did not enhance the immunogenicity of either intact or microneedle-treated skin and showed low stimulatory activity on dendritic cells [94].

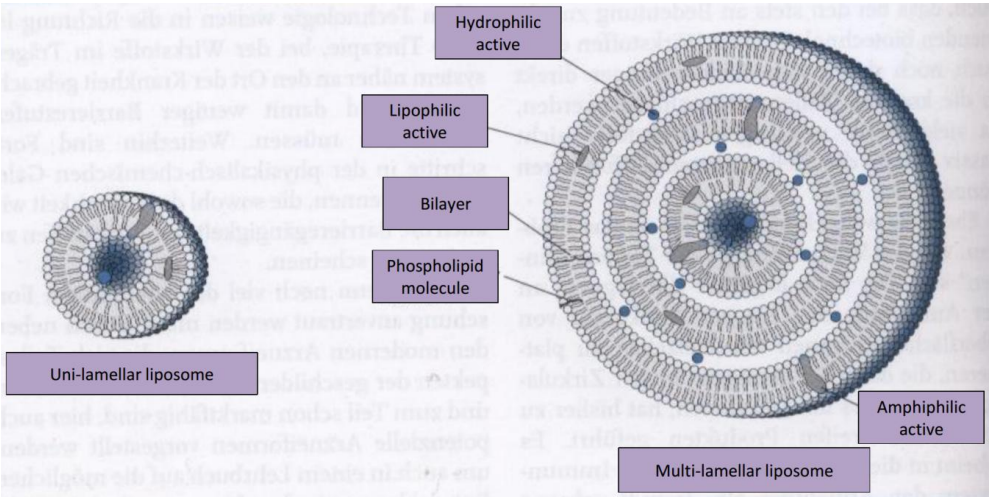

Figure 10: Schematic representation uni-lamellar and multi-lamellar liposomes according to Voigt [16].

3.5.4.1. Niosomes

Besides phospholipids, niosomal bilayers are composed of non-ionic surfactants such as sorbitan fatty acid esters (Span® of various types). These additives offer, in contrast to conventional liposomal formulations, several merits including low cost, high purity, content uniformity, greater stability, and ease of storage. Studies among topical vaccination with niosomes proved these carrier vesicles as suitable to elicit a comparable antibody titer and endogenous cytokines levels when compared with i.m. application of HBsAG [95].

3.5.4.2. Transferosomes

Transferosomes are designed in order to provide transdermal drug delivery by the use of elastic vesicles. The outstanding deformability enables transferosomes to squeeze themselves through intercellular regions across the SC under the influence of a transdermal water gradient [96].

Studies comparing tetanus toxoid (TT) loaded transferosomes, niosomes, and standard liposomes with i.m. applied alumn-adsorbed tetanus toxoid (AATT) showed mixed results. Topically given TT containing transferosomes, after secondary immunization, could elicit equivalent anti-TT-IgG titer when compared with an i.m. immunization. In contrast hereto, niosomes but also standard liposomes did not match these anti-TT-IgG titer levels. Interestingly, this study additionally conducted *in vitro* investigations towards antigen permeation in a Franz Diffusion cell model. Transferosomes demonstrated highest permeation results, however poor antigen transport across the skin generally occurred. This circumstance was assumed to be attributed to the large molecular size of the antigen with a poor diffusivity through vesicular membranes [97, 98].

3.5.4.3. Ethosomes

Besides phospholipids and water, liposomal carriers containing relevant amounts of approximately 30% ethanol are termed ethosomes. Since ethanol acts as well-established penetration enhancer, this short chain alcohol is assumed to positively impact on API penetration across the SC. Indeed, in terms of transdermal delivery (minoxidil and testosterone as model APIs) ethosomal carriers drastically enhanced API penetration when compared with both, standard liposomes but also an ethanolic API solution. The observed permeation enhancement of ethosomes seems to be attributed to a synergistic effect of ethanol and liposomal carriers [26].

3.5.5. Nanoparticles

Particles in a scale range of 1-300nm, depending on the author, are termed as nanoparticles. One can distinguish between nanocapsules and nano spherules. Nanocapsules contain microfine emulsion droplets or solids of a colloidal diameter with a fixed coated surface. In contrast to coated nanocapsules, nano spherules contain the active embedded in a matrix. Substrates for nanoparticles are either of natural or synthetic origin. These include gelatin, albumin, polysaccharides, fats, and waxes or in case of synthetic polymers polycyanoacrylates, polyvinylpyrrolidon, and

polylactides. By selecting appropriate polymer types, nanoparticles may provide a controlled drug delivery according to respective requirements.

Manufacturing processes of nanoparticles are based on versatile techniques from the various field of pharmaceutical technology. These include polymerization of mono- or oligomers from aqueous phases, O/W or W/O emulsions, surface polymerization, and surface condensation. Additionally, there are physical techniques on the basis of solvent deposition but also solvent evaporation. Drug loading of nanoparticles is commonly performed during or, less frequently, after the manufacturing process. However, nanoparticle techniques are not without its disadvantages. Particularly challenges with polymer based nanoparticles need to be overcome. These include residues from the organic solvent used in the manufacturing process, polymer toxicity, and the scaling up of the production process to industrial levels [16].

Besides the above mentioned nanoparticles, solid lipid nanoparticles (SLN) offer promising characteristics such as a broad administration field (dermal, p.o., and i.v.), high pressure homogenization as manufacturing process, avoidance of organic solvents, solvent matrix compositions of physiological and well-tolerated lipids, and the ability to produce and sterilize formulations on an industrial scale. These advantages emphasize the potential of solid lipid based nanoparticles in a nutshell [99].

Since antigens and likewise adjuvants with their large, complex, and commonly distinctly hydrophilic structures do not meet the ideal criteria to overcome the human SC, innovative carriers systems are urgently needed. Therefore, nanoparticles may represent a valuable tool in order to provide antigen stabilization, permeation, and concomitantly modify antigen release.

Due to their resemblance in size to native microorganisms, particle based antigens are more easily recognized and phagocyted by APCs. Concomitantly, they elicit the immune response to a greater extent when compared with dissolved antigens [100, 101]. Hence, from a pharmacological point of view, nanoparticular antigens and-even more importantly immunopotentiators represent an interesting concept for TCI development.

Although nanoparticles for dermal administration offer comprehensible advantages, numerous scientists tackle the issue whether and to which extent nanoparticles are

suitable to overcome the intact skin barrier. Indeed, it could be demonstrated that intact skin is impermeable to micro- but also nanoparticles [102-105]. However, particularly research efforts of Lademann and colleges substantiated the follicular route as a possible and previously underestimated penetration pathway. This could be proved on the basis that particles of approx. 650nm gained a maximum penetration depth in excised porcine ear skin [22, 106, 107]. A further justification for the role of a transfollicular impact on TCI was described by comparing immune responses after HBsAg administration in both, black-haired mice and nude mice, respectively. Here, black-haired mice achieved comparable antigen titers after dermal antigen challenging compared with an i.m. injection. By contrast, no immune response could be elicited by nude mice after dermal immunization [108].

3.6. Manufacturing techniques for particulate formulations

3.6.1. High pressure homogenization

Emulsions are disperse systems of two or more immiscible liquids with droplet sizes larger than 1µm in case of macroemulsions. In contrast hereto, microemulsions contain droplets below 100nm. Emulsions generally contain an inner phase dispersed in an outer phase. Commonly, one phase has a hydrophilic character whereas the other phase owns lipophilic properties. The use of emulsifiers decreases surface tension, a fact that positively impacts on both, stability but also manufacturability of emulsions.

The process of emulsification depends on energy supplied during manufacturing. Hydrodynamic forces cause a dissipation of both phases and in consequence a reorder of water/ oil interfaces. Generally, stable emulsions with a high degree of dispersion require a dispersion process with a subsequent homogenization procedure. Instrumental efforts during manufacturing strongly depend on size, viscosity, and surface tension of the respective emulsion. Manufacturing techniques include rotor stator devices (Silverson®, Ultra Turrax®), colloid mills, ultrasonic systems, and high pressure homogenizers. To date, high pressure systems enable appropriate droplet sizes of lower than 200nm.

The basic design of high pressure homogenizers generally implies a high pressure pump which can be electrically or pneumatically actuated and the actual high pressure dispersion unit. Figure 11 shows physical properties on the march of pressure more in detail.

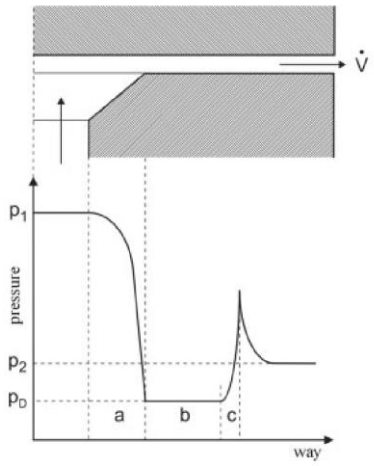

Figure 11: Graphical representation of pressure depending on passed way of fluid during high pressure homogenization process. Fluid flows in a valve with a given homogenization pressure. In the inlet bore “a” the fluid is very strongly accelerated thus the static pressure drops to a great extend. When vapor pressure of the fluid is reached vapor bubbles (cavitation blisters) and the single phase flow turns into a two phase liquid/ vapor flow “b”. The subsonic flow turns into a supersonic flow and in the further march of the flow it comes to a compression shock. Here, the pressure rises to a higher level so that in consequence the bubbles collapse and the flow becomes slower again “c”. Finally, the pressure in the valve outlet decreases to the ultimate pressure, mostly the ambient pressure [109].

3.6.2. Freeze drying:

Freeze drying, also known as lyophilization, is a particularly gentle dehydration technique commonly used to remove water from frozen samples. It positively impacts on the stability of various thermolabile and hydrolysis-sensitive substances. These include antibiotics, vitamins, hormones, blood plasma, serums, vaccines, proteins, sensitive plant extracts but also colloidal preparations such as liposomes [16]. Freeze drying bases on the principle that water, even in a frozen state, owns a distinct vapor pressure. Consequently, frozen water removal based on sublimation is driven by the fact that the vacuum value within in freeze dryer is beneath the partial water vapor pressure. An ice condenser assures a consecutive removal of water vapor. Figure 12 describes the physical principles of sublimation process.

Freeze drying processes can be divided into three stages:

i) Freezing

ii) Primary drying

iii) Secondary drying

Freezing is commonly performed under room pressure. During the freezing process pure water freezes first. A resulting increase of salt concentration especially occurs when saline buffers are used. A high salt concentration or precipitation of salts may negatively impact on stability of proteins or other sensitive substances. A parallel amorphous solidifying of concentrated salt solutions occurs at the presence of sugars. Sugars but also sugar fatty esters such as sucrose fatty esters thus act as kryoprotectants.

During primary drying, frozen water is removed by sublimation. The resulting water vapor deposits on a cooling coil at a temperature of nearly -60°C. Sample temperatures are set to approximately -20°, depending on the sample characteristic, during the course of primary drying. Since water vaporization results in a decrease of product temperature a hotplate compensates the evaporation based cooling.

A secondary drying process ensures a complete removal of the residual moisture. This process is performed at 20 – 25°C.

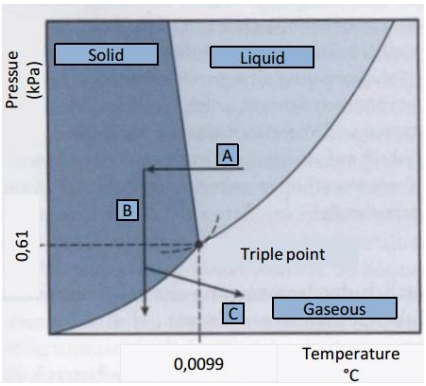

Figure 12: Graphical representation of triple point of water enabling sublimation processes. (A) describes freezing, (B) primary drying and (C) and secondary drying according to Voigt [16].

3.7. Analytical techniques used for formulation characterization

3.7.1. Franz Diffusion cells

Franz diffusion cells allow users to determine drug delivery characteristics of semi-solid dosage forms. Additionally, the operator can draw conclusions as to which extend excipients used within the semi-solid formulation may impact on drug release characteristics. Figure 13 illustrates a modern modified Franz Diffusion cell as it has been used within this work. This diffusion cell model is composed of two chambers. The inner chamber contains the acceptor medium whereas the outer sleeve provides a consecutive water flow. The surrounding water maintains a defined temperature of the acceptor medium. Other than commonly used 37°C in case of dissolution apparatuses, Franz diffusion cell investigations are performed at 32°C in order to mimic skin surface temperature. A magnetic stirrer agitates the acceptor medium in order to guarantee a uniform distribution of active substance dissolved therein. The sample is placed on either a synthetic membrane or ablated skin. Skin sections may be of animal (pigs or rodents) or human origin. A defined amount of semi-solid sample is placed on the upper surface of the membrane/ skin. After a pre-defined time period several µl of acceptor phase are withdrawn by the sampling tube and replaced with fresh acceptor medium.

To date, no compendial apparatus, procedures, or requirements for *in vitro* testing of semi-solid topical dosage forms are described in relevant pharmacopoeias [110]. Data on differences of parameters (such as number of synthetic membranes, agitation, and receptor medium) demonstrated the acceptor medium to be the most important and critical variable that influenced drug release. Moreover, these investigations described a ruggedness of *in vitro* diffusion cell systems used for drug release [111].

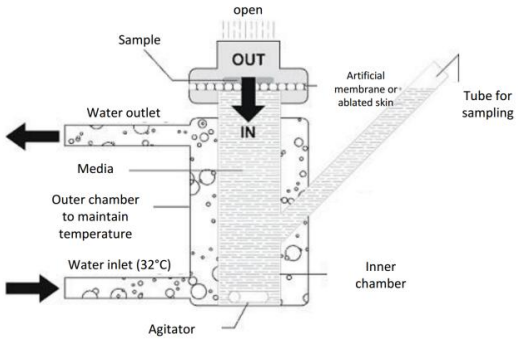

Figure 13: Graphical representation of a modified Franz – diffusion – cell according to Labswiss [112].

3.7.2. UV-Vis/ HPLC detection

Within a molecule, only electrons that are furthest from the atomic nuclei are of particular interest. Due to their energy richness, these electrons can be energetically exceeded by irradiating them with UV-Vis light. Molecules containing π electrons (such as double or multiple bonds) or n electrons (non bonding electrons) then absorb the energy from UV or visible light. Thus, a detectable transition from π to π* or n to π*occurs [113]. Energetic difference between HOMO (highest occupied molecular orbital) and LUMO (lowest unoccupied molecular orbital) is termed the HOMO-LUMO gap. The more easily excited the electrons, which means a lower energy gap between HOMO and LUMO, the longer the wavelength of light it can absorb.

According to Lambert-Beer's law, dissolved API concentrations may be precisely detected by:

$$c = \frac{A}{\varepsilon * b}$$

A = Absorption
ε = Absorption coefficient
c = concentration
b = thickness of the cuvette

The absorbance measured is directly proportional to the concentration. In order to achieve high measuring accuracy, absorptions need to be in a field between 0.2 and 1.4 [113].

High performance liquid chromatography (HPLC) is a technique to separate, identify, and quantify components in a liquid phase. Generally, HPLC involves a liquid sample being passed over a solid adsorbent material packed into a column. High pressure provides a consecutive flow of liquid solvent. Each substance dissolved in the mobile phase interacts slightly different with the stationary phase. In case of a weak interaction between the stationary phase and the substance of interest, this

substance flows off the column at a short time period. Conversely, a strong interaction effects a long term elution. In contrast to typical liquid chromatography, HPLC does not rely on gravity but on high operational pressures. In case of the method used within this work, pressure values were detected at approximately 110bar. Schematically, HPLC instruments include a sampler, pumps, and a detector. Purpose of the sampler is to carry the sample into a stream of liquid phase which carries it into the column. Required pressure is provided by pumps in order to enable sufficient passage times through the column. Subsequently, separated substances are quantified by an appropriate detector. To date, due to the lipophilic character of drugs most frequently reversed phase (RP) C-8, or alternatively C-18 columns are used.

3.7.3. Light- and polarized light microscopy

Light microscopy represents an easy to perform technique in order to optically observe particles. Light microscopes use visible light and a system of lenses for enlarging images of specimen. Common magnifications of light microscopes range in an order of 40 – 1000fold. On the basis that light microscopes are limited by diffraction to about 200nm resolution, particles of a submicron scale are preferably detected by electron microscopes.

Polarized light microscopy is an optical light microscopy technique involving polarized light. It is extensively used in optical mineralogy enabling the identification of crystal structures in a sample. A polarization microscope contains two polarization filters termed as polarizer and analyzer. The polarizer is positioned beneath the specimen stage, whereas the analyzer is located above the object. Purpose of the polarizer is to linearly polarize emitted light of the light source. Consequently, the polarization direction of light is aligned parallel to the polarizer. The analyzer as the second polarization filter is aligned in a 90°angle to the polarizer. These crossed polars now generate a black image. A specimen at the object slide may influence optical conditions. Certain substances such as crystals do, under certain circumstances, rotate the pane of polarization light. Such substances are termed birefringent, or

optically unisotropic. Due to changes of polarization plane, somewhat light penetrates the analyzer thus visualizing unisotropic structures.

3.7.4. Transmission electron microscopy

Electron microscopes use electron beams instead of visible light photons to illuminate the specimen. Electron beams are transmitted through an ultra thin specimen. The resulting interaction of the electron beam as it passes through the specimen thereby forms an image. This image than is focused and magnified on a fluorescent screen. Alternatively, the image can be focused by a CCD camera. This circumstance of using electrons instead of light photons results in a higher resolving power. Using electron microscopy one can achieve maximum resolutions of up to 50pm [114].

3.7.5. Rheological basics of semi-solid formulations

Semi-solid dosage forms such as ointments and creams generally do not behave ideal viscous. Typically, viscosity decreases at an increasing shear rate which is considered to be structurally viscous or pseudo plastic flow. This pseudo plastic behavior is often accompanied with thixotropy. Thixotropic systems strongly decrease their viscosity due to collapsing of inner structure in relation to the acting shear stress. After a subsequent recovering period thixotropic systems retrieve their original structure conditions.

Moreover, commonly used creams and ointments own a yield point. Below this yield point, the semi-solid system possesses solid like characteristics. After exceeding the yield point, most creams commonly behave pseudo plastic. This plastic behavior allows a good handling and thus is desirable for many semi-solid systems. Creams and ointments leave the tube as a continuous bar. Then, the occurring shear stress due to cream application onto the skin decreases the viscosity, a fact that consequently improves the applicability. After a short recovery period the cream remains reliably onto the skin surface ensuring drug delivery.

3.7.6 Dynamic light scattering and zeta potential

Dynamic light scattering (DLS) is a measurement technique in order to determine sizes of molecules and particles in the submicron region. Possible applications of DLS are particle size measurements but also particle size distributions, emulsions, and molecules dispersed or dissolved in a liquid. DLS measurement techniques are driven by the fact that particles in a liquid or a gas phase collide with molecules from their surrounding media. These collisions result in a randomized particle movement. Described by Stokes-Einstein theory, the Brownian motion depends on viscosity of the suspending fluid, temperature, and size of particles. DLS illuminates particles with a laser beam in order to detect time dependant fluctuation intensities. Fluctuation intensity depends on particle sizes. Hereby, smaller particles are moved further and more rapidly by solvent molecules than large particles do.

Besides particle sizes, electrostatic repulsive forces play a role in suspension type formulations. Since suspended particles own the tendency to agglomerate in order to decrease surface free energy, stabilization measures may be required to ensure a sufficient suspension stability. Therefore, the zeta potential acts as an indicator for suspension stability. It describes the degree of repulsion between adjacent, similarly charged dispersed particles. If the value of the zeta potential falls below a certain level, the forces of attraction may exceed the forces of repulsion. In consequence, flocculation and agglomeration occur [115].

3.7.7 Flow cytometry

Flow cytometry as a laser-based technique is employed in cell counting, cell sorting, biomarker detection, and protein engineering. Hereto, a suspension of cells passes a laser beam. Particles and cells in an order of magnitude of 0.2µm up to 150µm are detectable. Cells are detectable by scattering the laser beam, or due to a previous labelling of cells with a specific fluorescent dye. The resulting scattering or fluorescent light is then picked up by detectors. Fluorescence-activated cell sorting (FACS) as it is a specialized type of flow cytometry provides the partitioning of a heterogeneous cell mixture. It bases on the specific light scattering and fluorescent characteristic of each cell. Hereby, it is a useful scientific instrument in order to

provide a fast and quantitative recognition of fluorescent signals from individual cells but also enable a physical separation of cells of particular interest.

3.8. Imiquimod based transcutaneous immunization

Imiquimod represents a small molecule with a molecular weight of 240.3 Da. The active is termed by IUPAC as 4-Amino-1-isobutyl-1*H*-imidazo[4,5-c]chinolin (Figure 14). As a member of the imidazoquinoline family, similar to resiquimod, imiquimod activates the immune system via Toll-like receptor 7 (TLR 7)-MyD88-dependent signaling pathway [116]. This immunostimulating pathway stands in contrast to the Th2 response pattern of CT and LT. Investigations on cytokines emphasized a substantial IFNγ production compared with the $CD4^+$ mediated IL-4 production. Both, imiquimod but also resiquimod have provided crucial evidence in a murine model as adjuvants for DNA vaccination [117]. Since the activation of TLR 7 receptors induces a Th1 response, imiquimod is a potential immunostimulant in order to fight virus infected cells but also cancer cells. In order to facilitate a direct immune response by dermal administration, imiquimod activates dermis resident LHs.

Imiquimod is commonly used to treat human papilloma virus induced genital warts. Additionally, imiquimod has shown its capacity to eliminate several cancerous and precancerous skin lesions. In contrast to cytostatics with their serious side effects, imiquimod has no direct cytostatic effect. Previous investigations on the effect of imiquimod have shown the ability to eliminate tumor cells in mice after transcutaneous immunization [118, 119]. Frequently, imiquimod is used for treatment regimens of genital- and perianal warts (condylomata acuminata), a HPV (human papilloma virus) induced sexual transmitted disease. In contrast to cauterization or surgery, imiquimod offers a non-ablative treatment option based on a semi-solid formulation called Aldara® 5% creme. Besides the treatment of genital HPV induced warts, Aldara® 5% creme is approved to treat several cancerous and precancerous skin lesions. These include small superficial basal cell carcinoma (sBCC), non-hyperkertotic non-hypertrophic actinic keratoses (AKs) on the face and scalp. Aldara® 5% creme is a device for self administration by the patient. Commonly, this cream is

applied in the evening in order to ensure an appropriate residence time at the site of action. As the most frequently occurring adverse effect, Aldara® 5% creme causes local reactions at administration site. On the basis of a three times per week administration, 33.7% of patients reported itching or burning sensations at application site. Moreover, systemic side effects such as headache, flu-like symptoms, and myalgias were reported by 3.7, 1.1, and 1.5% of patients [120].

Next to Aldara® 5% creme, further treatment options for patients suffering from genital warts are available on the German market. These include Chondylox®, a podophyllotoxin based solution, but also green tea dry-extract containing Veregen® 10% ointment.

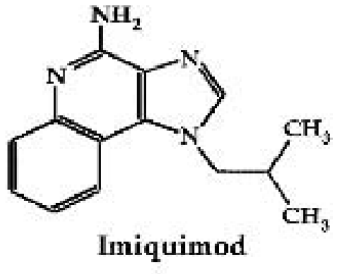

Figure 14: Chemical structure of TLR-7 agonist imiquimod, termed as 4-Amino-1-isobutyl-1*H*-imidazo[4,5-c]chinolin by IUPAC. Structural chemical formula is according to Schön [121].

4. Material and Methods

4.1. Components

Acetonitrile HPLC grade	VWR, Darmstadt, Germany
Aldara® 5% creme	Meda AB; donated by the Pharmacy of the University Mainz, Germany
Animals	C57BL/6 mice at 6-8 weeks were obtained from the local animal facility of the University of Mainz.
APC-conjugated IFNγ (clone XMG1.2)	eBioscience, Frankfurt, Germany
APC-Cy7-conjugated Anti-CD8 (clone 53-6.7)	eBioscience, Frankfurt, Germany
Avocado oil, refined, DAC	Carl Roth, Karlsruhe, Germany
Brefeldin A	Sigma Aldrich, Steinheim, Germany
Ethanol, HPLC grade	VWR, Darmstadt, Germany
Glacial acetic acid, high-purity, Ph. Eur.	Carl Roth, Karlsruhe, Germany
Hydrochloric acid, p.a.	Carl Roth, Karlsruhe, Germany
Imiquimod	Amino Chemicals Ltd., Marsa, Malta (CoA see section “appendix”)
Jojoba wax, virgin	Carl Roth, Karlsruhe, Germany
Li Ke Ji cream	Ke Yi Pharma, Hubei, People’s Republic of China
Laurocapram (CAS no. 59227-89-3)	Chemos GmbH, Regenstauf, Germany
Med Shine Li Di cream	Med-Shine Pharma, Sichuan, People’s Republic of China
Methanol p.a. grade	Carl Roth, Karlsruhe, Germany

Middle chain triglycerides	Carl Roth, Karlsruhe, Germany
Nan Bo cream	Top Fond Pharma, Henan, People's Republic of China
Officinal cremor basalis, DAC	Caesar & Loretz GmbH, Hilden, Germany
Oleic acid ≥ 99%	Carl Roth, Karlsruhe, Germany
Polyacrylic acid	Carl Roth, Karlsruhe, Germany
Polysorbate 80, Ph. Eur.	Carl Roth, Karlsruhe, Germany
Polyvinylpyrrolidon K30, high-purity	Carl Roth, Karlsruhe, Germany
Polyvinylpyrrolidon K90, high-purity	Carl Roth, Karlsruhe, Germany
Potassium dihydrogen phthalate, p.a.	Carl Roth, Karlsruhe, Germany
Saponin	Sigma Aldrich, Steinheim, Germany
Sodium acetate trihydrate, p.a.	Carl Roth, Karlsruhe, Germany
Sucrose fatty ester S-1670	Harke Pharma GmbH, Mülheim, Germany
Squalen, > 98%	Carl Roth, Karlsruhe, Germany
SIINFEKL	Dr. Stevanovic, Department Immunology, Institute of Cell Biology, University of Tübingen, Germany
Sudan III	Carl Roth, Karlsruhe, Germany
Trifluoroacetic acid HPLC grade	Sigma Aldrich, Steinheim, Germany
You Bi Qing cream	Zhuhai United Labs, Guangdong, People's Republic of China

4.2. Instruments

Analytical balance	Sartorius LE225D-OCE, Sartorius AG, Göttingen, Germany
Cannulas	Sterican® B.Braun Melsungen AG, Melsungen, Germany
CCD camera electron microscope	4kx4k TemCam-F416, TVIPS, Munich, Germany
Electric clipper	HC-240c, Remington, Ellwangen, Germany
Electron microscope	Tecnai12, FEI, Eindhoven, Netherlands
Flow cytometer	LSRII Flow Cytometer BD Pharmingen, Hamburg, Germany
Freeze dryer	Christ alpha 1-4, Martin Christ Gefriertrocknungsanlagen GmbH, Osterode am Harz, Germany
Freezer	Sanyo VIP Series, Sanyo, Wiesloch bei Heidelberg, Germany
High pressure homogenizer	Avestin Emulsi-Flex C3, AVESTIN Europe GmbH, Mannheim, Germany
HPLC column	300 C8 5µm reversed phase column (250*4.6mm) Mainz Analysentechnik, Mainz, Germany
HPLC detector	Jasco UV-975 detector, JASCO Germany GmbH, Groß-Umstadt, Germany
HPLC pump	Jasco PU-980 Intelligent HPLC pump, JASCO Germany GmbH, Gross-Umstadt, Germany
Laboratory balance	S-2002, Denver instrument, Bohemia, USA

Light microscope	DMIL Leica Microsystems GmbH, Wetzlar, Germany
Light microscope	Lomo 1, Leningradskoje optikoechanitscheskoje obedinenije, Sankt Petersburg, Russland
Modified Franz diffusion cell	EDC-07 diffusion cell, Labswiss International AG, Muttenz, Switzerland
Pipettes	Abimed discovery, Langenfeld, Germany
Planetary Mill	Pulverisette 6 classic line, Fritsch GmbH, Idar-Oberstein, Germany
Rheometer	HAAKE™ RheoStress™ 1 Rotational Rheometer, Thermo Fisher Scientific Inc. Karlsruhe, Germany
Rheometer measurement device	Cone and plate device PiT-L 35, Thermo Fisher Scientific Inc., Karlsruhe, Germany
Synthetic membranes (10kDA cutoff)	Diachema FRG, Munich, Germany
Syringes Franz diffusion cell	Omnifix-F, B.Braun Melsungen AG, Melsungen, Germany
Syringes HPH	Omnifix Luer Lock 50ml, B.Braun Melsungen AG, Melsungen, Germany
Ultra sound bath	Brandelin Sonorex, Geo-Reinigungstechnik, Gescher, Germany
Ultra Turrax	IKA®-Werke GmbH & CO. KG, Staufen, Germany
UV-cuvettes	Plastibrand UV-cuvettes, Carl Roth, Karlsruhe, Germany
UV-Photometer	Lambda 35 UV/Vis photometer, PerkinElmer Rodgau, Germany

Vortex	Vortex Genie 2, Süd Laborbedarf, Grauting, Germany
Water bath	Köttermann, Köttermann GmbH & Co KG, Uetze/Häningen, Germany
Zeta sizer	Zeta sizer nano, Malvern Instruments GmbH, Herrenberg, Germany
Zirconium oxide grinding ball (0.5mm and 1.0mm diameter)	Fritsch, Idar-Oberstein, Germany

4.3. Software

Excel 2007, Microsoft Corporation, Redmond, USA

FACSDiva software BD Pharmingen, Hamburg, Germany

GraphPad Prism 5.02, GraphPad Software Inc.

ImageJ 1.44p, National Institutes of Health, USA

RheoWin 4 data manager 4.30.0001, Thermo Fischer Scientific

ScopeTek 300, Hangzhou Scopetec Opto-Electric Co., Ltd., Zhejiang Province, PR China

Sigma Plot, Systat Software Inc., San Jose, USA

Word 2007, Microsoft Corporation, Redmond, USA

Zetasizer software 6.20, Malvern Instruments Ltd.

4.4. *In vitro* methods

4.4.1. Drug liberation and solubility evaluation

Investigations on drug liberation from pharmaceutical dosage forms are provided by versatile apparatus. A common requirement is the avoidance of drug saturation in the

acceptor medium during the course of measurement. This circumstance requires high solubility in the acceptor medium addressed by sink conditions described by the following term:

$$C_t < 0.2 * C_s$$

C_t = Concentration value at the time t

C_s = Saturated concentration

However, depending on the author [13], limits differ in a range of $C_t < 0.1 * C_s$ to $C_t < 0.3 * C_s$.

Initially, solubility of imiquimod has to be ensured in case of either the 25ml acceptor media containing Franz diffusion cells and the 7.50ml containing modified Franz diffusion cell model.

In case of Franz diffusion cells (see section 4.4.3.) 50mg of Aldara® 5% creme was applied on each diffusion cell with a resulting amount of 2.5mg imiquimod. As it is described in the literature, imiquimod is well soluble in a blend of methanol and an acetate buffer pH 4.0 (7/3 V/V) [122]. Instead of an acetate buffer a phthalate buffer pH 3.6 according to Ph.Eur.7.0 was used.

In case of modified Franz diffusion cell measurements, the exclusive use of a murine skin setup distinctly diminished the amount of API within the acceptor phase. Hence, a more physiological acceptor medium which is also suitable for HPLC detection was developed. This acceptor medium comprises of a 20mM acetate buffer and ethanol. For the acetate buffer, 1.0ml glacial acetic acid and 48.0mg sodium acetate trihydrat were diluted in 800ml double distilled water. pH value was set precisely to 3.6. Then, a 1000ml volumetric flask was filled up to the mark with double distilled water.

In order to evaluate a suitable acetate buffer/ ethanol blend, several mixtures (table 2), 7.50ml each, were investigated in terms of their capacity to dissolve 7.50mg imiquimod. Respective volumes of buffer and ethanol were measured before mixing each blend in order to avoid a falsification on the results due to volume contraction. Immediately after dissolving but also after a storage period of one week under room conditions (23°C) samples were checked for residual imiquimod. Other than blend

no. 3-7, blend no. 1 and no. 2 did not show any solid imiquimod substance after a one week period. All other blends resulted in incomplete imiquimod dissolved states. Consequently, blend no. 2 was the acceptor buffer of choice for modified Franz diffusion cell investigations.

Previous to each permeation investigation 7 volume parts of acetate buffer were mixed with 3 volume parts of HPLC grade ethanol. In order to lowering the risk of health hazard for the operator but also environmental impact, methanol was eliminated in favor of less toxic ethanol that also meets the test-relevant requirements. Alike the Franz diffusion cell model, 50mg of each imiquimod formulation was applied with a resulting maximum of 2.5mg reaching the acceptor phase.

Table 2: Ethanol/ acetate buffer pH 3.6 (20mM) ratio described as V/V in order to evaluate imiquimod solubility.

Blend no.	Ethanol (volume parts)	Acetate buffer pH 3.6 (volume parts)
1	20	**80**
2	30	**70**
3	40	**60**
4	50	**50**
5	60	**40**
6	70	**30**
7	80	**20**

4.4.2. Freeze drying

Within this work the respective samples were placed directly on a metal product plate. The thickness of each aqueous sample within the product plate was approximately 5mm. The sample containing product plate but also the hotplate were frozen at -82°C for twenty minutes in a freezer. Then, sample plate and hotplate were placed within the freeze dryer. The temperature for the primary drying process was set to -21°C. The required pressure was determined by instrument and set to

0.920mbar. The primary drying process was performed for twenty four hours. Subsequently, the secondary drying was realized at 25°C at a maximum vacuum for additional two hours.

In order to prevent SN6 squalen containing formulation from too low temperatures, the manufacturing conditions deviated from the above described freeze drying process. The aqueous formulation was placed on a metal product plate. Then, product plate and hotplate were placed within the freeze dryer. The temperature was set to 10°C and vacuum was carefully adjusted to 0,920mbar. This primary drying step was performed for 24 hours. An additional secondary drying process at 25°C was then performed for two hours, according to the method described above.

4.4.3. Franz diffusion cell

Within this work the simple Franz diffusion cell model was used in order to obtain *in vitro* drug release profiles. Additionally, the simple Franz diffusion model was utilized to assess whether synthetic membranes but also murine skin in combination with different types of acceptor medium impact on drug permeation characteristics. The results obtained by different setups were compared with *in vivo* generated data in order to test for correlations.

Mice were either sacrificed by cervical dislocation or preferably by carbon dioxide. Then, animals were shaved with an electric clipper. Skin was ablated and fatty tissue was removed carefully by a scalpel.

50mg of each imiquimod containing sample was placed onto an area (skin or synthetic membrane) of 0.79cm^2. As acceptor medium a solution of 7 volume parts methanol and 3 volume parts phthalate buffer pH 3.6 according to Ph.Eur. 7.0 was used. Each Franz diffusion cell contained 25ml of acceptor solution. Temperature of the acceptor medium was set to 32°C in order to mimic skin surface temperature. Due to highly pH dependant solubility [123], only a markedly decreased pH compared with physiological environment would ensure sink conditions during the course of the measurement. Furthermore, 0.1N hydrochloric acid was tested as acceptor medium following commonly used practices [123, 124]. Samples from the acceptor chambers were collected after 1, 2, 3, 5, 6, 7, 8.5 and 24 hours and replaced with fresh

degassed methanol/ buffer pH 3.6 solution or HCl, respectively. Imiquimod concentration within each sample was analyzed by UV-Vis detection (see section 4.4.5.)

4.4.4. Modified Franz Diffusion cell

Determination of drug permeation across murine skin was also studied by an EDC-07 Franz diffusion cell model provided by Labswiss. Each acceptor chamber contained a volume of 7.50ml. With respect to both, poor solubility of imiquimod in aqueous solutions, but also HPLC requirements, a blend of sodium acetate trihydrate/ glacial acetic acid buffer (with a total salt concentration of 20µM) and ethanol (7/3 V/V) with a resulting pH of 3.6 served as acceptor medium in order to maintain sink conditions during the course of measurement. Previously the acceptor medium was degassed by an ultra sound bath for approximately 30 minutes. Temperature was set to 32.0°C in order to mimic skin surface temperature. The acceptor medium was constantly agitated by a magnetic stirrer and a magnetic stir bar at 500rpm.

Skin samples were placed on each diffusion-cell chamber. 50mg of imiquimod formulation was evenly distributed on the skin surface of each diffusion cell using a spatula. 100µl of acceptor solution was withdrawn after 1, 2, 3, 5, 7, 8.5, and 24 hours and immediately replaced with fresh degassed medium. Imiquimod concentrations were detected by HPLC using a UV-Vis detector (see section 4.4.6.).

4.4.5. UV-Vis detection

Imiquimod concentrations in the acceptor medium were determined by UV absorption at 319nm wavelength. This wavelength was evaluated to be well suited by a wavelength check. Buffer media used here are described in detail in section 4.4.3. “Franz diffusion cell”. Linearity range evaluated at a Perkin Elmer Lambda 35 UV-Vis photometer was 0.34 – 25µg/ml with a resulting r^2 of 0.9999.

4.4.6. HPLC detection

In order to elute imiquimod, a 300 C8 5µm reversed phase RP 250*4.6mm column was used. The mobile phase comprises double distilled water, trifluoric acid and acetonitril (70: 0.0125: 30 V/V). This mobile phase ensured a pH value of 2.8 in order to avoid imiquimod precipitation in the column. The flow rate was 1.0ml/min generated by a Jasco PU-980 Intelligent HPLC pump. For quantitative API detection UV absorbance was determined by a Jasco UV-975 detector at 245nm wavelength. Imiquimod eluted after 5:30 minutes. Sample injection volume was 50.0µl. Detectable concentration ranges were from 35-1790 ng/ml. Jasco-Borwin HSS-2000 software was used to analyze the revealed peaks. During Franz Diffusion cell experiments approximately 110µl of sample solution was removed carefully by a 1.0ml syringe. Samples were collected in 1.5ml microcentrifuge-vials. Then, 100.0 or 50.0µl, depending on the expected concentration, of imiquimod containing samples were diluted with either 300.0 or 350.0µl buffer solution pH 3.6 in HPLC glass vials. In order to measure a homogenous solution, HPLC vials were twice turned upside down. More detailed data concerning validation procedure see section “Appendix”.

4.4.7. Dynamic light scattering

Within this work imiquimod particle sizes were measured in a 9mg polysorbate 80 per ml water containing solution. To ascertain whether crystal growth inhibitors such as PVP K30 and PVP K90 affect imiquimod particle sizes but also particle size distribution, an equal amount of crystal growth inhibitor compared with imiquimod was added to the aqueous imiquimod polysorbate 80 suspension.

On the basis that DLS measurements require a slightly milky suspension, 50.0µl of each sample was diluted with 4.0ml of double distilled water. Then, 100.0µl of the resulting suspension was additionally diluted with 1.30ml of double distilled water in a disposable cuvette. Measurements with a Malvern Zeta Sizer Nano were performed directly after the manufacturing process but also 1, 7, 10, and 70 days post manufacturing. Each sample was prepared three times in order to determine average particle sizes, and PDI values.

Similarly to particle size determinations, zeta potential measurements were performed with equal dilutions.

4.4.8. Light- and polarized light microscopy

Cream specimen from PR of China but also Aldara® 5% creme were diluted with distilled water. After subsequent application on an object slide, additionally lipophilic dye Sudan III served as colorant agent to detect whether all formulations show oil in water cream characteristics. In order to distinguish between API crystals and oil droplets, a polarization filter in a parallel but also a crossed setup was used. Images were detected at 400fold magnification.

4.4.9. Transmission electron microscopy

Samples were spread on a glass slide and then adsorbed onto a continuous carbon grid. They were washed three times with 20µl H_2O distilled prior to staining with 5µl of a 1% uranyl acetate solution. After the staining solution was blotted off grids were air dried. They were transferred to an electron microscope and images were recorded using a 4kx4k TemCam-F416 (TVIPS, Munich, Germany).

4.4.10. Rheological measurements

Rheograms were obtained by a Haake Rheostress1 equipped with a plate-plate measuring device termed as PiT-L 35. Data from rheological measurements were exploited by RheoWin 4 data manager. Flow curves displaying shear stress vs. shear rate were generated under a controlled shear rate setup of 0-200 s^{-1} recording the resulting shear stress.

Thixotropie was also determined by a controlled shear rate setup with a rate of 0-1000s^{-1} for 60s, following a 1000s^{-1} phase for 30s and subsequent reduction of the shear rate from 1000-0s^{-1} for further 60s.

The obtained measurement data were performed at a temperature of 23.0°C with an appropriate preheating time. Moreover, after each sample was placed at the RS1 application surface, a minimum of ten min ensured a recovery of inner structure. The measurement settings were chosen according to the manufacturers recommendations.

4.4.11. F1 and F2 test

In terms of *in vitro* data evaluation, several possibilities to characterize drug release characteristics are conceivable. Generally, comparing API release values at a defined point in time is easiest. However, such a comparison only takes a certain point into account thereby disregarding the curve progression, a circumstance that may falsify results. In contrast hereto, calculating difference factor f1 and similarity factor f2 may eliminate the above mentioned disadvantage. This from licensing authorities accepted calculations enables monitoring of an entire curve progression when compared with single point measurements at e.g. 24h [125]. The threshold values are < 15 in case of f1, or > 50 in case of f2, respectively [125, 126]. Both factors are calculated as

$$f_1 = \left(\sum_{t=1}^{n} |R_t - T_t|\right) / \left(\sum_{t=1}^{n} R_t\right) * 100$$

$$f_2 = 50 * log\left[\frac{1}{\sqrt{1 + \frac{1}{n}\sum_{t=1}^{n}(R_t - T_t)^2}} * 100\right]$$

N = number of sample collections

R_t = cumulative released shares [%] of reference formulation

T_t = cumulative released shares [%] of test formulation

To SUPAC (scale up and post approval changes) drug release curves are valid as similar if f2 factors exceed the value of 50.

In terms of comparing the innovators product Aldara® 5% creme with formulations from PR of China both factors were calculated for both, synthetic membrane setup but also the murine skin setup.

4.5. *In vivo* methods

In vivo measurements have been described in detail by Stein [127]. This includes the experiments described as follows.

4.5.1. Transcutaneous immunization protocols

Transcutaneous immunizations protocols were described previously [128]. In short, dorsal hair of anesthetized mice was completely removed with electric clippers. Afterwards, 50mg of imiquimod containing formulations together with 100µg SIINFEKL ($OVA_{257-264}$) dissolved in DMSO were applied on days 0 and 1. In contrast hereto, SIINFEKL has not been added directly in case of several nano- to submicron particle imiquimod formulations in virtue of high imiquimod solubility. Here SIINFEKL has been

i) applied by i.d. injection

ii) directly added (in case of the freeze dried concepts) as component of the formulation

iii) applied via a suitable vehicle (in case of the emulsion gel concept) previous to the administration of the imiquimod formulation. The vehicle cream initially was a non imiquimod containing formulation. Later on, officinal cremor basalis served as imiquimod-free vehicle cream.

4.5.2. IFNγ determination

Interferon gamma, a dimerized soluble cytokine has antiviral, immunoregulatory, and anti-tumor activity [129]. Additionally, IFNγ is also an important activator of macrophages. IFNγ-production by $CD8^+$ T-cells was determined after *ex vivo* restimulation of blood cells for 6 hours either with or without $OVA_{257-264}$ (100 nM) together with Brefeldin A (1 µg/ml, Sigma). After washing with FACS buffer, samples were stained for CD8 surface expression. Before intracellular IFNγ-staining, cells were fixed and permeabilized with 4 % paraformaldehyd. After a washing step with PBS containing 0.1 % BSA and 0.05 % Saponin cells were stained for IFNγ.

4.5.3. Cytotoxicity test

In order to determine the magnitude of imiquimod based CTL stimulation a cytotoxicity test was used. Hereto, peptide loaded and carboxyfluorescein succinimidyl ester (CFSE) marked spleen cells create the basis for this *in vivo* performance test. Previously immunized mice were given these spleen cells (0.4 µM $CFSE^{low}$) acting as target structure by tail vein incision. Non peptide loaded spleen cells act as reference cells. To distinguish between target and reference spleen cells, the latter ones were loaded with a higher CFSE concentration (4 µM $CFSE^{high}$). Blood samples of immunized and control mice were collected and respective CFSE populations were analyzed among each other by flow cytometry. The ratio between CFSE high and CFSE low allows direct conclusion as to which extent the marked cells are eliminated.

4.5.4. Tetramer staining

Antigen specific cytotoxic T-cells can be specifically stained in order to assess their activity. For this staining process a tetramer comprising of peptide loaded MHC-I molecules additionally linked with Phycoeritrin (PE) was used. PE acts as a fluorescent dye suitable for FACS determination. To avoid falsification on the result, a propidium iodide solution was added in order to differentiate between dead and living cells.

4.5.5. Murine ear swelling test

Imiquimod as an immunostimulant may lead to a local inflammatory reaction. Such a local reaction may be associated with a swelling of tissue. To measure the inflammatory response, imiquimod containing preparations were applied after 2 consecutive days on the ears (each site 50 mg per treatment). Ear swelling was assessed by measuring the ear thickness before and after treatments. Although representing a simple to detect method the ear swelling test allows reliable conclusions on the inflammatory effect of the respective formulations.

4.5.6. Tumor rejection assay

Activation of CTL affects both, the eradication of virus infected cells but also tumor cells. Hence, rejection of implanted tumors gives an impression of effectiveness not only as surrogate parameter but as a final outcome. Tumors were implanted by s.c. injection of 4 x 105 EG.7 thymoma cells (from ATCC) as described previously [118]. Tumors were allowed to grow until palpable (10-12 days after inoculation) before treatments were initiated. Tumor size was monitored three times per week with a caliper measuring the diameter in two dimensions. Mice were killed when tumor size exceeded 20mm in both diameters.

4.6. Development of imiquimod formulations

4.6.1. Freeze dried concepts

Attempts on a lyophilized nanoemulsion concept comprising of at least one sucrose fatty ester and pharmaceutically acceptable oil have proven this concept as a possible candidate for parenteral nutrition. Since numerous active ingredients are poorly soluble in water, the oil phase of a nanoemulsion may act as solvent for lipophilic active substances. Additionally, this formulation concept may be freeze dried and, after redispersion with water, still be intravenously administered [130]. Interestingly, this nanoemulsion offers a certain spreading quality. Hence, the composition of this patent was modified in terms of enhanced spreadabilty. Moreover, the resulting formulation approach contained imiquimod not in a dissolved but in a suspended state.

Purified water, sucrose fatty ester S-1670, and imiquimod were stirred in a 50ml beaker for five minutes. A preliminary milling step included the milling of the aqueous imiquimod suspension by a Pulverisette 6 ball mill using 25g zirconium oxide grinding spheres of 1.0mm diameter in an almost completely filled 45ml zirconium oxide grinding vessel for two cycles at 650rpm, 20minutes each, with a respective recovery/ cooling period of ten minutes. After planetary milling, the aqueous suspension was thoroughly poured through a sieve with an aperture of 0.5mm in order to exclude a blockage of the HPH due to 1.0mm zirconium oxide grinding balls. Then, the resulting

suspension underwent high pressure homogenization in an Avestin EmulsiFlex-C3 high pressure homogenizer at 500bar and 1000bar for four and eight cycles, respectively. Thereafter, the respective oil component was added and pre-emulsified by an Ultra Turrax® for five minutes at 8000rmp. In order to create a nano emulsification, an additional high pressure homogenization step was performed with 500, 1000 and 1500 bar, 4 cycles each. The overall sucrose fatty ester S-1670/ oil ratio was 2.0/ 7.5 (m/m). Other than this ratio, the oleic acid based SN required equal parts of both, sucrose fatty ester S-1670 and oleic acid in order to ensure a sufficient stability. In case of laurocapram containing SN formulations, the enhancer was added along with the oil phase previous to the second HPH step.

The antigen SIINFEKL was added previous to the preliminary milling step to the aqueous imiquimod suspension.

General compositions of SN (except oleic acid) formulations are described in table 3a. Table 3b describes the respective oil component of each SN formulation more in particular.

Since oleic acid based SN formulations showed lacking stability, the general composition differed from SN 1 – SN 6. Table 3c describes the oleic acid based SN in detail.

Table 3a: General compositions of SN formulations described as percent by weight.

Component	Percent by weight
Sucrose fatty ester S-1670	20.0
Imiquimod	5.0
Purified water *	300.0
Respective oil**	70.0
Laurocapram***	5.0
SIINFEKL ****	0.20

* purified water was removed during the freeze drying process.

** details concerning respective oil components are described in table 3b.

*** in case of absence of laurocapram, the proportional weight of 5% was equalized by respective oil components in case of SN 1 – SN 4.

**** presence of SIINFEKL in case of SN 5 – SN 6.

Table 3b: Details on composition of respective SN formulations thereby addressing the presence or absence of antigens but also respective use of laurocapram as penetration enhancer.

	lipophilic component	penetration enhancer	antigen
SN 1	middle chain triglycerides	-	-
SN 2	avocado oil	-	-
SN 3	jojoba wax	-	-
SN 4	squalen	-	-
SN 5	middle chain triglycerides	laurocapram	SIINFEKL
SN 6	squalen/ tocopherol	laurocapram	SIINFEKL

Table 3c: Details on composition of the oleic acid based SN formulation.

Component	Percent by weight
Sucrose fatty ester S-1670	47.5
Imiquimod	5.0
Purified water*	300.0
Oleic acid	47.5

* purified water was removed during the freeze drying process.

4.6.1.1 Stability testing of SN formulations

As described in the section above, each SN formulation contains a specific oil component. Differences in physicochemical properties such as color, odor, liquidity but also presence or absence of double bonds within the molecule, may thus impact on formulation stability. In order to assess oil related influences on stability, each formulation was stored under room conditions at 23°C directly after the manufacturing process. After a fourteen days period, possible changes referring to color, odor, and powdery appearance were investigated.

4.6.2. Emulsion gel

4.6.2.1 Preliminary studies on crystal growth inhibitors

In general, the emulsion gel contains imiquimod particles suspended in a nano-crystalline state. Nanoparticles are inevitably more unstable than microparticles because of the extra Gibbs free energy contribution related to the particle size and primarily due to surface energy [131, 132]. As a semi-solid aqueous formulation approach the use of crystal growth inhibitors was assessed previous to the further development steps. Polyvinylpyrrolidone derivates such as PVP K30 are suitable for the use as polymeric stabilizers. Other than polymeric stabilizers, polysorbate 80 acts as a non-ionic surfactant stabilizer [133, 134]. Preliminary studies regarding the effect of PVP K30, PVP K90, and polysorbate 80 were performed. Therefore, three aqueous imiquimod crystal suspensions with the active suspended in 9mg/ml polysorbate 80 were tested. The presence of polysorbate 80 was mandatory due to the poor wettability of imiquimod. Two suspensions additionally contained either PVP K30 or PVP K90 in equal amounts to imiquimod. Except polysorbate 80, the third suspension did not contain further crystal growth inhibitors. The suspensions were stored in test tubes under room conditions at 23°C. Measurement conditions for particle size but also zeta potential determination are described at section 4.4.7. “dynamic light scattering”.

4.6.2.2 Manufacturing of the emulsion gel

Manufacturing the emulsion gel is based on the following steps:

i) pre-homogenization of an aqueous imiquimod suspension by a planetary mill

ii) adding jojoba wax, polysorbate 80 and laurocapram

iii) manufacturing and precisely neutralizing a 3% aqueous polyacrylate gel

iv) HPH of the i and ii

v) Adding a stoichiometric amount of iii in order to ensure a 5% API content of the emulsion gel

For pre-homogenization, 3.0g imiquimod were added to 17.0ml of an aqueous polysorbate 80 (9mg polysorbate 80/ml) solution. The resulting 15% (M/M) imiquimod containing aqueous suspension was poured in a 45ml grinding vessel. Then, 25g of zirconium oxide grinding balls with a diameter of 0.5mm were added. Both, aqueous imiquimod suspension and grinding balls almost completely filled the grinding vessel. Milling was performed by a Fritsch Pulverisette 6 planetary mill for six cycles, 20min each, with a respective cooling period of 10min between cycles. Rotation direction setup of the instrument was reverse. After planetary milling, the aqueous suspension was thoroughly poured through a sieve with an aperture of 0.25mm in order to exclude a blockage of the HPH due to 0.5mm zirconium oxide grinding balls.

Then, the emulsifier polysorbate 80 was added to the aqueous imiquimod suspension to produce a stable emulsion. At this manufacturing step, laurocapram and jojoba wax were added to create a formulation with a final amount of 5 % polysorbate 80, 2.5 % laurocapram, and 42.5 % jojoba wax, respectively.

The resulting two-phase mixture was pre emulsified by a Vortex Genie®2 for two minutes at maximum level. Then, HPH was performed by an Emulsiflex™ C3 (Avestin) for five cycles at 500bar and ten cycles at 1000bar. The resulting oil in water emulsion with suspended imiquimod nanoparticles occurred as a yellow fluid. In order to create a semi-solid formulation a previously prepared and precisely neutralized polyacrylic acid gel was added. Hereto, polyacrylic acid was suspended in purified water using a pharmaceutical mortar and pestle. Then, a 0.1N sodium hydroxide solution was carefully added in order to neutralize the suspension. The resulting gel was tested for pH value by a commonly used pH paper. In order protect imiquimod particles against acidity the pH value of the aqueous gel was set to at least 7.

Table 4: Composition of 5% imiquimod emulsion gel

	Component	Percentage [w/w] of each component within the emulsion gel
1)	Aqueous polysorbate 80 (9mg/ml) Imiquimod suspension 15% (W/W)	33.33
2)	Polysorbate 80	5.0
3)	Laurocapram	2.5
4)	Jojoba wax	42.5
5)	Aqueous polyacrylate gel 3%(W/W)	16.67

Based on the assumption that 7.0g aqueous imiquimod suspension 15% (W/W) (suspended in 9mg/ml polysorbate 80) remain after pouring the suspension through a sieve, this will result in 21.0g emulsion gel end product. This end product is – besides the 7% aqueous polysorbate 80 imiquimod suspension (15%) – composed of:

- ➔ polysorbate 80: 1,05g
- ➔ laurocapram: 0,525g
- ➔ jojoba wax: 8,925g
- ➔ (carbomer gel: 3,50g)

After mixing all and vortexing the components except for the carbomer gel in a grainer tube HPH is performed as described above.

Subsequent to the HPH, the amount of the yellowish emulsified fluid, comprising of aqueous imiquimod suspension, polysorbate 80, laurocapram and jojoba wax is precisely determined. Basing on a total amount of 21.0 g including 3.5 g of carbomer gel, the missing portion carbomer gel needed to complete the emulsion gel can be calculated. For instance 14.4 g of the yellowish emulsion remain after HPH. Then, in consequence 2.88 g carbomer gel have to be added.

5. Results

5.1. Comparison of commercially available semi-solid imiquimod formulations

The following section does not primarily aim at comparing Peoples Republic of China and Europe as competitors, but to examine the extent as to which different formulations differ between each other. Special attention is devoted to both, pharmaceutical characteristics but also *in vivo* generated effects in C57BL/6 mice. Differences detected were a valuable tool in order to gain deeper insights into imiquimod based TCI. The precious possibility to investigate five different dermal formulations allowed a systematic comparison of different *in vitro* methods. Moreover, it represented an opportunity to give hints regarding development efforts in terms of novel improved imiquimod based TCI concepts.

5.1.1. Rheological characterization

Flow curves obtained by plotting shear stress Ƭ (Pa) versus shear rate (s^{-1}) demonstrated a roughly tenfold difference in viscosity at low shear rates (approx. 25 s^{-1}) between products (figures 15a-b). Pseudo plastic flow behavior but also thixotropy were observed in all investigated formulations, however distinct differences concerning flow limit were obvious.

A shear thinning effect was detectable particularly in case of “Nan Bo”, but shear stress induced phase separation with a supernatant oil phase occurred in all formulations, to a varying extent, during the measurements. This phase separation with a resulting supernatant oleic phase is particularly evident in case of “Nan Bo”, already appearing at slight shear rates of approximately $50s^{-1}$. This might explain the substantial decline of viscosity in case of “Nan Bo” (figure 15a) that, on the other hand, offered apparently the highest viscosity in application handling when applied on skin samples. Besides “Nan Bo”, lacking stability also occurred in case of the innovators product Aldara® 5% creme, a circumstance that is in line with stability issues mentioned in the literature [135].

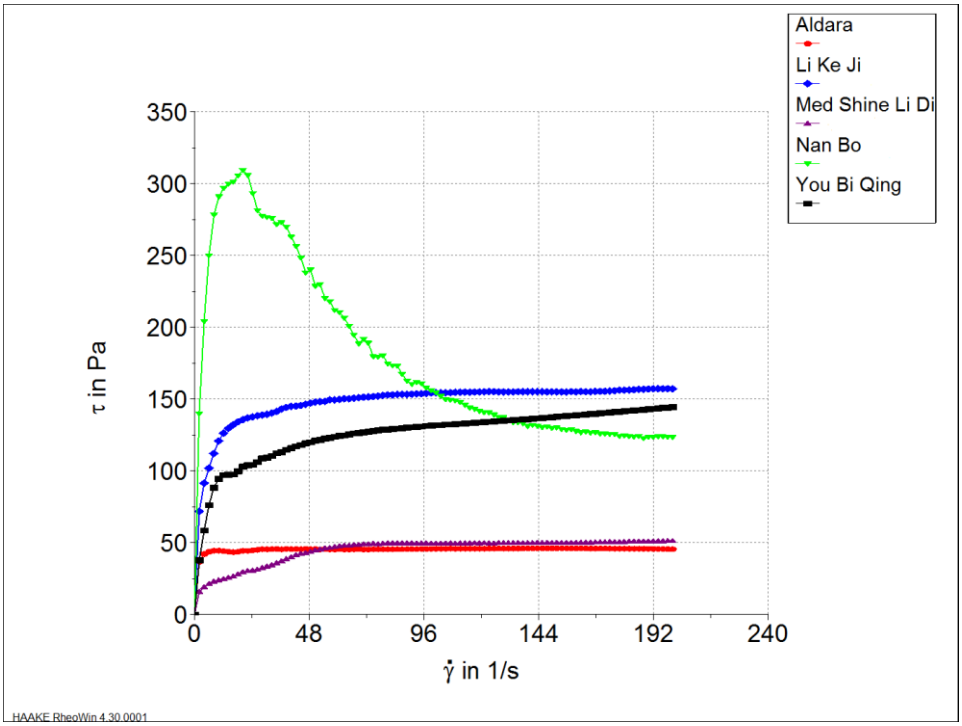

Figure 15a: Flow curves of different imiquimod containing formulations displaying shear stress (τ) versus shear rate (γ).

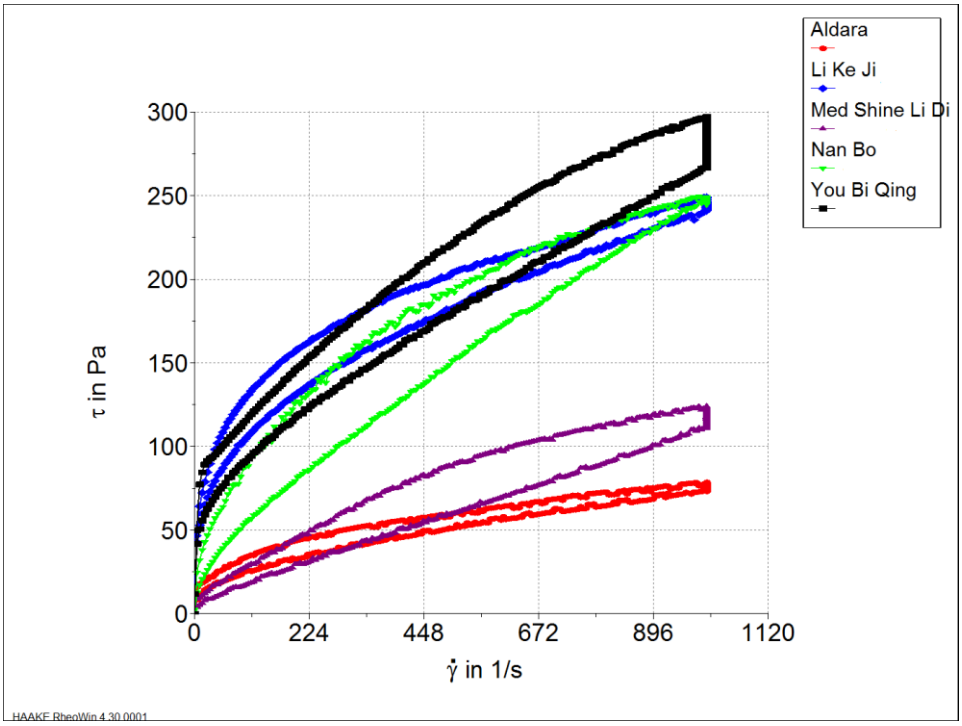

Figure 15b: Thixotropic properties of imiquimod containing formulations displaying shear stress (τ) versus shear rate (γ).

5.1.2. Light microscopic images

Light microscopic images attested all formulations water-miscibility with well dyeable dispersed state oil droplets when using Sudan III (stained droplets not shown). In order to detect whether or not cream samples contain imiquimod in a dissolved state, the use of a polarization setup showed distinct differences concerning the various products. In order to gain a general idea of an aqueous imiquimod suspension figure 16 depicts unprocessed imiquimod crystals. Imiquimod crystals of up to 60µm in length occurred in case of “Li Ke Ji” (figure 18). In the same manner, “You Bi Qing” (figure 21) contains crystalline active however, particle sizes were only in a range of 2 – 5µm and unlike “Li Ke Ji”, incorporated into the inner oil phase of the cream. “Med Shine Li Di” (figure 19), “Nan Bo” (figure 20), and Aldara® 5% creme (figure 17) did not show any presence of crystalline active.

Interestingly, in case of “Med Shine Li Di”, several optically anisotropic artefacts in a scale range of up to 1000µm in length occurred (figure 19a). Likewise “Li Ke Ji” contained anisotropic fibrous artefacts embedded in the cream formulation (specimen not shown).

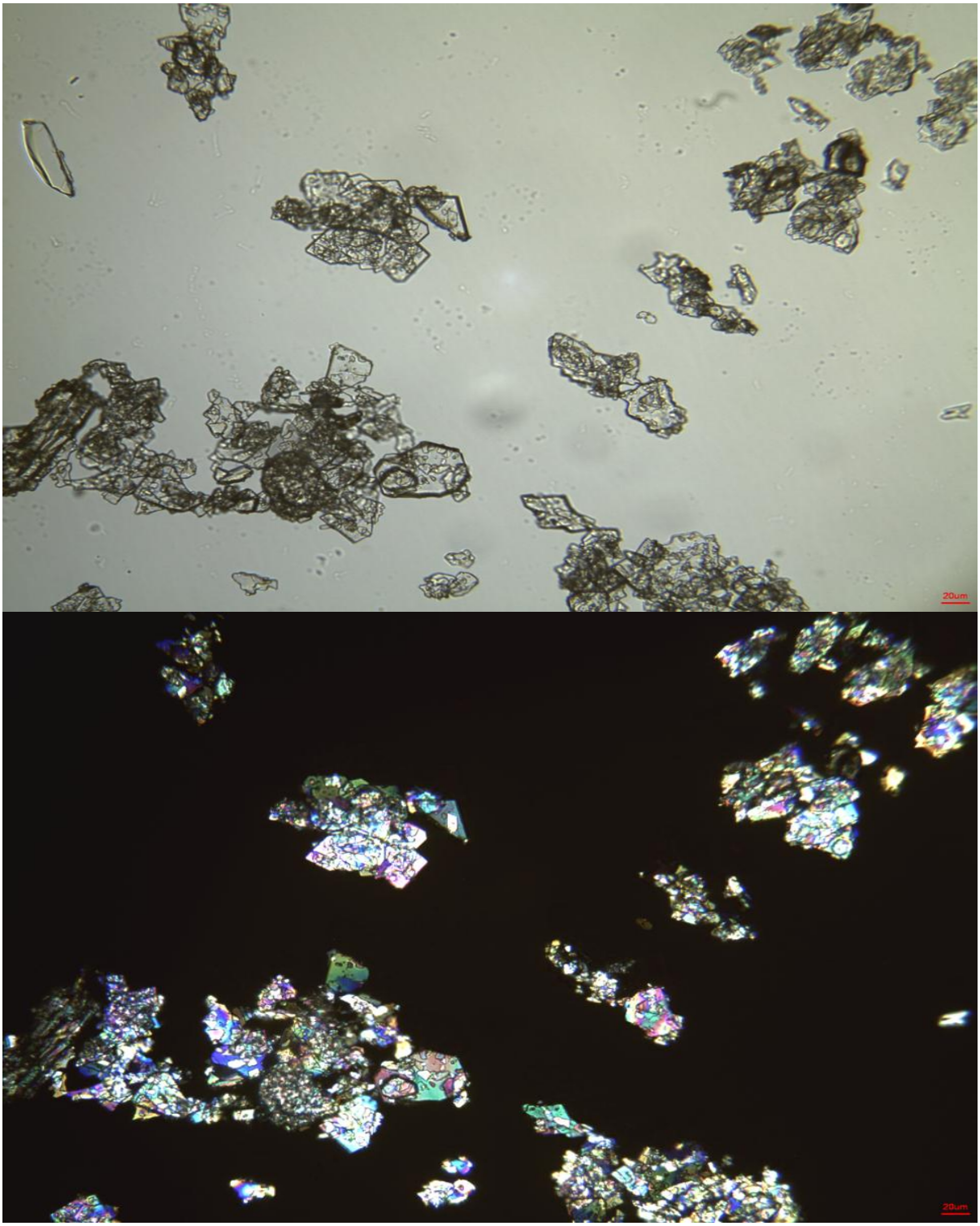

Figure 16: Microscopic contemplation of imiquimod raw crystals with polarization filters parallel (upper picture) and crossed (lower picture) demonstrate a distinct optically anisotropic effect of the API (100fold magnification). The red bar on the right sight at the bottom of the contemplation displays a length of 20 µm.

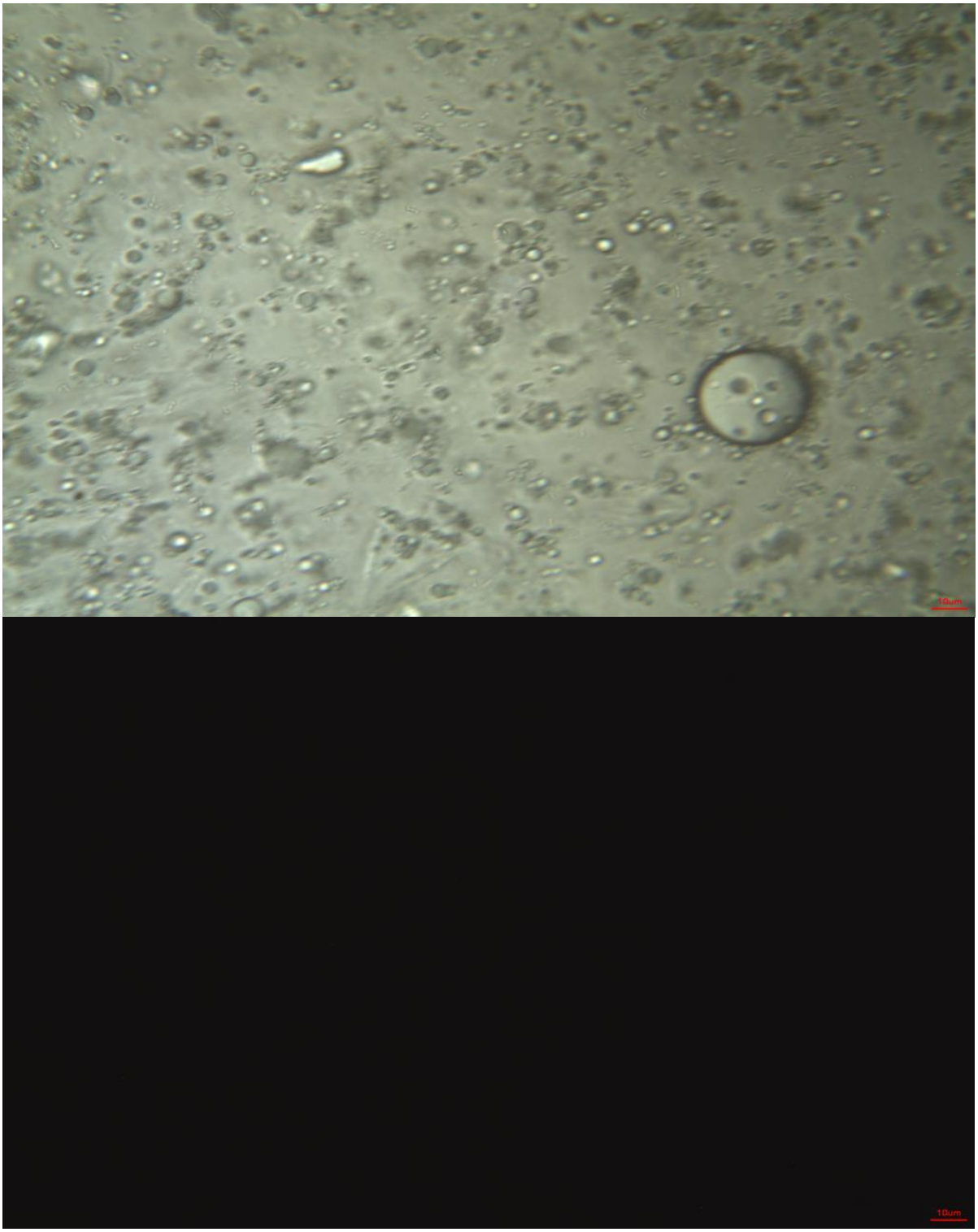

Figure 17: Microscopic contemplation of Aldara® 5% creme with polarization filters parallel (upper picture) and crossed (lower picture) (400fold magnification). Due to the absence of optically unisotropic structures the lower image indicates that the innovator product contains the API in a completely dissolved state. The red bar on the right sight at the bottom of the contemplation displays a length of 10 µm.

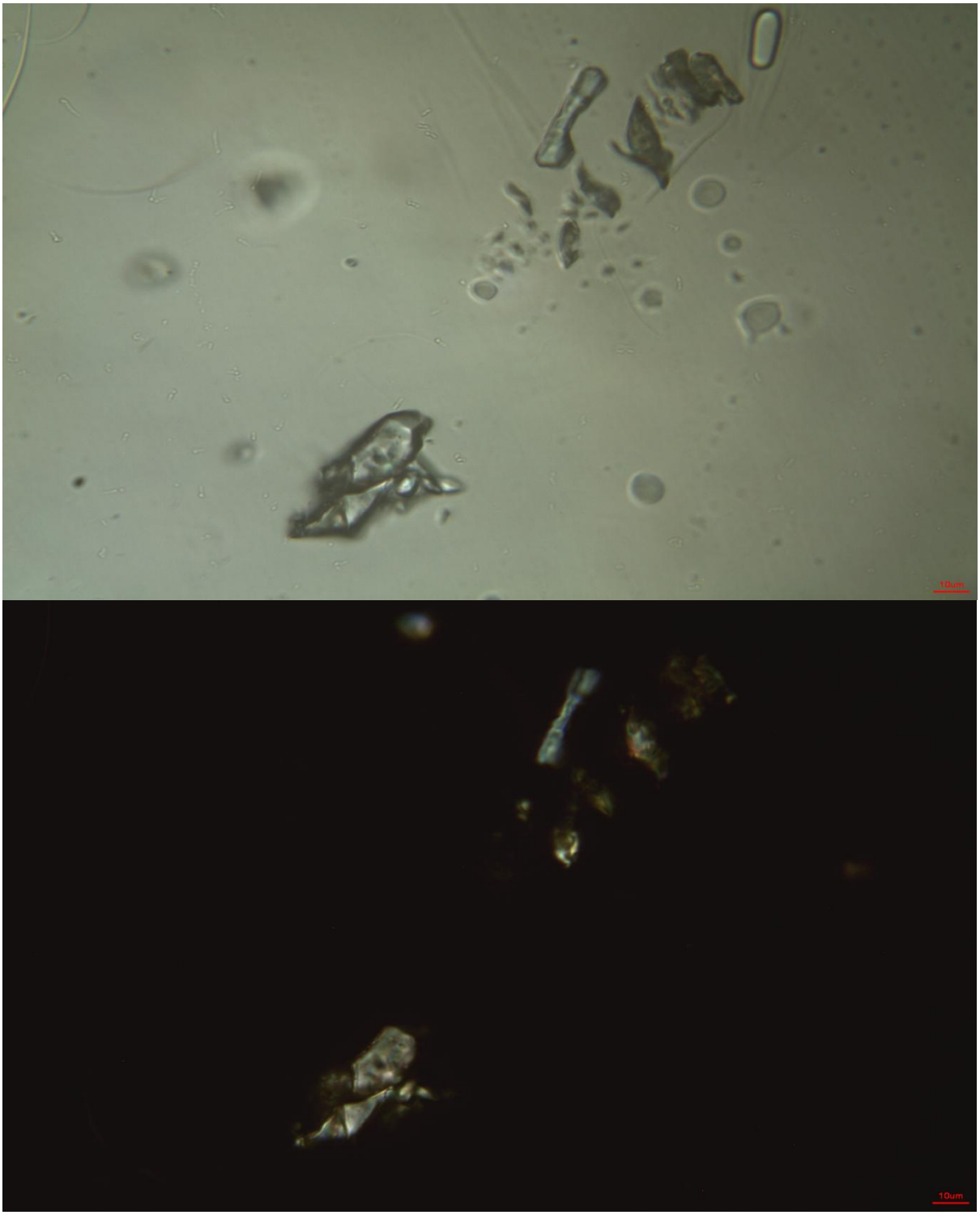

Figure 18: Microscopic contemplation of “Li Ke Ji” with polarization filters parallel (upper picture) and crossed (lower picture) (400fold magnification). Crystalline structures in this formulation are located at the outer (aqueous) phase of the cream. The red bar on the right sight at the bottom of the contemplation displays a length of 10 µm.

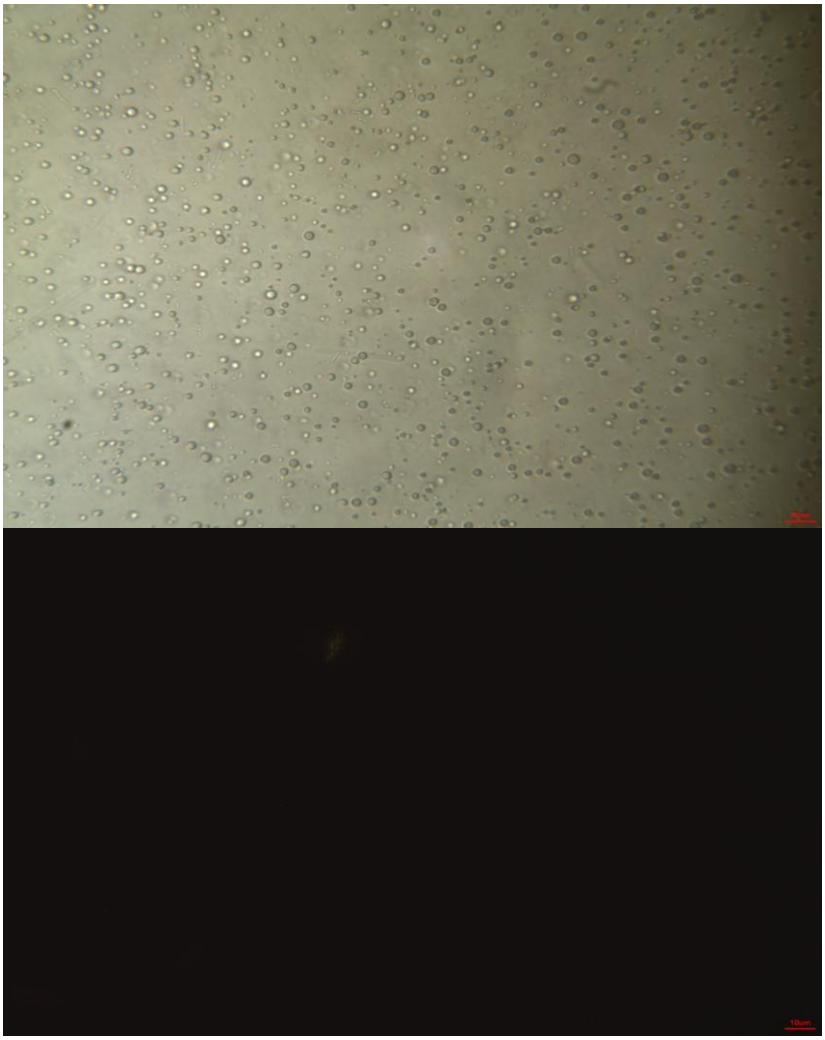

Figure 19: Microscopic contemplation of “Med Shine Li Di” with polarization filters parallel (upper picture) and crossed (lower picture) (400fold magnification). Alike Aldara® 5% creme this cream formulation contains the API in a completely dissolved state. The red bar on the right sight at the bottom of the contemplation displays a length of 10 µm.

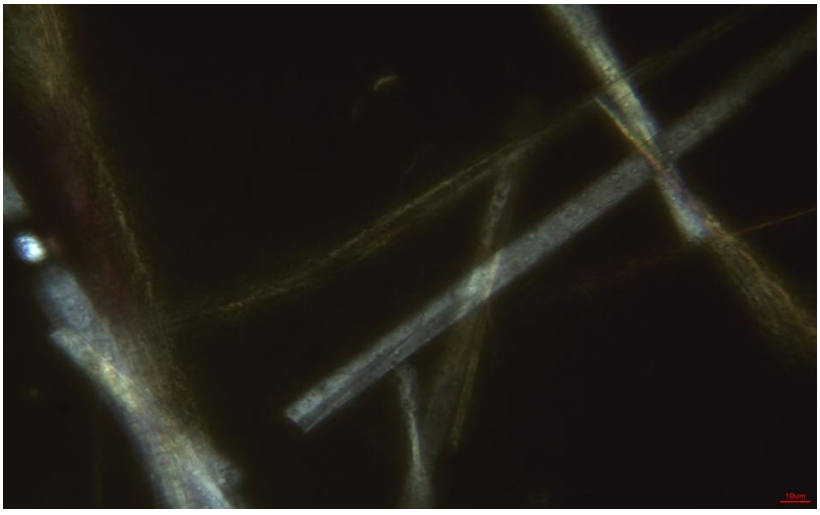

Figure 19a: Microscopic contemplation with polarization filters crossed of anisotropic fibrous structures occurring in “Med Shine Li Di”. The red bar on the right sight at the bottom of the contemplation displays a length of 10 µm.

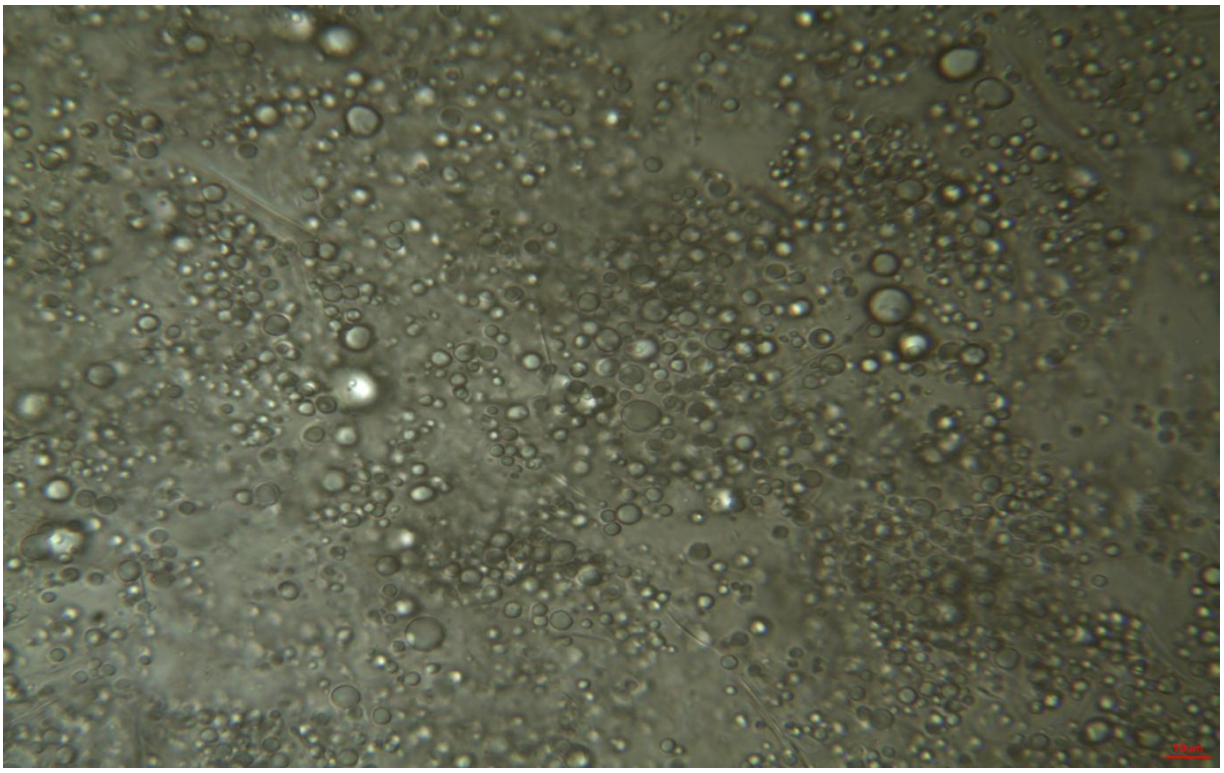

Figure 20: Microscopic contemplation of “Nan Bo” with polarization filters parallel (upper picture) and crossed (lower picture) (400fold magnification). Exactly as in the specimen of Aldara® 5% creme but also “Med Shine Li Di” no crystalline structures were detectable when polarization filters are crossed. The red bar on the right sight at the bottom of the contemplation displays a length of 10 µm.

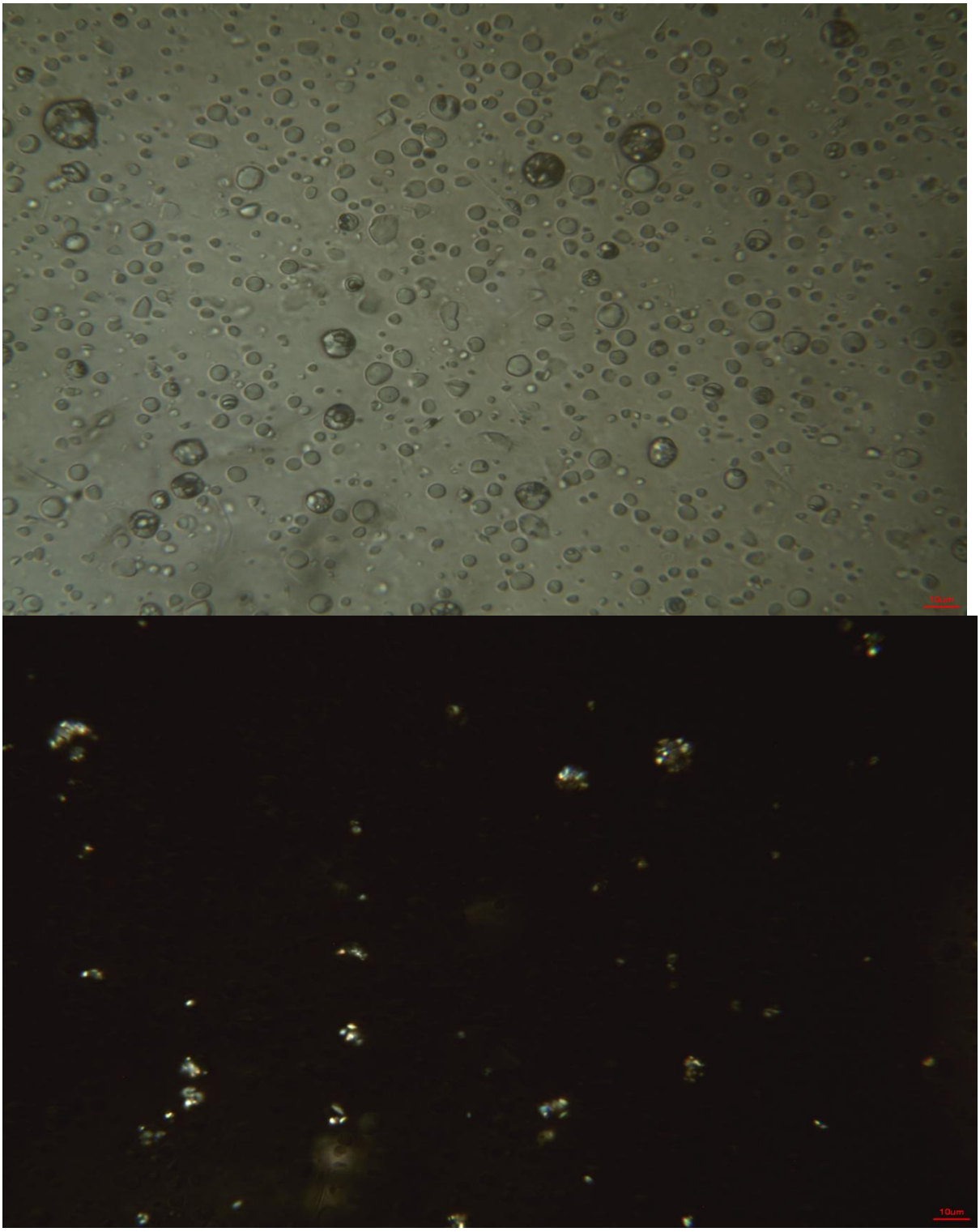

Figure 21: Microscopic contemplation of “You Bi Qing” with polarization filters parallel (upper picture) and crossed (lower picture) (400fold magnification). The specimen of “You Bi Qing” shows the presence of crystals embedded in the inner (oil) phase of the cream. API particles are distinctly smaller in comparison with “Li Ke Ji”. The red bar on the right sight at the bottom of the contemplation displays a length of 10 µm.

5.1.3. Franz Diffusion cell results comparing artificial membranes and murine skin

Investigations in the field of imiquimod release in a synthetic membrane related Franz diffusion cell setup but also permeation across ablated murine skin showed noticeable differences between products as it is obvious by figures 22a-c.

In terms of release rate, dissolved state formulations Aldara® 5% creme and “Nan Bo” gained highest values. Furthermore, curve progressions were similar, particularly when methanol/ phthalate buffer pH 3.6 blend served as acceptor medium (figure 22a). Since f1 values ≤ 15 and f2 values ≥ 50 are considered equivalent, calculated values of 5.25 and 59.58 verified this equivalence.

“You Bi Qing” with oil incorporated crystalline API demonstrated the lowest imiquimod release independent of experimental *in vitro* setup (figure 22a-c). On the other hand, the occurrence of crystalline imiquimod embedded in a cream formulation did not necessarily imply magnitudes of lower API release rates from the product. This was reflected by crystal based “Li Ke Ji” that performed alike the crystal free “Med Shine Li Di” when methanol/ phthalate buffer pH 3.6 blend served as acceptor medium.

In contrast to the methanol/ phthalate buffer solution, curve progressions of hydrochloric acid based acceptor solution were steepened. Moreover, lacking API release in case of “You Bi Qing” was more perceptible when compared with the methanol comprising acceptor solution (figure 22b).

Unlike membrane related Franz diffusion cell setup, imiquimod permeation across ablated murine skin (figure 22c) was considerably enhanced in case of dissolved state creams Aldara® 5% creme, “Nan Bo” and “Med Shine Li Di”. As it becomes apparent by “Li Ke Ji” but also “You Bi Qing”, suspended state imiquimod containing creams generally demonstrated permeation values significantly below dissolved state creams.

Permeation values on the basis of murine skin, calculated as f1 but also f2 values, attested none of the investigated formulations to gain equal or increased results in comparison to Aldara® 5% creme. Unlike synthetic membrane related Franz diffusion cell results, imiquimod permeation curves of dissolved state formulations “Nan Bo” and “Med Shine Li Di” showed similarity (f1 = 10.73) among each other.

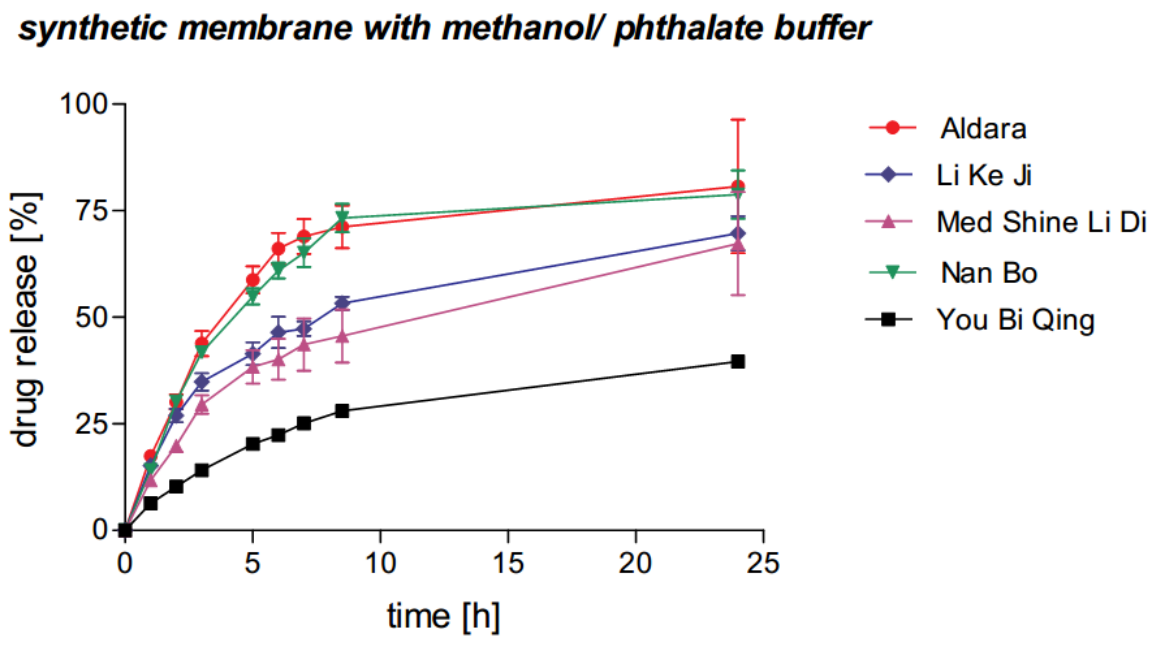

Figure 22a: Imiquimod release from commercially available creams during a 24 hours measurement in a Franz diffusion cell model (n=4). The acceptor phase consisted of a blend of phthalate buffer pH 3.6 and methanol in a 3/7 (V/V) ratio. Error bars described as standard deviation.

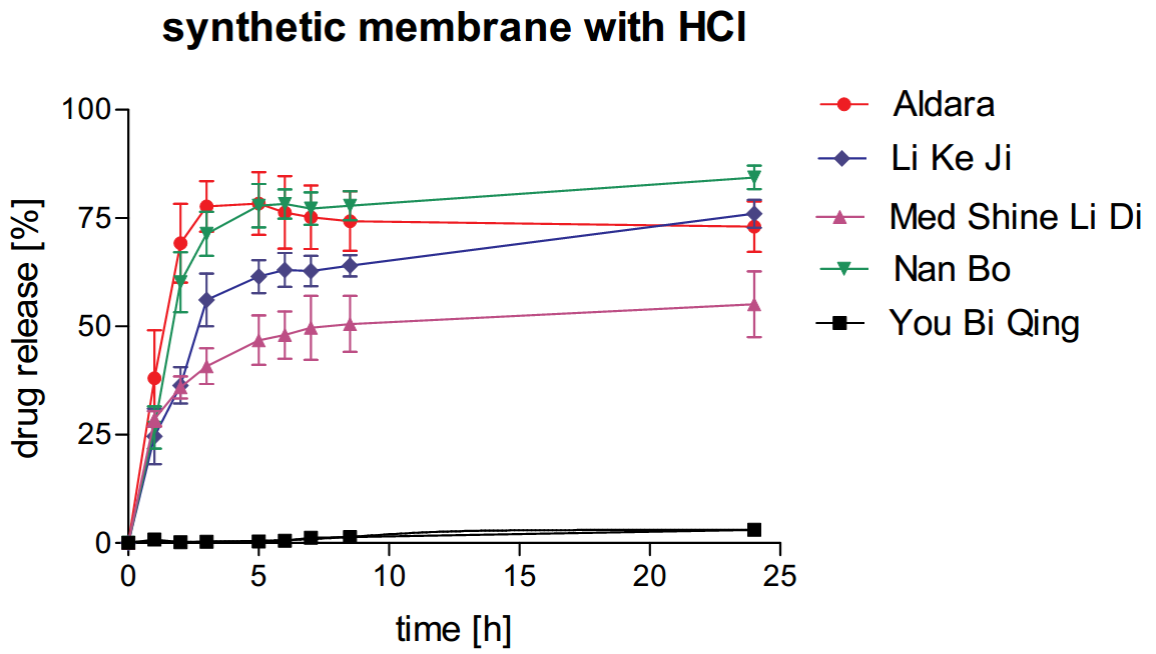

Figure 22b: Imiquimod release from commercially available creams during a 24 hours measurement in a Franz diffusion cell model (n=4). The acceptor phase consisted of a 0.1M HCl solution following commonly used practices [123] Error bars described as standard deviation.

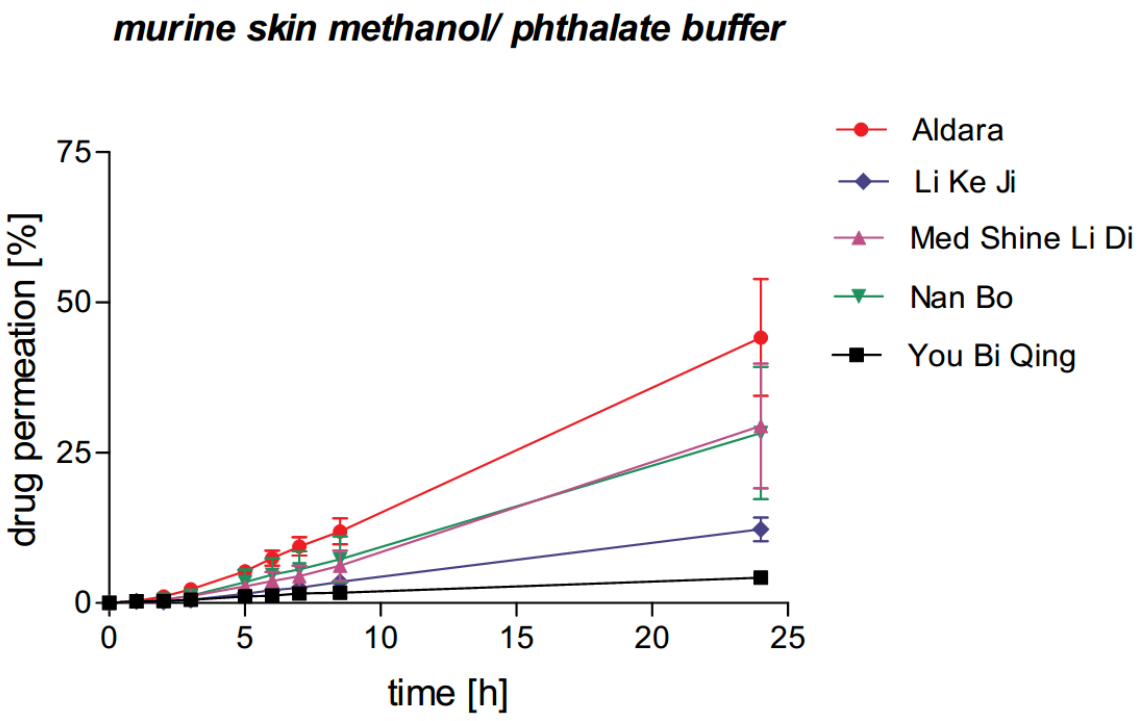

Figure 22c: Imiquimod permeation across shaved and ablated murine skin of commercially available creams during a 24 hours measurement in a Franz diffusion cell model (n=4). Equivalent to the situation described by figure 22a, the acceptor phase consisted of a blend of phthalate buffer pH 3.6 and methanol in a 3/7 (V/V) ratio. Error bars described as standard deviation.

5.1.4. Cytotoxic T-cell activity, tetramer staining, IFNγ, and ear swelling test

To directly address the extent as to which imiquimod containing formulations described here affect specific immune responses *in vivo,* a murine model based on C57BL/6 mice was intended to provide further information. 100 µg SIINFEKL, dissolved in DMSO, were incorporated in 50 mg of each formulation. This homogeneous cream was then applied onto the shaved backs of mice, in order to induce a peptide specific immune response [117, 128]. Specific $CD8^+$ T-cell quantification revealed that each formulation induced a significant population of peptide-specific T-cells compared to the untreated control group (figure 23a). Aldara® 5% creme showed slightly but not significantly increased numbers of specific $CD8^+$ T-cells compared with the miscellaneous formulations for imiquimod treated group. To further investigate their capacity to induce immune responses, the intracellular production of IFNγ was determined. As already outlined by tetramer staining, each formulation used for TCI triggered the IFNγ production after re-stimulation of blood cells in a significant manner when compared to the untreated control group. Indeed,

on an overall basis “You Bi Qing”, “Nan Bo”, and “Li Ke Ji” showed comparable levels of $IFN\gamma^+CD8^+$ T-cells. In contrast hereto, a slightly increased population was detected after treatment with “Med Shine Li Di”. To this end, Aldara® 5% creme based TCI induced significantly enhanced amounts of IFNγ-producing cells compared with the other products (figure 23b). In line with these results were those obtained from *in vivo* cytotoxicity assay (figure 23c). Compared to the unimmunized control where no specific lysis could be detected, all other groups showed cytolytic activity with the strongest results for “Med Shine Li Di” and Aldara® 5% creme depicted in the highest ratio of killing peptide-loaded target cells.

Analyzing the antigen-unspecific inflammatory effects, imiquimod containing creams were applied on the ears of mice. Since imiquimod induced immune response effects skin irritation including augment of murine ear tissue thickness, detection of ear swelling acts as an indicator in order to draw conclusions in terms of respective cream efficiency [136]. As depicted in figure 24 “Med Shine Li Di” induced the strongest ear swelling followed by Aldara® 5% creme. In case of “Li Ke Ji” and “You Bi Qing” lower ear swelling responses with larger standard deviations were observed. The preparation “Nan Bo” did not induce a response, comparable to the vehicle-treated group. “Nan Bo” generally did not behave according to expectations, since it contains the active in a dissolved state and thus higher pharmacodynamic responses were expected. Nevertheless it is also obvious that the viscosity of the “Nan Bo” formulation is highest, which should lead to a reduced diffusivity of the active dissolved therein.

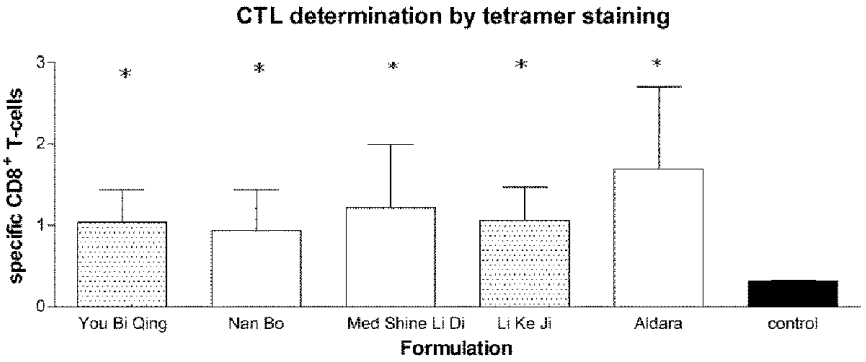

Figure 23a: Induction of specific immune response after treatment with different imiquimod-containing formulations. C57BL/6 mice were immunized with different imiquimod-containing formulations (50 mg, on 2 days) together with $OVA_{257-264}$ (100 µg) as indicated. Seven days after immunization the amount of peptide-specific $CD8^+$ T cells ($n = 11$) was assessed. A non-medicated ointment containing the antigen SIINFEKL was used as control group.

*Significantly higher immunostimulating effect in comparison with the untreated control group ($p < 0.05$ by Mann–Whitney test).

Dotted area bars represent API crystal containing formulations. Error bars described as standard deviation.

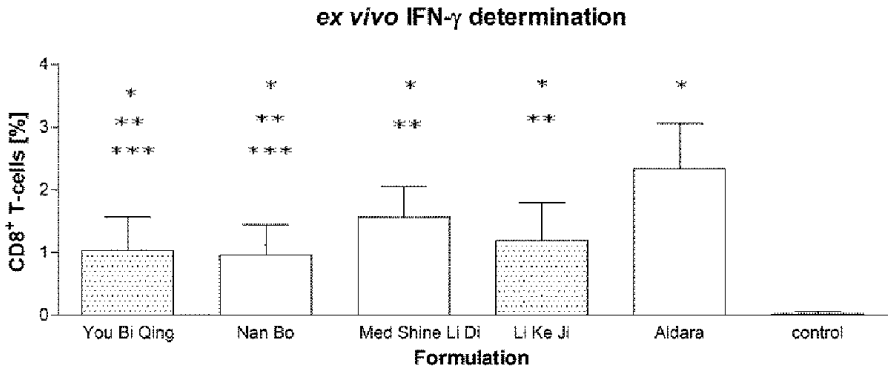

Figure 23b: Induction of specific immune response after treatment with different imiquimod-containing formulations. C57BL/6 mice were immunized with different imiquimod-containing formulations (50 mg, on 2 days) together with $OVA_{257-264}$ (100 µg) as indicated. Seven days after immunization the percentage of IFNγ-producing $CD8^+$ T cells after *ex vivo* restimulation ($n = 9$) was assessed. A non-medicated ointment containing the antigen SIINFEKL was used as control group.

*Significantly higher immunostimulating effect in comparison with the untreated control group ($p < 0.05$ by Mann–Whitney test).

**Significantly higher immunostimulating effect of Aldara® 5% creme when compared with respective formulation ($p < 0.05$ by Mann–Whitney test).

***Significantly higher immunostimulating effect of 'Med Shine Li Di' when compared with respective formulation ($p < 0.05$ by Mann–Whitney test).

Dotted area bars represent API crystal containing formulations. Error bars described as standard deviation.

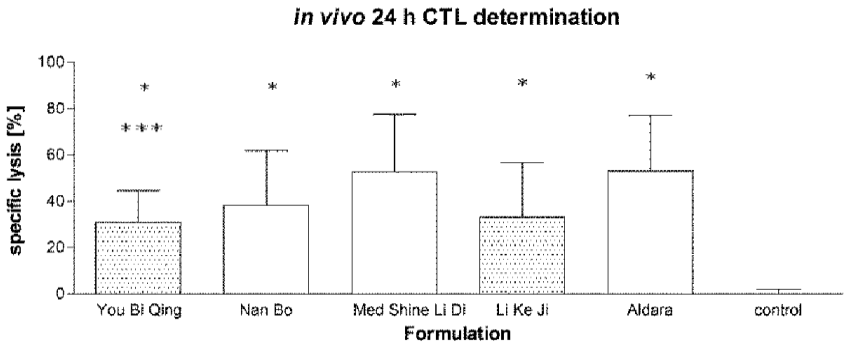

Figure 23c: Induction of specific immune response after treatment with different imiquimod-containing formulations. C57BL/6 mice were immunized with different imiquimod-containing formulations (50 mg, on 2 days) together with $OVA_{257-264}$ (100 µg) as indicated. Seven days after immunization the *in vivo* cytolytic activity after transfer of target cells was assessed ($n = 11$). A non-medicated ointment containing the antigen SIINFEKL was used as control group.

*Significantly higher immunostimulating effect in comparison with the untreated control group ($p < 0.05$ by Mann–Whitney test).

***Significantly higher immunostimulating effect of 'Med Shine Li Di' when compared with respective formulation ($p < 0.05$ by Mann–Whitney test).

Dotted area bars represent API crystal containing formulations. Error bars described as standard deviation.

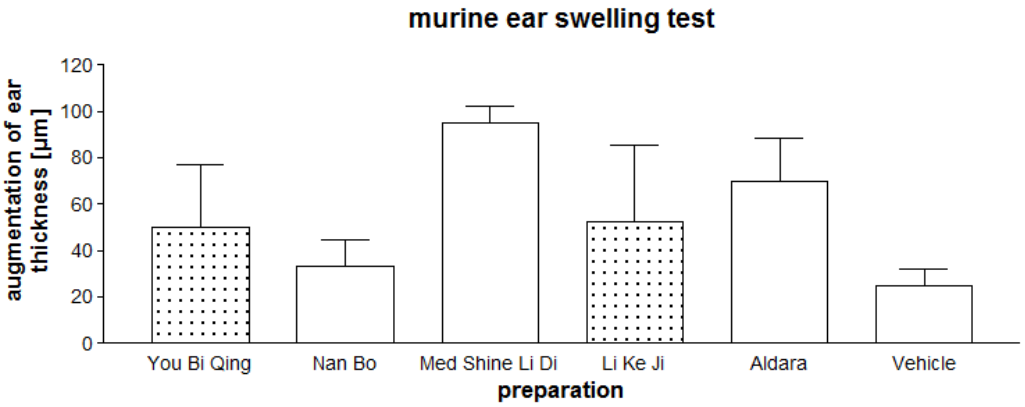

Figure 24: Imiquimod containing formulations mediate unspecific inflammatory responses. Imiquimod-containing formulations (50 mg, on 2 days) were applied to the ears of C57BL/6 mice. The ear swelling response was assessed by determination of ear thickness before and 1 day after treatments (n=2). Dotted area bars represent API crystal containing formulations. Error bars described as standard deviation. A non-medicated ointment (vehicle) containing the antigen SIINFEKL was used as control group.

Despite considerable variability concerning immune responses, it became apparent that the products containing crystalline API generally showed the lowest immunization activities at equal doses which corresponds well with the results from

the *in vitro* permeation tests across ablated murine skin samples. Nevertheless, it is also obvious that the differences between the products observed *in vivo* are much less than suggested by any of the *in vitro* tests.

5.1.5. Correlation plot of *in vitro* and *in vivo* parameters

Attempts of correlating *in vitro* with *in vivo* data showed mixed results.

In general, a membrane related Franz diffusion cell setup pointed out different release results between the versatile formulations. However, poor correlations regarding artificial membrane-controlled drug release and *in vivo* effects were detectable under all investigated conditions (figure 25 a, c, and e). Resulting r^2 values of the synthetic membrane based setup ranged from 0.157 – 0.313. A slope significantly deviating from zero only occurred in case of IFNγ. However, no significant correlation was detected for any synthetic membrane based Franz diffusion cell setup (table 5). With regard to the pharmaceutical characteristic of each formulation this method in general seemed unsuitable to draw conclusion on both, the pharmaceutical characteristic of respective formulation but also the resulting *in vivo* performance. Differences concerning the acceptor medium did not noticeably impact on the ranking of release rates, however it is obvious that particularly in case of “You Bi Qing” a drug release from the cream sample without using an organic cosolvent in the reservoir solution completely failed.

On the other hand, drug permeation rates across ablated murine skin yielded slopes significantly deviating from zero when plotted against the magnitudes of the *in vivo* responses. Resulting r^2 values ranged from 0.535 – 0.777 (table 5). With respect to the according *in vivo* results only the use of a murine skin setup (figure 25b, d, and f) demonstrated its capacity to draw conclusions on the resulting performance in a laboratory scale. Looking at the different parameters measured *in vivo* a significant correlation rate was achieved by measuring the cytotoxic T-cell activity against i.v. applied labeled target spleen cells (figure 25d). Hence, this *in vivo* model was preferred for further in vivo measurements.

Table 5: Permeation across either synthetic membranes or ablated murine skin versus *in vivo* detected parameters based on five versatile semi-solid formulations. The table describes whether the resulting slope is significantly deviating from zero, a correlation between in vitro and in vivo occurs, and the resulting r^2 value.

	Skin permeation vs. IFNγ	**Skin permeation vs. lysis of SIINEKL labeled spleen cells**	**Skin permeation vs. $CD8^+$ T-cells, detected by tetramer staining**	**Membrane permeation vs. IFNγ**	**Membrane permeation vs. lysis of SIINEKL labeled spleen cells**	**Membrane permeation vs. $CD8^+$ T-cells, detected by tetramer staining**
Slope significantly non zero	x	x	x	x	-	-
Significant correlation	-	x	-	-	-	-
r^2	0.606	0.777	0.535	0.212	0.313	0.157

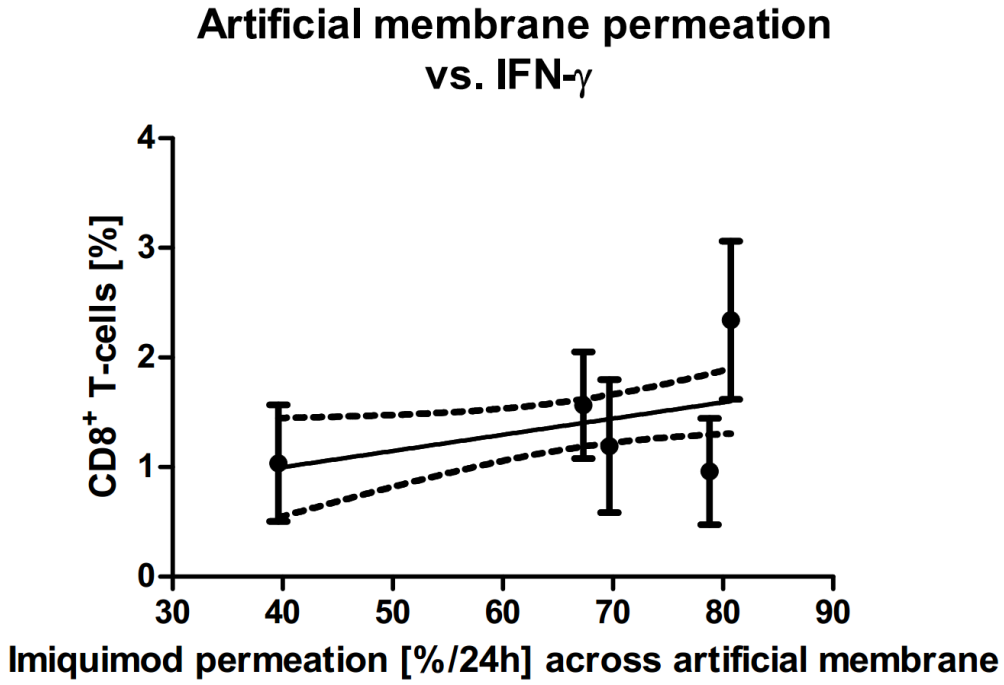

Figure 25a: *In vitro/ in vivo* correlation based on five versatile semi-solid formulations. Average percent values of imiquimod permeation across a synthetic membrane (10kDa MW cutoff) are plotted versus percentage of IFNγ-producing $CD8^+$ T-cells after *ex vivo* re-stimulation ($n = 9$). Imiquimod permeation is defined as percentage of the administered active substance detected within the acceptor chamber after 24h in a Franz diffusion cell model (n=4; error bars described as standard deviation).

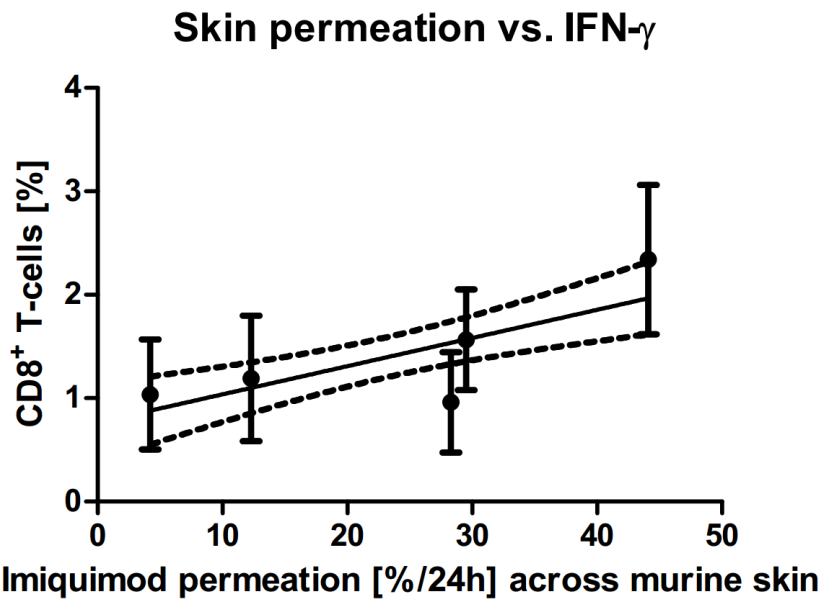

Figure 25b: *In vitro/ in vivo* correlation based on five versatile semi-solid formulations. Average percent values of imiquimod permeation across ablated murine skin are plotted versus percentage of IFNγ-producing $CD8^+$ T-cells after *ex vivo* re-stimulation ($n = 9$). Imiquimod permeation is defined as percentage of the administered active substance detected within the acceptor chamber after 24h in a Franz diffusion cell model (n=4; error bars described as standard deviation).

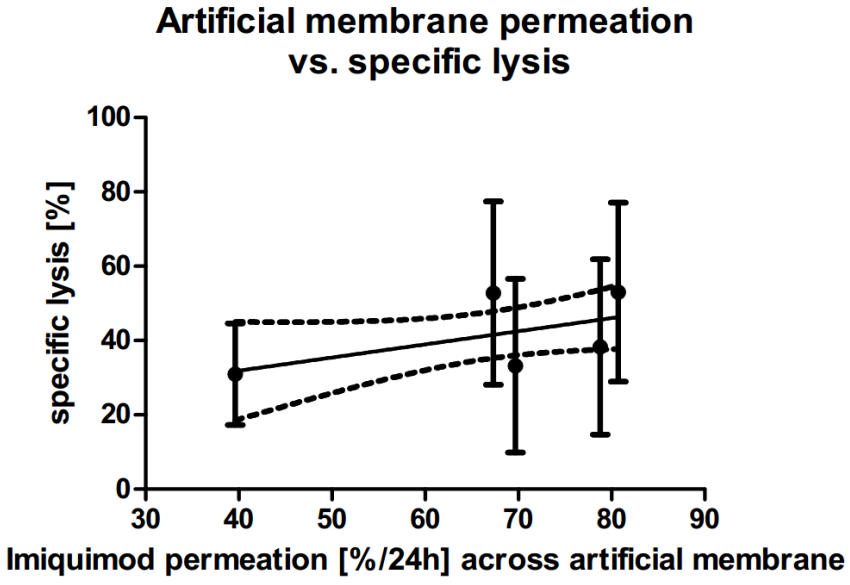

Figure 25c: *In vitro/ in vivo* correlation based on five versatile semi-solid formulations. Average percent values of imiquimod permeation across a synthetic membrane (10kDa MW cutoff) are plotted versus *in vivo* generated $CD8^+$ T-cell activity against i.v. administered SIINFEKL labeled spleen cells (n=11). Imiquimod permeation is defined as percentage of the administered active substance detected within the acceptor chamber after 24h in a Franz diffusion cell model (n=4; error bars described as standard deviation).

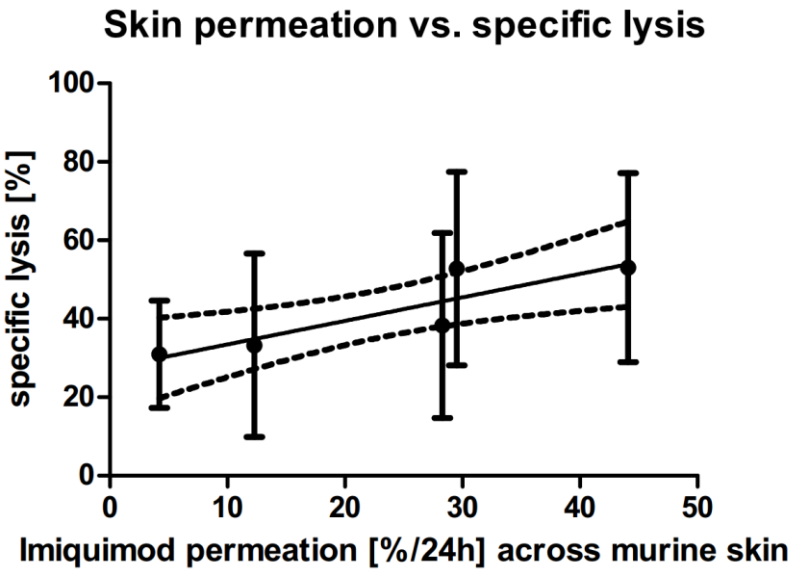

Figure 25d: *In vitro/ in vivo* correlation based on five versatile semi-solid formulations. Average percent values of imiquimod permeation across ablated murine skin are plotted versus *in vivo* generated $CD8^+$ T-cell activity against i.v. administered SIINFEKL labeled spleen cells (n=11). Imiquimod permeation is defined as percentage of the administered active substance detected within the acceptor chamber after 24h in a Franz diffusion cell model (n=4; error bars described as standard deviation).

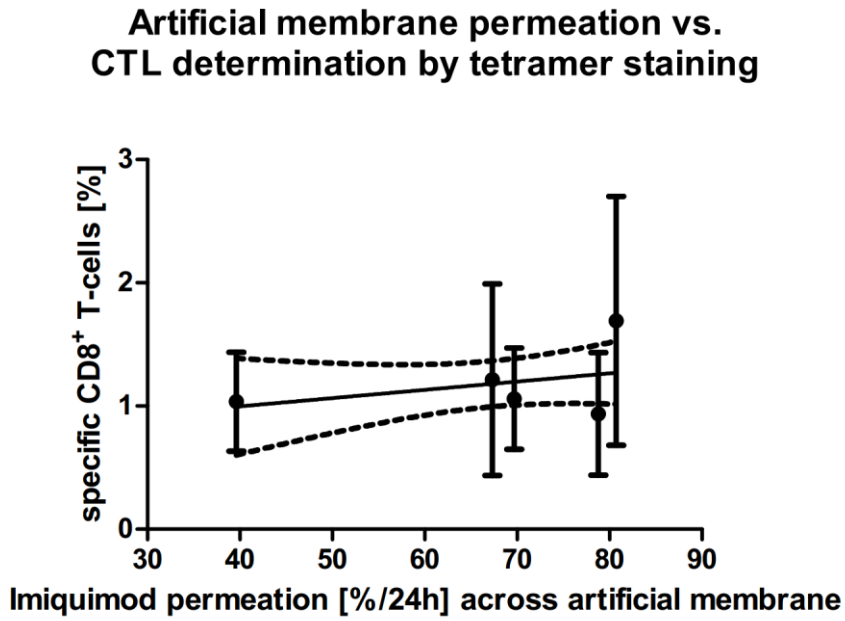

Figure 25e: *In vitro/ in vivo* correlation based on five versatile semi-solid formulations. Average percent values of imiquimod permeation across a synthetic membrane (10kDa MW cutoff) are plotted versus percentage of specific $CD8^+$ T-cells detected by tetramer staining (n=11). Imiquimod permeation is defined as percentage of the administered active substance detected within the acceptor chamber after 24h in a Franz diffusion cell model (n=4; error bars described as standard deviation).

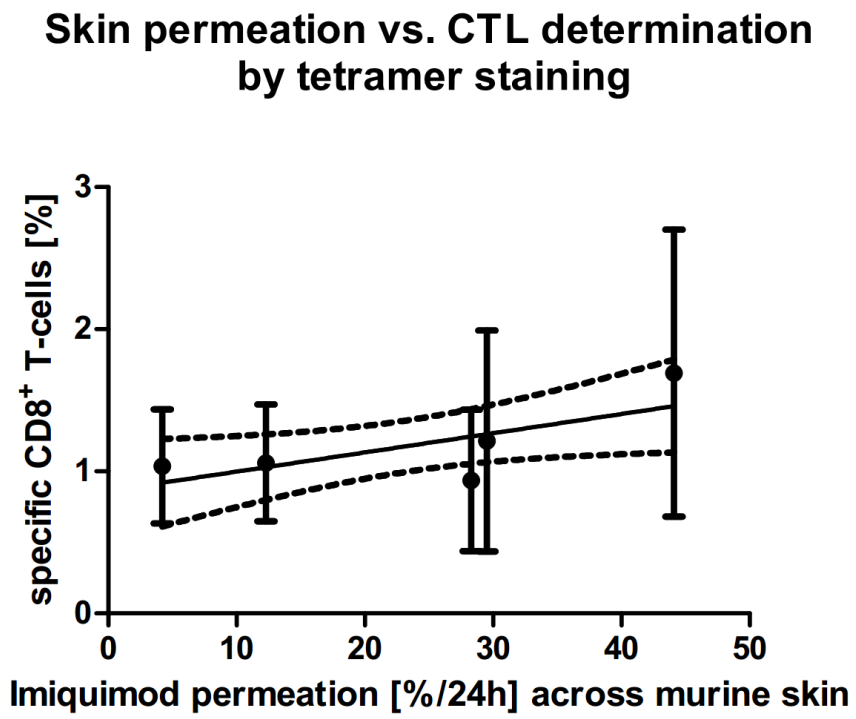

Figure 25f: *In vitro/ in vivo* correlation based on five versatile semi-solid formulations. Average percent values of imiquimod permeation across ablated murine skin are plotted plotted versus percentage of specific $CD8^+$ T-cells detected by tetramer staining (n=11). Imiquimod permeation is defined as percentage of the administered active substance detected within the acceptor chamber after 24h in a Franz diffusion cell model (n=4; error bars described as standard deviation).

5.2. Anhydrous formulation concept based on sucrose fatty esters and freeze drying

Since investigations of multisource products, described in the section above, emphasized a noticeable influence of pharmaceutical characteristics towards *in vivo* generated immune stimulation, the following section describes a novel formulation concept. Despite the fact that commercially available imiquimod formulations with the active in a dissolved state perform better [137], this section primarily deals with a concept based on nano- to submicron imiquimod particles. Moreover, physicochemical properties of imiquimod such as poor solubility are predestinated for a particle based formulation concept. Hence, this section aims at developing a stable freeze dried formulation by concomitantly focusing on effects of different pharmaceutical oils but also further excipients such as laurocapram as penetration

enhancer. In addition, the following section includes a dissolved state formulation in order to display differences between formulation concepts.

5.2.1. Stability issues of solid nano emulsions

Directly after the freeze drying process, all formulations appeared as white to off-white powder. Application on the skin effected an irreversible liquefaction due to the induced mechanical stress. Thus, the freeze dried powder termed as solid nanoemulsion (SN) facilitates a dermal application which is similar to a commonly used cream formulation.

There are several options for the formulation of a SN with respect to the oil component. The characteristics of oil components may be described as follows:

(1) Middle chain triglycerides (MCT), is a commonly used well tolerated lipophilic excipient for dermal administration. It comprises of C_8-C_{12} saturated fatty acids esterified with glycerol [16]. SN formulations based on MCT in general proved to be superior regarding their storage stability compared with unsaturated oil containing formulations. Neither a discoloration or rancid odor nor the leaking of oil was observed.

(2) Avocado oil, harvested from Avocado fruits (Persea Americana MILL.), is a widespread oil used particularly for cosmetic purposes. Due to a natural content of 0.007 – 0.02% tocopherol it is described as insensitive against oxidation processes [138]. This oil approximately has a content of 85% triglycerides including saturated but also unsaturated fatty acids. Oleic acid, linoleic acid, and palmitic acid represent the majority of C_{18} fatty acids [139]. SN formulation based on Avocado oil demonstrated a slightly lacking stability since discoloration occurred after a one week period and an additional week, a rancid odor occurred.

(3) Jojoba wax, often simply thought of inaccurately as jojoba oil, contains esters of 11-eicosenic acid including their C_{18}- and C_{22} homologues with the monovalent alcohol 11-eicosenol [138]. Jojoba wax is well suitable for a broad variety of cosmetic and pharmaceutical purposes as it offers non toxicity to human skin [140] but also

good skin tolerability. Likewise MCT, no odor or discoloration occurred in case of jojoba wax containing SN formulations.

(4) Squalen as an unsaturated triterpene compound is produced in all higher organisms. This widely disseminated oil comprises noticeable amounts of olive oil, wheat-germ oil, amaranth oil, and rice bran oil [141]. On the basis of six double bounds per molecule, squalen easily undergoes oxidative degradation processes. In order to avoid oxidative processes, alpha tocopherol may be added as an antioxidant [142]. Squalen containing SN formulations distinctly demonstrated poor stability and obvious decomposition. In order to avoid oxidative processes further squalen based formulations contained a blend of 60% squalen and 40% tocopherol.

(5) Oleic acid is a monounsaturated fatty acid commonly occurring in various animal and vegetable fats and oils. Besides its use as suspension stabilizer and lubricant for valves in metered dose inhalers, it acts as a penetration enhancing excipient for dermal formulations [16]. On the basis that oleic acid offers a proven capability to dissolve imiquimod [123] in a sufficient amount to generate a completely dissolved state formulation, an oleic acid based formulation was designed on a dissolved state formulation in accordance to the innovators product Aldara® 5% creme. Obviously, directly after manufacturing, poor stability became apparent thus oleic acid based dissolved imiquimod formulations represented a serious challenge. In order to create a manageable formulation, other than the oil based formulations described by table 3a, the ratio of sucrose ester / oleic acid was set to 1 / 1 instead of 1 / 3.5 (table 3c).

5.2.2. Electron micrographs of imiquimod particles

Electron micrographs were recorded in order to examine whether imiquimod is available in crystalline form but also to determine particle sizes. Electron micrographic analysis proved the presence of crystalline active shown as an example in figure 26. Detection of particle sizes (table 6) resulted in slight variations between the different oil containing SNs.

Table 6: Average particle sizes in nanometers of electron microscopically detected imiquimod crystals. Particle sizes were measured according to Martin' diameter with 100 particles for each specimen, standard deviation was then calculated. Single values of particle size detection see section "Appendix" table 8.

Formulation	Average particle size [nm]	Standard deviation [nm]
SN 1	525	225
SN 2	568	306
SN 3	617	275
SN 4	663	231

Particle size distribution of SN 2, 3 and 4 but not SN 1 pointed out a Gaussian particle size distribution. A list of particle sizes of SN 1 – SN 4 is attached at the appendix section.

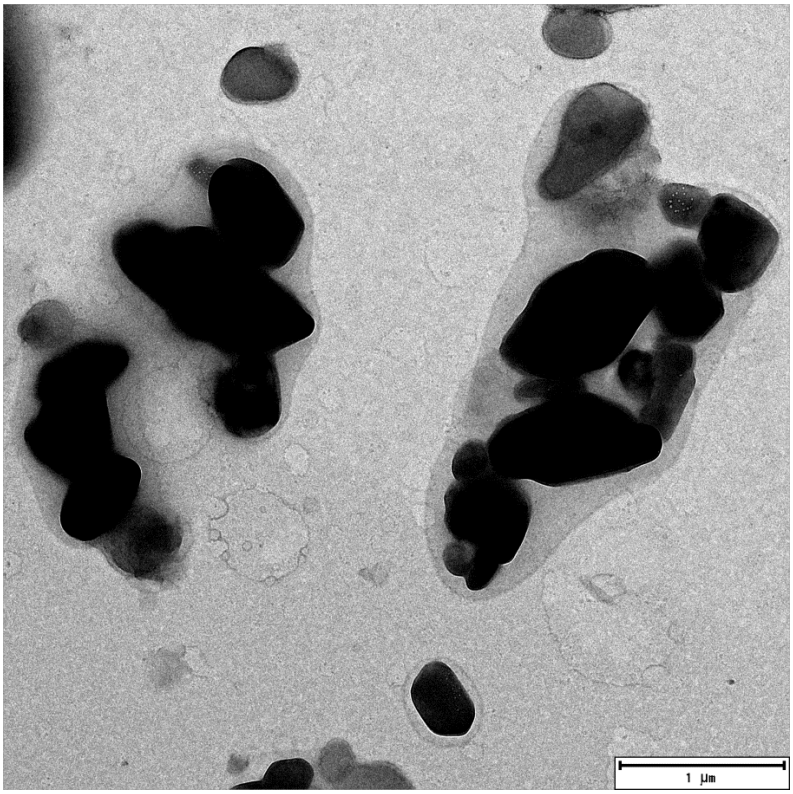

Figure 26: Transmission electron microscopic image of SN 1 shows imiquimod crystals embedded within the oil phase (middle chain triglycerides) of the specimen presented as an example for nano- to submicron particle occurrence.

5.2.3. *In vitro* imiquimod permeation across ablated murine skin

Permeation plots of imiquimod formulations across murine skin showed the highest level of imiquimod permeation across skin samples in case of the innovators product Aldara® 5% creme. Curve progressions of avocado oil and MCT based SNs did not differ between each other to a noticeable extent (figure 27). Unlike MCT and avocado oil, jojoba wax showed a highly detrimental effect on imiquimod permeation as it became apparent by SN 3. An approximately tenfold decreased imiquimod concentration in the acceptor medium after a measurement course of 24h was observed in case of jojoba wax containing SN 3 in comparison with Aldara® 5% creme. Based on the fact that a murine skin related setup in a Franz diffusion cell model demonstrated its capability to discriminate between particle-based and dissolved state formulations, the lacking permeation of SN 3 was thus attributed to the jojoba wax component in the formulation.

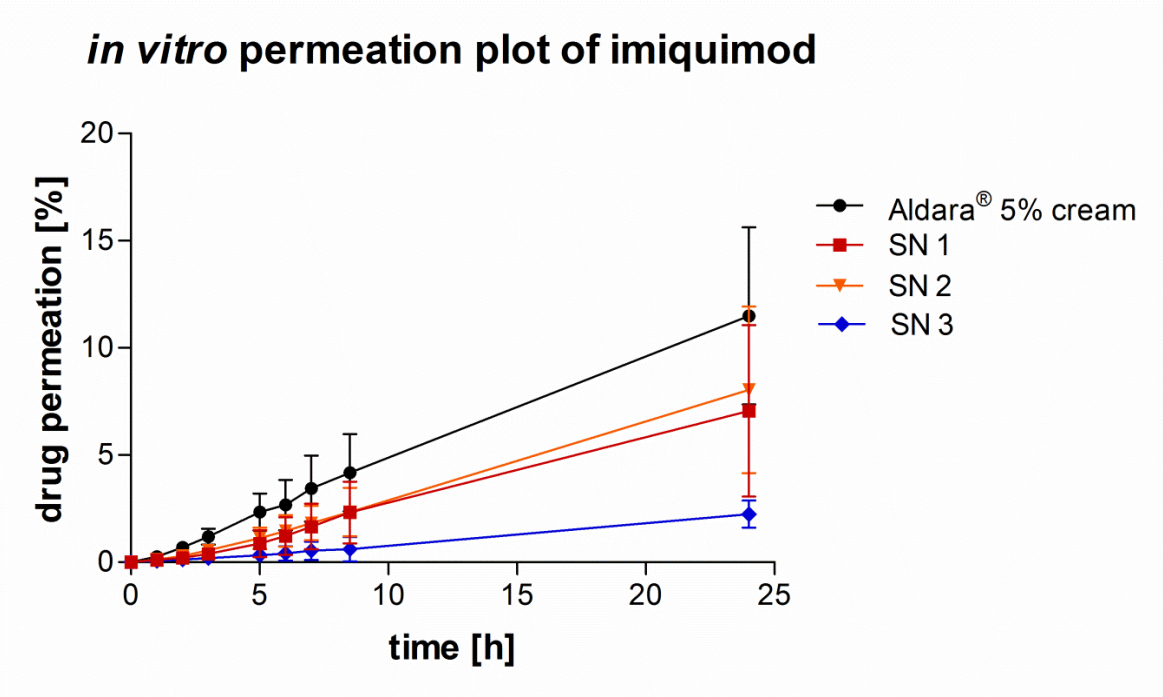

Figure 27: *In vitro* imiquimod permeation from solid nanoemulsions in comparison with the innovators product Aldara® 5% creme. A modified Franz diffusion cell model was used with a shaved and ablated murine skin setup (n=6). A blend of a 20mM acetate buffer pH 3.6/ ethanol in a ratio of 7/3 (V/V) served as acceptor medium. Error bars described as standard deviation.

5.2.4. Impact of laurocapram and pharmaceutical oil components on *in vitro* imiquimod permeation

Obviously, oil components demonstrate a strong impact on imiquimod permeation as it is can be seen in figure 27. Since an increased permeation, so far, correlates with an augment of *in vivo* performance, a penetration enhancer was added in order to increase and accelerate the rate of imiquimod permeation across skin samples. The use of laurocapram which is mixable, to varying extents, with commonly used pharmaceutical oils [39] showed that the anticipated increase of skin permeation did not occur as expected. As apparent from figure 28, laurocapram did not noticeably enhance imiquimod permeation across ablated murine skin. This is particularly evident in case of SN 1 and SN 5, both showing an identical curve progression, however the sole difference is the presence of laurocapram in case of SN 5. *In vitro* permeation across murine skin in case of SN 6, based on squalen/ tocopherol, is in line with the results of SN 1 and SN 5.

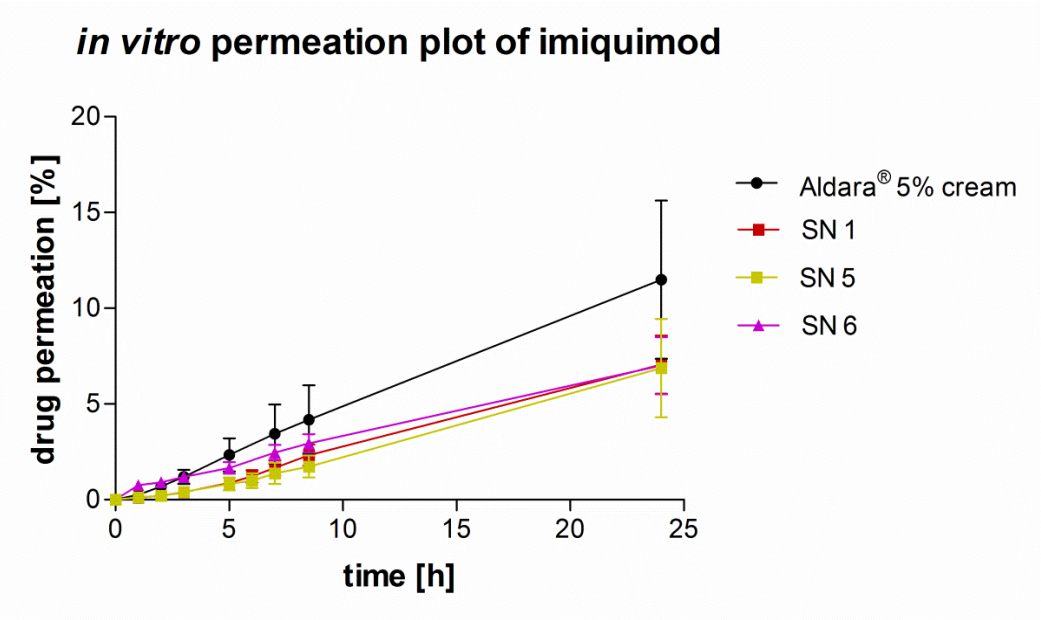

Figure 28: *In vitro* imiquimod permeation from solid nanoemulsions in comparison with the innovators product Aldara® 5% creme. SN 1 and SN 5 are distinguished by the presence of laurocapram in case of SN 5. SN 6 bases on squalen and tocopherol. Alike SN 5, it contains an additional amount of 5% laurocapram in order to evaluate whether laurocapram impacts on API permeation. A modified Franz diffusion cell model was used with a shaved and ablated murine skin setup (n=6, including SD). A blend of a 20mM acetate buffer pH 3.6/ ethanol in a ratio of 7/3 (V/V) served as acceptor medium. Error bars described as standard deviation.

5.2.5. Impact of laurocapram and pharmaceutical oil components on cytotoxic T-cell activity

As described in the section above, oil related influences were markedly detected in case of jojoba wax since this excipient noticeably decreased the permeation rate of imiquimod in case of SN 3. In order to examine whether *in vivo* results are in line with *in vitro* findings, excipient related influences SN 1 – SN 4 were evaluated in small groups of animals. Despite lacking stability, the tocopherol free squalen containing formulation SN 4 was included into this series of tests. To exclude the influence of the respective SN formulations on antigen penetration, in the context of this experimental section, SIINFEKL was applied intra dermally. Regarding spleen cell lysis, both, SN1 but also SN4 revealed the highest immune stimulating performance. Despite lacking skin permeation, jojoba wax containing SN 3 sufficient induced spleen cell lysis in C57BL/6 mice. Obviously, avocado oil demonstrated a noticeable reduction of *in vivo* performance in comparison with both, Aldara® 5% creme but also respective solid nanoemulsified formulations (figure 29).

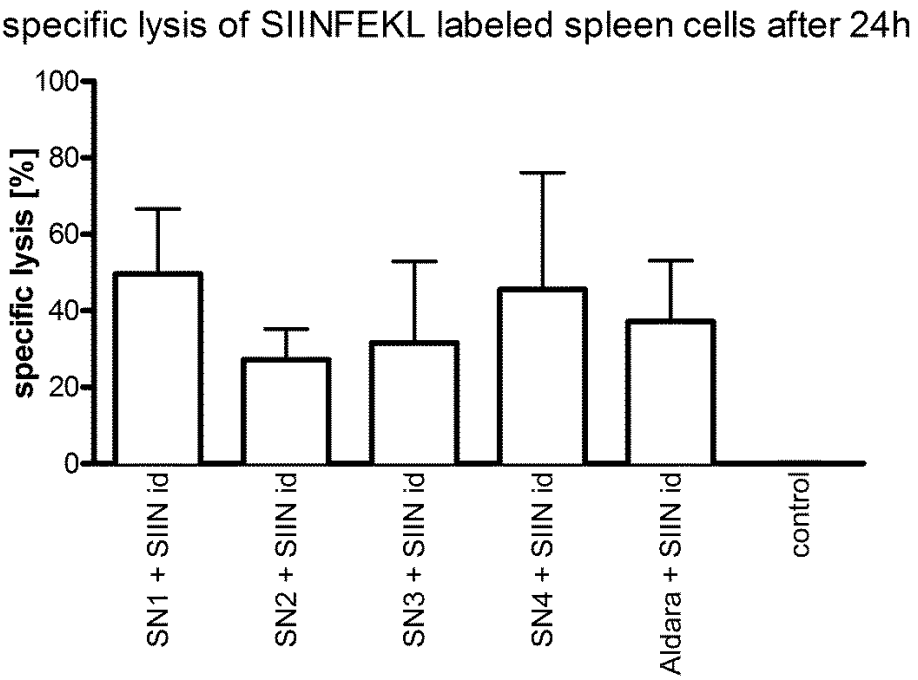

Figure 29: Cytotoxic T-cell induced spleen cell lysis in C57BL/6 mice 24h after TCI with different oil containing SN formulations. In order to generally assess whether an oil related difference occurs regarding imiquimod the antigen was administered intra dermally (n=4). Error bars described as standard deviation. No significance was observed by a two tailed Mann-Whitney test.

Results

Regarding *in vivo* test series SN 1 – SN 4, there was some evidence that particularly MCT and squalen were feasible to create an efficient approach towards CTL activation. Based on the above mentioned results, the question is as follows:

i) Is it possible to create an antigen containing formulation based on either MCT or squalen with a laurocapram content of 5%?

ii) Could an improved composition of SN4 lead to a stable and appropriate TCI formulation?

Addressing i)

Since SN 1 but also SN 4 induced slightly increased immune responses compared with avocado oil but also jojoba wax, MCT and squalen were used for further formulation improvements. The rationale of choosing MCT is based on its stability towards environmental influences. Squalen was chosen due to its additional TLR-7 independent immunostimulating effect [143].

Laurocapram as a possible penetration enhancer is miscible with versatile pharmaceutical oils. Moreover, it has a capacity of penetration enhancement in case of both, lipophilic but also hydrophilic actives. In addition, laurocapram did not dissolve imiquimod crystals as observed in previously performed experiments. Hence, it represents a promising enhancer for the SN formulation approach. Both formulations SN 5 and SN 6 contain the model antigen SIINFEKL as it has been added during the manufacturing process. Thus these two formulations represent a ready to use concept avoiding the additional treatment of SIINFEKL embedded in a vehicle system such as officinal cremor basalis prior to the application of the imiquimod containing formulation.

Results obtained by SN 5 and SN 6 emphasize a distinct influence of excipients on imiquimod based TCI efficiency. Moreover, this formulation concept proved to simultaneously allocate the model antigen SIINFEKL to the site of action.

Addressing ii)

As it is apparent in figure 29, SN 4 demonstrates a sufficient capacity to induce an immune reaction. However, stability of this formulation was poor. Consequently, tocopherol as a lipophilc antioxidant was added. The resulting composition based on squalen/ tocopherol (SN 6) resulted in a stable formulation. Moreover, SN 6 significantly ($p \leq 0.05$) augmented the cytotoxic T-cell answer in comparison with both, the innovators product Aldara® 5% creme but also MCT based SN 5. The latter one demonstrated a slightly diminished *in vivo* performance when compared with Aldara® 5% creme (figure 30).

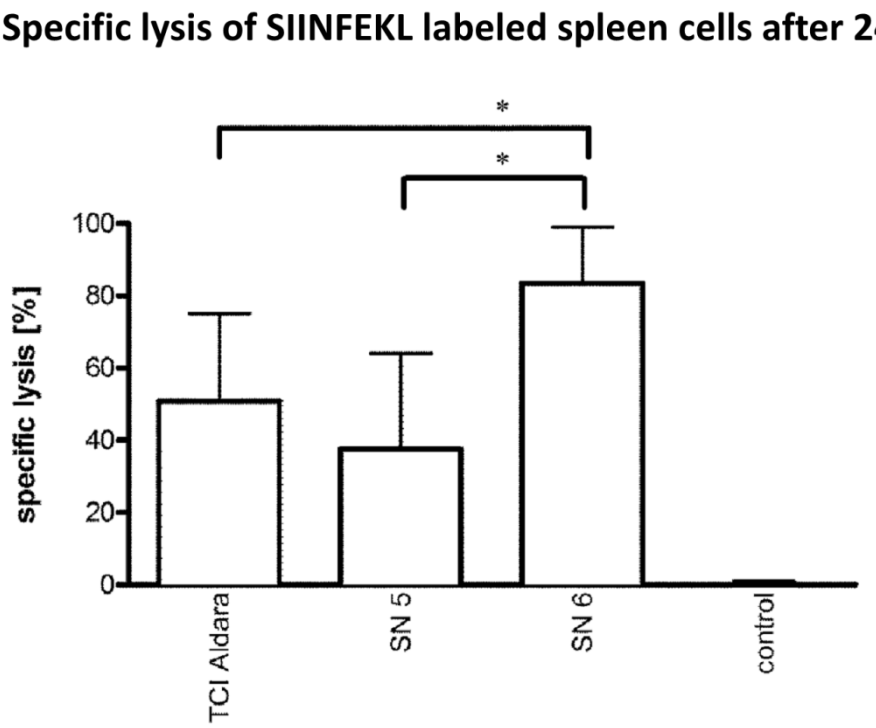

Figure 30: Comparison of MCT based SN 5 and squalen/ tocopherol based SN 6 with Aldara® 5% creme induced cytotoxic T-cell answer in C57BL/6 mice. Both laurocapram containing SNs have in common that the antigen SIINFEKL was added during the manufacturing step (n=19 in case of Aldara® 5% creme, n=10 in case of SN 5, n= 9 in case of SN 6) which was also the case for Aldara® 5% cream. Error bars described as standard deviation. Cremor basalis DAC as a non-medicated ointment containing the antigen SIINFEKL was used as untreated control group.

* describes a significant difference of SN 6 compared with either SN 5 or Aldara® 5% creme ($p<0.05$) in T-cell answer calculated by a two tailed Mann Whitney test. No significant difference could be observed between the innovators product and SN 5.

5.3. Aqueous imiquimod based emulsion gel

As observed in case of “You Bi Qing” and “Li Ke Ji” formulations, these imiquimod particle based products generally showed lower immunization potency compared to products which contain only dissolved drug. This could be due to the fact that particle sizes in these suspension type ointments were in a range of a few microns. The emulsion gel concept supplies imiquimod particles in a submicron scale range in order to sufficiently activate cytotoxic T-cells. The particles are suspended in an aqueous gel formulation. Moreover, with respect to an improved *in vivo* performance, an oil phase was integrated on the basis of jojoba wax leading to an aqueous emulsion gel. Since jojoba wax decelerated imiquimod permeation across murine skin, the train of thought is to prolong imiquimod persistence at the site of DC activation. With this in mind the following section describes an emulsion gel containing both, jojoba wax as a retarder but also laurocapram as enhancer to overcome the SC. This formulation was investigated in terms of *in vitro* permeation and rheology. As the emulsion gel contains particles of considerably lower size when compared with the SN approach, dynamic light scattering measures served as a valuable tool in order the assess whether crystal growth inhibitors such as PVP K30 and PVP K90 may positively impact on particle sizes of suspended state imiquimod.

5.3.1. Electron micrographs of imiquimod particles

Alike the SN formulation concept, electron microscopic photographs proved the presence of crystalline imiquimod (figure 31). Other than SN formulations, imiquimod particles were in a scale range of approximately 100nm up to 500nm. Average particle size detection based on DLS measurement technique was determined as 285nm. In contrast to imiquimod particles described within the SN section of this work, particles detected here were considerably smaller. Since both concepts are based on a top-down method in manufacturing, the presence of smaller particles here might thus be associated with either enhanced amounts of HPH cycles at 1000bar but also with a reduced viscosity of the aqueous polysorbate 80 solution when compared with more viscous sucrose fatty ester solution.

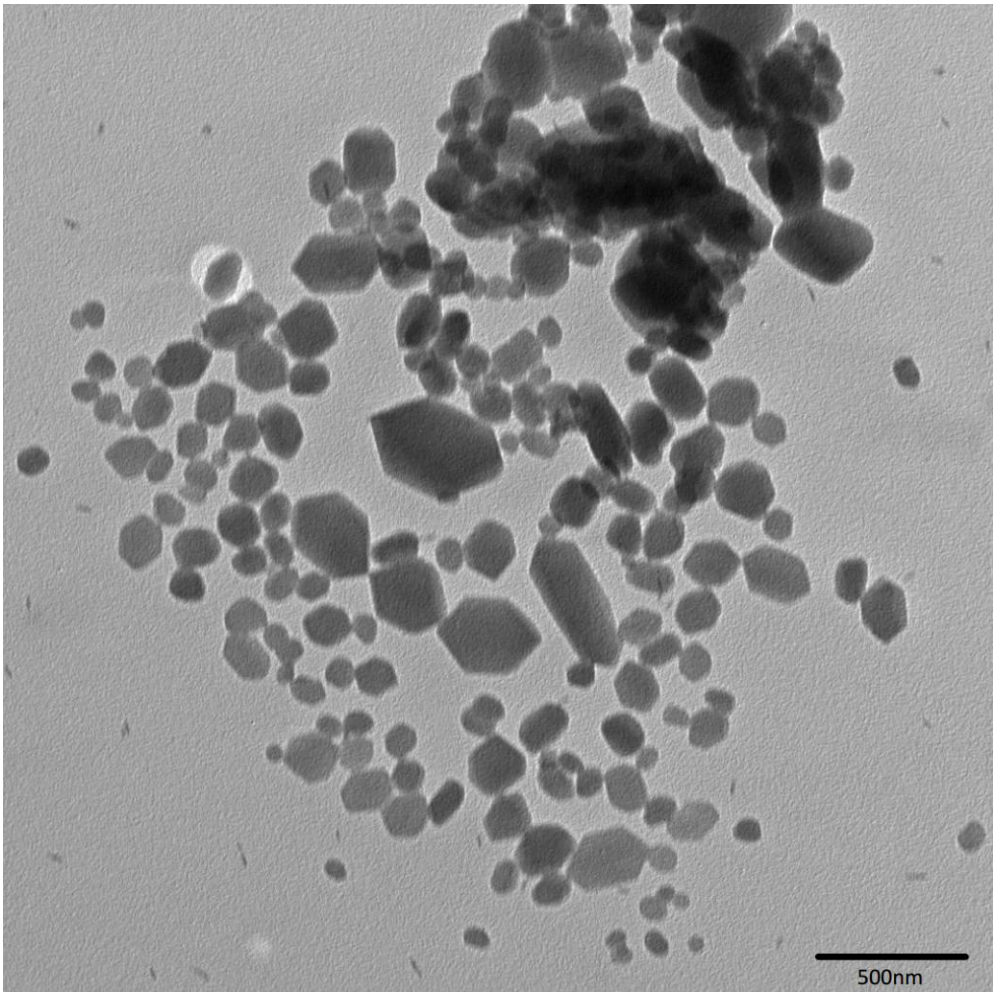

Figure 31: Transmission electron micrograph of imiquimod crystals in an aqueous polysorbate 80 solution at a 5800fold magnification.

5.3.2. Influence of polyvinylpyrrolidon on imiquimod particle sizes

On the basis that suspended state particles tend to decrease the surface free energy by agglomeration, stabilizing efforts in pharmaceutical suspensions are commonly used by adding suspension stabilizers but also crystal growth inhibitors. PVP, as it has been described as an effective crystallization inhibitor [144] neither demonstrated a beneficial effect on particle sizes, nor on the polydispersity index. Average particle sizes of imiquimod remained stable after a one week period in case of both, PVP K30 and polysorbate 80. The presence of PVP K90 seemed to delay the particle size stabilizing. Here, a stabilization of particle sizes was detected after a ten days period. However, average particle sizes in case of PVP K30 and to a higher extent in case of PVP K90 were somewhat higher when compared with a polysorbate 80 based

imiquimod suspension. As it is apparent by figures 32a-f, the general trend of particle sizes stands in accordance with the respective PDI values.

Indeed, PVP K90 negatively impacted on the stability of the imiquimod suspension resulting in a noticeable sedimentation after few days of storage. Additionally, imiquimod particle sizes in case of the PVP K90 containing suspension were above both, the PVP K30 but also polysorbate 80 based suspension. Since PVP based crystal growth inhibitors emerged to be unsuitable to further stabilize imiquimod crystals, the use of PVP based excipients was henceforth omitted. In order to create a stable suspension thereby offering constant particle sizes but also PDI's, polysorbate 80 proved to fulfill this purpose. A negative zeta potential was detected either in presence and absence of further crystal growth inhibitors. A noticeable impact on the zeta potential values of the aqueous imiquimod suspension did not occur although particle sizes were slightly increased when PVP K30 and K90 were added to the suspension (table 7). Taken together, an aqueous imiquimod suspension based on polysorbate 80 offers the potential to maintain a stable formulation. Since polysorbate 80 represents a nontoxic and also well tolerable emulsifier it is described as suitable for the use of submicron o/w emulsions but also solid lipid nanoparticles [145].

Table 7: Average zeta potential values of aqueous imiquimod suspensions in case of either presence or absence of PVP K30 and PVP K90. Three measurements have been performed to calculate average mean and standard deviation.

Imiquimod particle suspended in	Zeta potential [mV]
polysorbate 80 (9 mg polysorbate 80 / ml water)	-33.1 ± 0.93
polysorbate 80 (9 mg polysorbate 80 / ml water) + PVP K30	-34.3 ± 0.32
polysorbate 80 (9 mg polysorbate 80 / ml water) + PVP K90	-33.4 ± 0.25

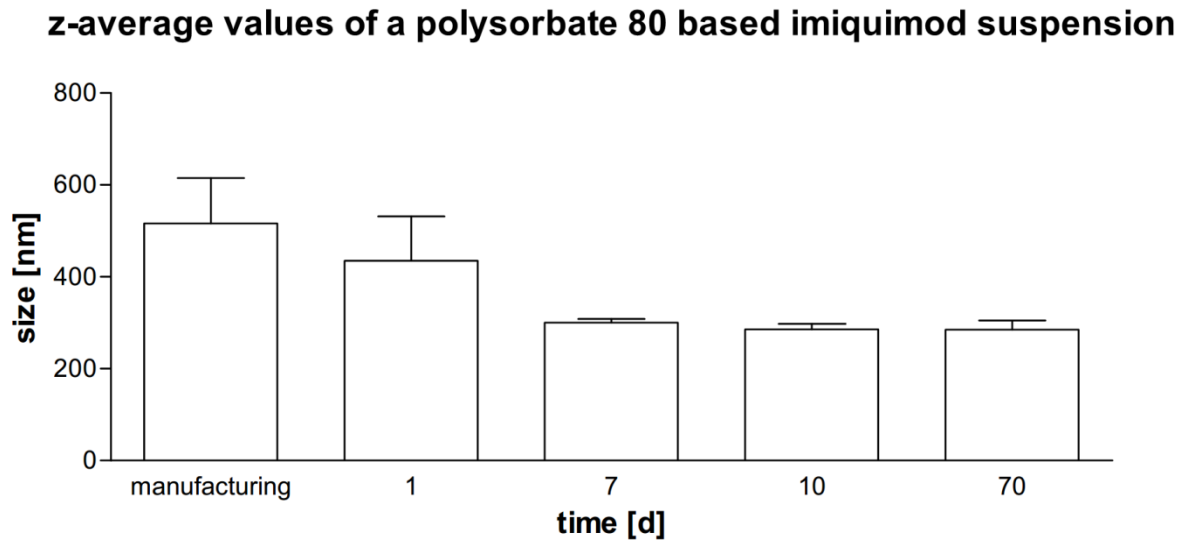

Figure 32a: Average particle size of an aqueous imiquimod suspension in a 9mg/ml polysorbate 80 detected by DLS (n=3). Particle sizes were measured directly after the manufacturing process and compared with particle sizes over a storage period of 70 days. Samples were stored in a greiner tube under room conditions (22°C – 24°C). Error bars described as standard.

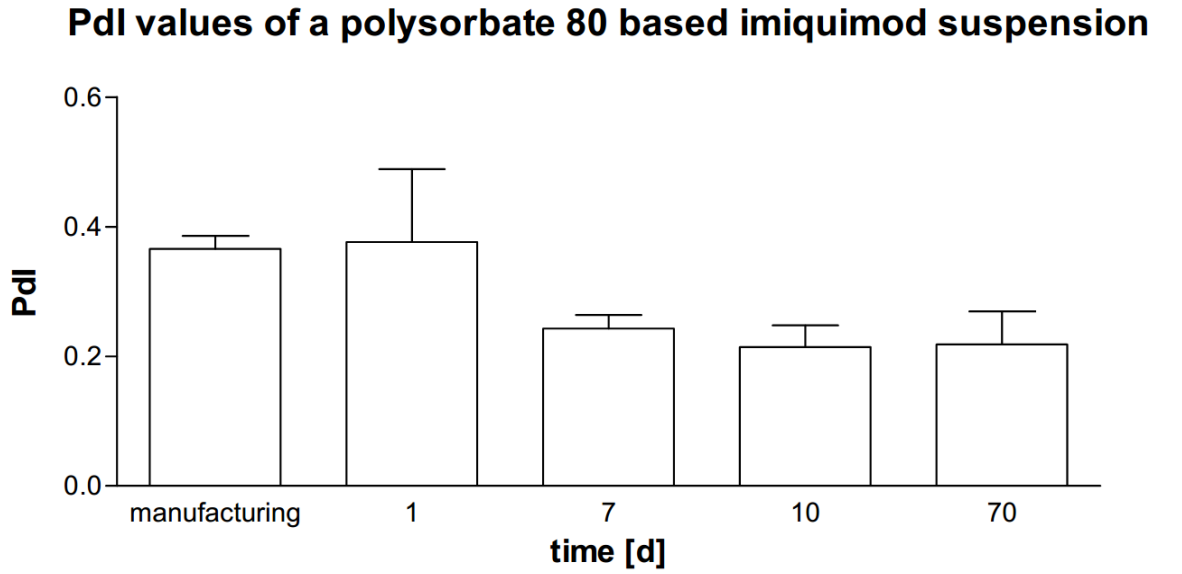

Figure 32b: Average PdI values of an aqueous imiquimod suspension in a 9mg/ml polysorbate 80 detected by DLS (n=3). PdI values were measured directly after the manufacturing process and compared with particle sizes over a storage period of 70 days. Samples were stored in a greiner tube under room conditions (22°C – 24°C). Error bars described as standard.

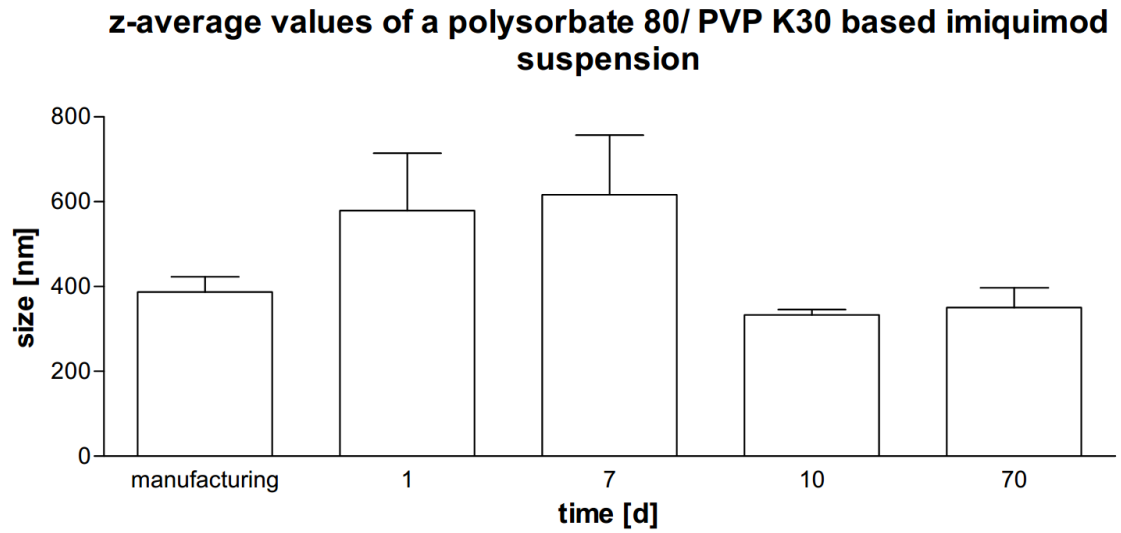

Figure 32c: Average particle size of an aqueous (9mg/ml polysorbate 80) imiquimod suspension with additionally added PVP K30 detected by DLS (n=3). Particle sizes were measured directly after the manufacturing process and compared with particle sizes over a storage period of 70 days. Samples were stored in a greiner tube under room conditions (22°C – 24°C). Error bars described as standard deviation.

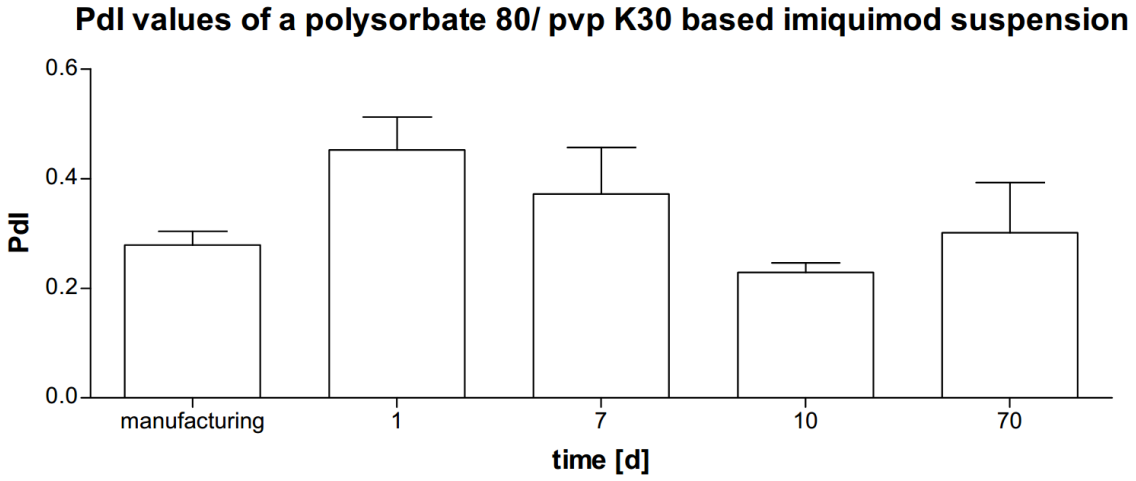

F

igure 32d: Average PdI values of an aqueous imiquimod suspension in a 9mg/ml polysorbate 80 with additionally added PVP K30 detected by DLS (n=3). PdI values were measured directly after the manufacturing process and compared with particle sizes over a storage period of 70 days. Samples were stored in a greiner tube under room conditions (22°C – 24°C). Error bars described as standard.

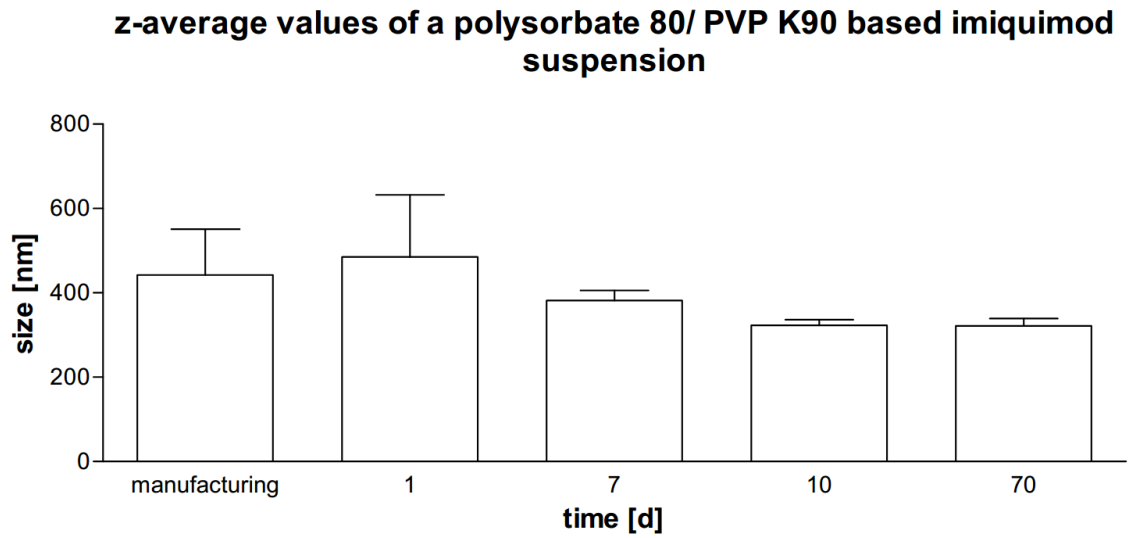

Figure 32e: Average particle size of an aqueous (9mg/ml polysorbate 80) imiquimod suspension with additionally added PVP K90 detected by DLS (n=3). Particle sizes were measured directly after the manufacturing process and compared with particle sizes over a storage period of 70 days. Samples were stored in a greiner tube under room conditions (22°C – 24°C). Error bars described as standard deviation.

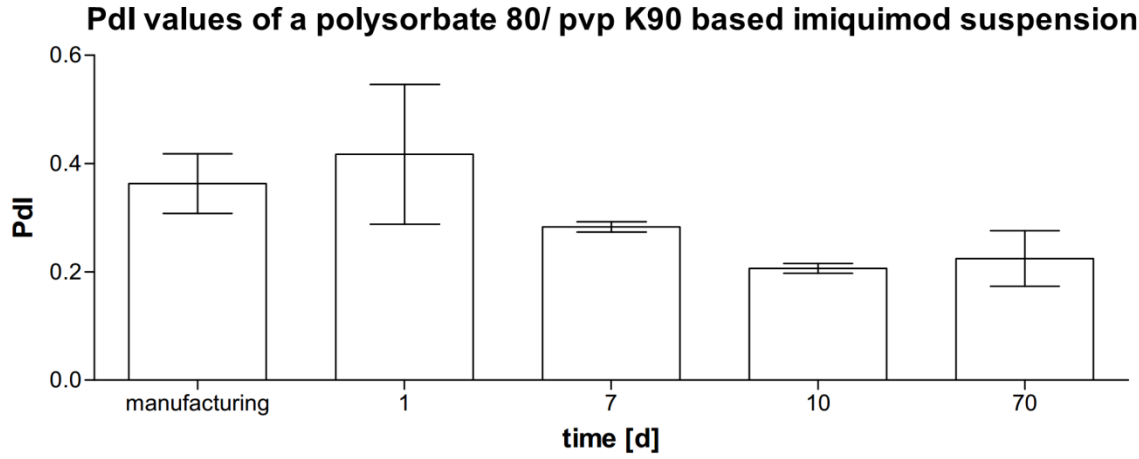

Figure 32f: Average PdI values of an aqueous imiquimod suspension in a 9mg/ml polysorbate 80 with additionally added PVP K90 detected by DLS (n=3). PdI values were measured directly after the manufacturing process and compared with particle sizes over a storage period of 70 days. Samples were stored in a greiner tube under room conditions (22°C – 24°C). Error bars described as standard.

Addressing long term stability, DLS measurement on particle size of imiquimod, formulated as emulsion gel, were performed directly after the manufacturing process but also after a storage period of nine months under room conditions in a pharmacy-customary jar at 22°C – 24°C. As seen in figure 33, imiquimod particles remained

stable after a long term storage period, a fact that is in line with the above mentioned findings confirming that crystal growth inhibitors are as additional formulation excipients unnecessary.

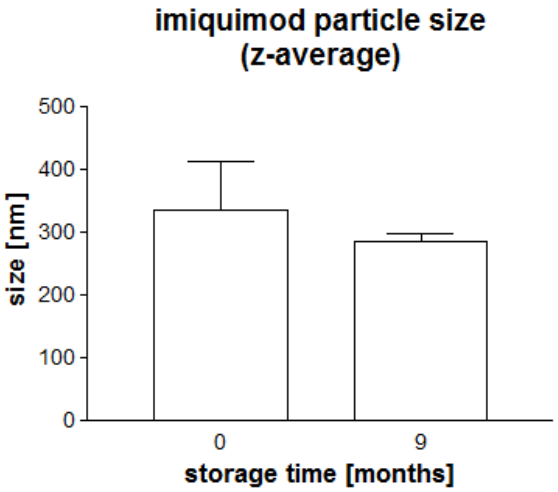

Figure 33: Imiquimod particles of the emulsion gel measured by DLS. Average particle size (n=3) was detected directly after the manufacturing process but also after a nine months storage under room conditions (22°C – 24°C). Error bars described as standard deviation.

5.3.3. Rheological characteristics of the emulsion gel

The emulsion gel formulation concept aims at a prolonged imiquimod residence on the skin since viscosity was considerably enhanced when compared with Aldara® 5% creme. Viscosimetric measurements indicated a broad disparity between Aldara® 5% creme and the emulsion gel. The innovators product Aldara® 5% creme shows thin fluid consistency which is similar to common dermally applied lotions. In contrast hereto, there was a substantially high-viscosity in case of the emulsion gel resulting in an approximately 20fold increased shear stress (figure 34) at similar shear rates.

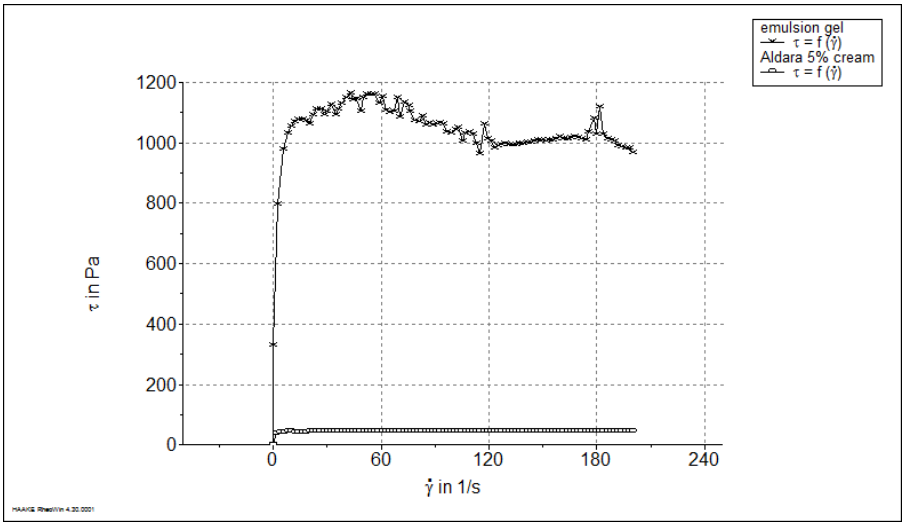

Figure 34: Flow curves of imiquimod containing formulations were obtained by a Haake RS1 rotation type viscosimeter using a parallel-plate setup. Measurements were performed at 23°C with an appropriate pre heating time.

5.3.4. Influence of jojoba wax on *in vitro* imiquimod permeation

In vitro results based on jojoba wax showed a strong decline of imiquimod permeation. In this case again, a strongly diminished API permeation was obtained by modified Franz diffusion cell measurements (figure 35). Permeation plots after 24hours demonstrated an almost eightfold increased amount in case of Aldara® 5% creme. As observed previously, the presence of laurocapram did not impact on *in vitro* imiquimod permeation data.

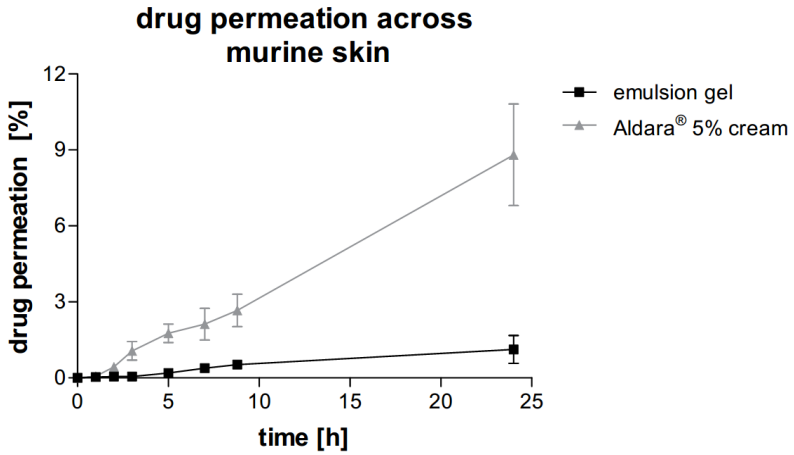

Figure 35: Imiquimod permeation across murine skin of the emulsion gel in comparison with Aldara® 5% creme. Data was obtained by a modified Franz diffusion cell apparatus using a murine skin setup (n=6). Error bars described as standard deviation. Acceptor medium was a 20mM acetate buffer pH 3.6/ ethanol (7/3 V/V).

5.3.5. Effect of formulation on cytotoxic T-cell activity

Based on a TCI protocol in C57BL/6 mice, the jojoba wax containing emulsion gel induced cytotoxic T-cells in a marginally increased magnitude when compared with Aldara® 5% creme (figure 36). The emulsion gel formulation, despite a significant reduction in skin permeation of imiquimod thus showed comparable imiquimod immunization results.

Jojoba wax, as it has proven useful to markedly decrease *in vitro* API permeation, again did not behave according permeation data obtained by modified Franz diffusion cell measurements.

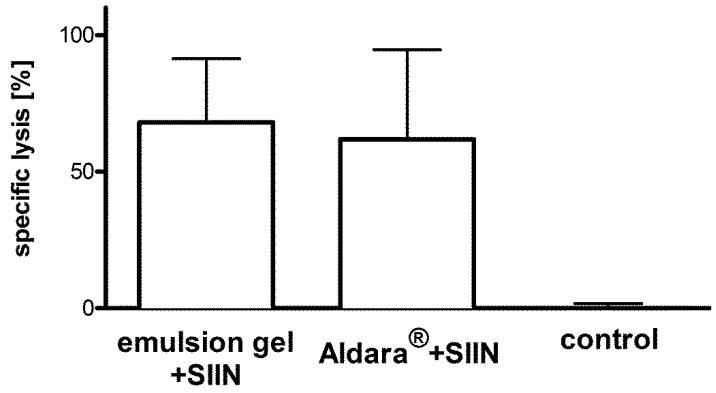

Figure 36: Cytotoxic T-cell induced lysis of labeled spleen cells in C57BL/6 mice (n=9) after 24hours. SIINFKL was either incorporated directly into Aldara® 5% creme or incorporated into offinical cremor basalis. In case of the latter one, the administration of SIINFEKL was subsequent to the emulsion gel (differences regarding the concomitant administration of SIINFEKL incorporated into Aldara® 5% creme but also an i.d. administration of SIINFEKL are described in the "appendix" section at figure 42). A non-medicated ointment containing the antigen SIINFEKL was used as control group. Error bars described as standard deviation.

5.3.6. Rejection of implanted tumors in C57BL/6 mice

In order to determine tumor rejection efficacy, C57BL/6 mice were challenged with EG.7 thymoma cells (4×10^5 s.c.), expressing SIINFEKL. After inoculated tumors were palpable, mice were treated dermally with either Aldara 5% creme or jojoba wax based emulsion gel (SIINFEKL was previously applied incorporated into officinal cremor basalis). Survival period was evaluated by a Mantel-Cox test. In contrast to the untreated control group, a significantly prolonged rate of survival was observed in case of both treatment groups. Further noticeably prolonged duration of survival

emerged in case of the emulsion gel, however this difference was not significant with a resulting p value of 0.17 (figure 37).

Other than duration of survival, decline of tumor size over a period of 60days showed a markedly improved efficacy of jojoba wax based emulsion gel in comparison with the innovators product (figure 38a-c). Within this graphical representation a reduction of tumor size but also a subsequent vanishing after approximately 25days was detected in seven of nine animals treated with the jojoba wax based imiquimod emulsion gel. Unlike these results, Aldara® 5% creme demonstrated to avoid tumor growth in only three animals. Data of the untreated control group demonstrated that tumor rejection emerged in none of these animals.

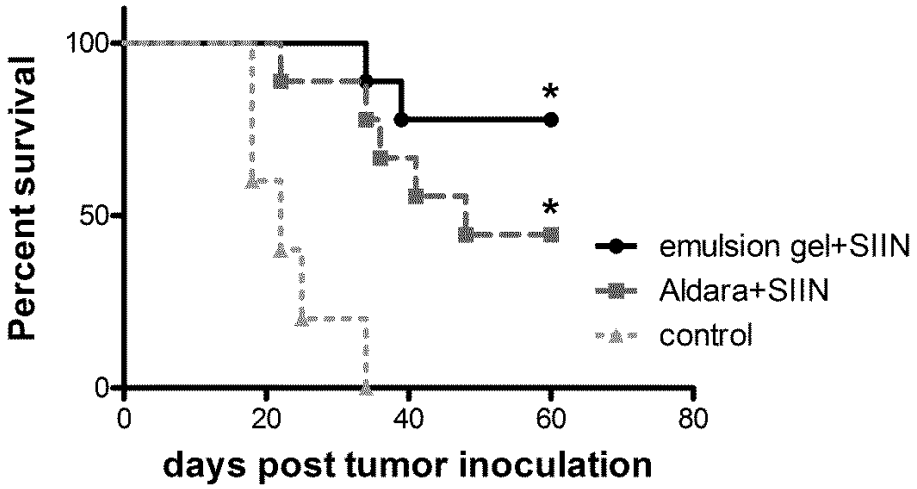

Figure 37: EG.7 thymoma cells (4 x 10^5 s.c.), expressing SIINFEKL, were injected into the flank of C57BL/6 mice. After the tumor was palpable mice were immunized as indicated on two consecutive days in weekly intervals over a period of three weeks or left untreated. Mice were sacrificed when tumor size exceeded 2cm^2. * describes a significant difference to the untreated control group, calculated by Mantel-Cox test. A non-medicated ointment containing the antigen SIINFEKL was used as control group.

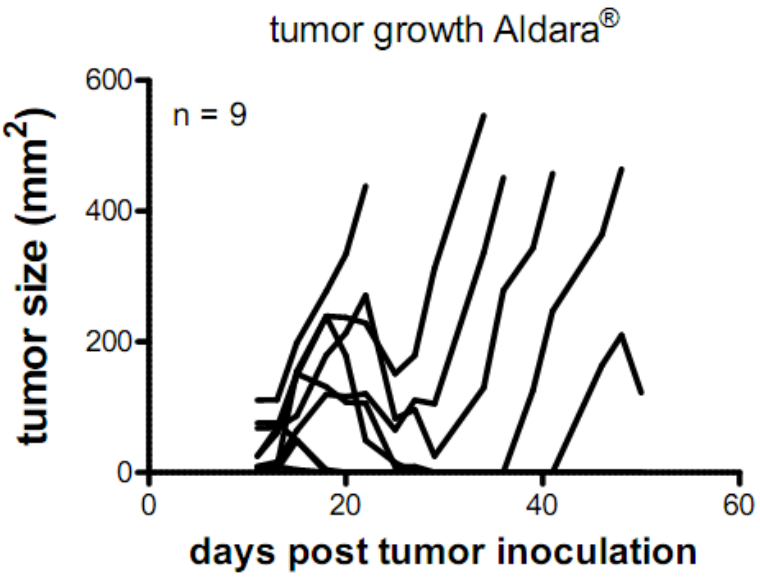

Figure 38a: Graphical representation of tumor progression in C57BL/6 mice after inoculation of EG.7 thymoma cells (4 x 10^5 s.c.). Thymoma cells are expressing SIINFEKL as a surrogate tumor antigen. Mice were dermally immunized with Aldara® 5% creme after tumors became palpable. The antigen SIINFEKL was incorporated into the cream. Mice were immunized in weekly intervals over a period of three weeks.

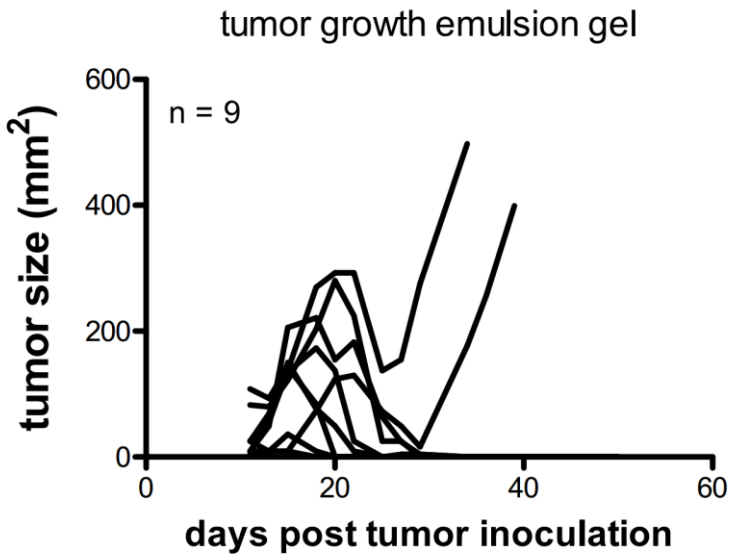

Figure 38b: Graphical representation of tumor progression in C57BL/6 mice after inoculation of EG.7 thymoma cells (4 x 10^5 s.c.). Thymoma cells are expressing SIINFEKL as a surrogate tumor antigen. Mice were dermally immunized with the emulsion gel after tumors became palpable. The antigen SIINFEKL was incorporated into officinal cremor basalis and administered subsequent to the jojoba wax containing emulsion gel. Mice were immunized in weekly intervals over a period of three weeks.

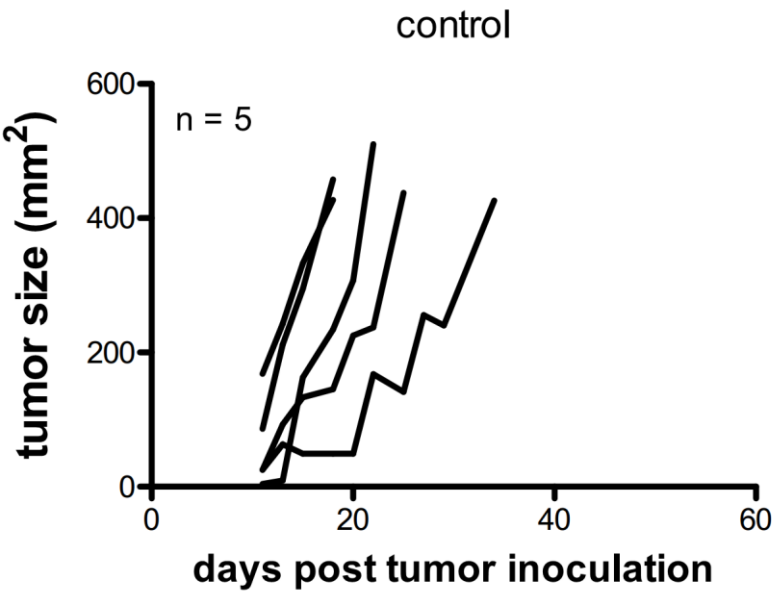

Figure 38c: Graphical representation of tumor progression in C57BL/6 mice after inoculation of EG.7 thymoma cells (4×10^5 s.c.).

6. Discussion

6.1. Prediction of immunization efficacy in a Franz diffusion cell model – opportunities and limitations

6.1.1. Biopharmaceutic aspects of imiquimod containing multisource products

In vitro and *in vivo* tests of Aldara® 5% creme and commercially available multisource products from PR of China showed differences from a pharmaceutical and biopharmaceutical perspective. Thus different formulation compositions in spite of equal amounts of imiquimod did not demonstrate concordant efficacy in a mouse model.

Although it is difficult to draw strong conclusions for the situation in humans, data suggests that the products offer a significant immunizing effect when applied on the skin in comparison to vehicle control treatment. Differences regarding *in vivo* but also *in vitro* data lead to the conclusion that the products may not be bioequivalent [124, 137]. The latter conclusion may also be justified by measured differences in physicochemical parameters such as viscosity and characteristics of the dispersed state phase.

Unfortunately the package inserts of the Chinese products did not contain any information on excipients incorporated and thus do not allow to draw any further conclusions, a fact that stands in contrast to European drug safety ascertains. Results obtained within this work raise the question whether the galenic system applied in case of Aldara® 5% creme represents the optimum composition in terms of potential for transcutaneous immunization. Obviously, as demonstrated in this study, dissolved state imiquimod containing creams offered superior immunization performance *in vivo*. An explanation for the advantageous skin permeation of dissolved state imiquimod formulations could be due to the high solution capacity of dissolved state ointments. Generally, a high affinity of the drug to the vehicle with a simultaneous high solution capacity of the vehicle for the drug results in a low bioavailability. However, within the same type of vehicle the permeation rate increases proportionally with an increasing API concentration. Maximal permeation is achieved if the dissolved concentration of the active is equal to the solubility in the

vehicle surface [146]. Imiquimod is known for its poor solubility. Besides drastically decreased pH values, isostearic acid, oleic acid, and linoleic acid are an exceptional case as they dissolve relatively high amounts of imiquimod. Although the solution capacity of isostearic acid is up to 17% [123], other components included in Aldara® 5% creme such as water do not dissolve relevant amounts of imiquimod. It can thus be assumed that five percent imiquimod nearly represents the maximum solution capacity of the vehicle cream used in Aldara®. This might be a possible explanation for the increased permeation of Aldara® 5% creme. On the other hand, the penetration rate from suspension based ointments is independent from the drug's solubility. The amount of suspended active thus has no influence on the intensity of action since the API is released fast enough [146]. Hence, suspension type formulations represent a valuable platform to design imiquimod formulations.

One of the principle aims of this work was to identify areas of improvement for imiquimod based TCI. As it has been demonstrated by "Med Shine Li Di" but also Aldara® 5% creme, dissolved state semi-solid formulations may offer equivalent performances. Nevertheless, none of formulations tested gained substantially higher cytotoxic T-cell activations compared with the innovators product.

Recent insight into drug transport mechanisms across intact skin emphasized transfollicular transport of small molecules and particles to play a more important role than estimated previously [147-149]. An explanation of diminished *in vivo* performance in cases of both, "You Bi Qing" but also "Li Ke Ji" is in line with the fact that particles above a size of 10µm are described unfeasible to penetrate into the stratum corneum [150]. Indeed, none of the tested formulations contained the API in a nano to submicron scale.

6.1.2. Opportunities of Franz diffusion cell investigations

In contrast to synthetic membranes, imiquimod permeation across ablated murine skin seemed better adaptable to predict *in vivo* generated immunization. In particular, cytotoxic T-cell induced spleen cell lysis and imiquimod permeation across murine skin correlated well with a resulting r^2 value of 0.777 (figure 25d). Unlike excised murine skin based permeation data, synthetic membrane related Franz diffusion cell

investigations did not correlate with any *in vivo* results. A slope significantly deviating from zero occurred in case of all *in vivo* parameters when plotted against *in vitro* imiquimod skin permeation. As an exception, a slope significantly deviating from zero was measured in case of membrane permeation against IFNγ determination.

In particular with a view to ascertaining whether imiquimod containing formulations contain the active in a dissolved or suspended state, murine skin as a membrane model should be preferred. Moreover, the skin based Franz diffusion cell model was suitable to give hints on differences regarding dissolved state formulation. In particular permeation of Aldara® 5% creme compared with “Nan Bo” and “Med Shine Li Di” showed noticeable differences within the dissolved state formulations (figure 22c).

Accordingly, Aldara® 5% creme achieved substantially higher skin permeation when compared with crystal free “Nan Bo” and “Med Shine Li Di”. The latter two products were evaluated equivalent in terms of permeation rates (f1 = 10.73).

These findings may be explained by the skin physiology. Due to a high degree of tortuosity to the path of water or any other solvent molecules [15], protein enriched corneocytes represent an obstacle to solvent diffusion across the SC from the acceptor chamber upwards into the cream sample. Consequently, a solvent transfer from the acceptor medium upwards into the cream sample thus seems to be minimized.

Unlike murine skin setup, leveling effects in case of synthetic membranes are most likely affected by acceptor solvent diffusion across membrane pores into the cream sample and will dissolve the drug. Thus, a highly concentrated API solution follows the concentration gradient back into the acceptor chamber.

Studies aiming at different parameters in Franz diffusion cells described the acceptor medium as most important and critical variable that influences drug release [111]. Numerous synthetic membranes tested resulted in similar penetration values. Pores of tested membranes were in a range of 0.45 to 0.50µm, whereas membrane thickness noticeably differed (150 – 450µm). Based on these findings, synthetic membranes were described to minimize the variability observed when using skin membranes [151].

Results obtained within this work contradict these findings; however this may be drug specific.

Indeed, acceptor medium related differences in drug release profiles occurred for identical formulations in synthetic membrane related Franz diffusion cell investigations. However both, 0.1M HCl and methanol/ pH 3.6 buffer blend did not affect the general imiquimod release order with Aldara® 5% creme demonstrating the most rapid release. In general the methanol/ phthalate buffer based setup showed a slower curve progression. Relevant differences occurred in case of “You Bi Qing” (figure 22a-b) where a considerably higher amount of imiquimod was detected in the acceptor chamber when methanol was used. This can be substantiated by the fact that imiquimod crystals are embedded in the inner oil phase of “You Bi Qing” cream. Due to the enhanced solubilization capacity of the methanol/ buffer blend, imiquimod is more likely eluted from the oil phase of the cream than by the hydrophilic aqueous HCl solution.

As a conclusion, it is advisable to use a murine skin setup in order to assess whether formulations differ but also to draw conclusions on *in vivo* effects.

6.1.3. Limitations of Franz diffusion cell investigations towards immunization efficacy

Despite considerable differences in permeation data across murine skin but also correlations to *in vivo* effects, this method has reached its limit by trying to differentiate between particulate formulations (suspension-type) containing imiquimod particles in a nano – to submicron scale.

This conclusion results from Franz diffusion cell data showing similarity of API permeation across murine skin in case all SN formulations except for SN 3 (figures 27-28). However, the situation *in vivo* did not go hand in hand with *in vitro* obtained data. This is also confirmed when considering emulsion gel data. Instead it turned out that *in vitro* permeation is decreased to a tenfold extent in case of SN 3 compared with Aldara® 5% creme. Nevertheless, both, *in vivo* CTL activation but also tumor rejection data were equal to slightly augmented in case of a jojoba wax based emulsion gel.

A general issue on TCI performance prediction is based on the fact that immunization processes take place in the viable epidermis but also dermis and deeper muscular tissues. Although bypassing the immune system of the skin, i.m. injections of vaccines by needle and syringe still hit the target. Despite the circumstance that LC are most prominent within the stratum spinosum they are present in all layers of the dermis and particularly around blood vessels [152].

Thus, attempts on TCI performance prediction by considering API permeation across ablated skin in several cases might lead to inconsistent results.

In contrast to drug loaded TTS such as fentanyl patches, providing a controlled release rate which correlates well with a measurable plasma API level, antigens and immunopotentiators trigger a complex immunological cascade. Hence it may generally seem challenging to predict immune effects by measuring penetration or permeation values.

A considerable impact of excipients on TCI performance is also illustrated by “Nan Bo” and “Med Shine Li Di”. Both formulations revealed similar permeation results however respective *in vivo* detected cytotoxic T-cell activations differed substantially (figures 23a – 23c).

6.2. Impact of excipients as formulation components on transcutaneous immunization results

Results obtained within this work opened up new opportunities to improve imiquimod based TCI.

A rationale for *in vivo* superiority following administration of Aldara® 5% creme in comparison with other tested dissolved state formulations may be related to the use of isostearic acid. This fatty acid may be acting as penetration enhancer, especially if C-16 branched, has shown an up to 17-fold enhanced drug penetration rate across the skin [153]. Indeed, Aldara® 5% creme with its total amount of five percent dissolved imiquimod consequently may contain high amounts of isostearic acid. Except for isostearic acid, only linoleic acid and oleic acid may serve as a possible

substitute to completely dissolve the required amount of five percent imiquimod [123] in a cream formulation.

Dissolving sufficient amounts of imiquimod in order to create a semi-solid dosage form is described in the literature as the assignment of two compounds with one or more hydrogen bond formers e.g. gentisic acid, salicylic acid, glycolic acid or lactic acid and a polar solvent system e.g. DMSO (dimethyl sulfoxide), ethanol, benzyl alcohol, or NMP (N-methyl Pyrrolidone) [135].

Although mentioned as feasible to dissolve large amounts of imiquimod conspicuously higher than 5%, these compound blends are estimated to cause skin irritations and itching. Likewise, the above mentioned fatty acids, mineral acids in general have a high capacity to dissolve imiquimod, however, required pH values consequently might have a deleterious effect on the skin due to pH shift.

Investigations on excipient related effects in SN formulations but also the aqueous emulsion gel confirmed a substantial impact of excipients on *in vivo* generated effects.

6.2.1. Inclusion of sucrose fatty acid esters in transcutaneous immunization formulations

In combination with sucrose fatty acid esters, a vehicle combining antigen and immunopotentiator can be designed. Additional formulation components include pharmaceutical acceptable oils and lipophilic or aqueous penetration enhancers. Starting from a highly dispersed oil in water nanoemulsion freeze drying can be applied to yield a solid nanoemulsion which may be applied externally.

Mitsubishi-Kagaku Food based nomenclature towards sucrose fatty acid ester in terms of food grade types is as follows [154]:

The leading letter represents the fatty acid type.

The last two numbers represent the percentage of the named fatty acid.

The first one or two numbers describe the HLB value of sucrose fatty acid ester.

Addressing stability issues of freeze dried TCI formulations such as insensitivity to room humidity and temperature during the course of manufacturing this concept offers several advantages related to its anhydrous character. Nevertheless, few aspects need to be taken into consideration. Saturated oil and wax containing formulations demonstrated to be highly stable. Formulations based on sucrose fatty ester S-1670 may be stored under room conditions due to their insensitiveness against humidity. Since freeze drying removes the outer (aqueous) phase of a (nano)-emulsion, high HLB values are required in order to manufacture an oil in water emulsion.

Besides sucrose fatty acid ester S-1670, previous formulation development efforts included sucrose fatty acid esters L 1695 but also M 1695. The latter two components showed distinctly hygroscopic properties. Directly after the manufacturing process SN formulations based on L 1695 tended to agglutinate with a noticeable liquefaction. Indeed, M 1695 showed instabilities in a similar manner. Since M 1695 and L 1695 also demonstrated these stability issues when stored in a commonly used glass jar, this agglutination is not associated with the manufacturing process of SN formulations in general.

Other than M 1695 and L 1695 an aqueous solution of S-1670 is susceptible to temperature higher than 35°C. Such a temperature load caused an irreversible gelling effect which makes a further manufacturing process impossible. Hence, during the manufacturing of the aqueous S-1670 solution, it has to be cooled for instance by ice water if required.

Interestingly, different types of sucrose fatty esters affect drug release characteristics in a chain length dependant manner [155]. Based on this study, sucrose fatty ester types used in TTS thus may represent a promising concept in terms of development efforts of patches for immunological purposes.

6.2.2. Particle sizes

According to the literature, particles in a nano- and submicron scale are described as suitable to ensure an appropriate residence time within hair follicles of up to ten days

by the follicular transport route [23]. Hair follicles are considered as promising target with respect to their dense network of blood capillaries and resident dendritic cells [156]. Results obtained within this work contradict the hypothesis that a pronounced cytotoxic T-cell response is facilitated exclusively by dissolved state formulations [137]. These formulations however did not contain imiquimod particles in a submicron- to nanoscale range. Addressing particle based imiquimod containing formulations, a further example of lacking performance based on an aqueous cellulose gel is described in the literature [123]. The authors described a micronization process however details addressing particle size were not described in particular. This can be elucidated by findings that particles exceeding 10µm neither penetrate into the follicular orifices nor the horny layer [106].

Regarding particle sizes of immune potentiator formulations developed in the context of this work, they have in common that the average diameter should be beneath 1µm. Transmission electron micrographs but also DLS measurements attested average sizes of approximately 600nm in case of SN formulations and 285nm in case of the emulsion gel, respectively. This was shown to generate enhanced and extended immune stimulation when compared with commercially available products. In terms of nano- to submicron particle related advantages, results obtained here are in line with findings of others [20, 157, 158]. Regarding potential side effects, both, SN concept but also the aqueous emulsion gel demonstrated a reduced API permeation in contrast to Aldara® 5% creme. Hence, these formulation concepts may provide a reduction of local and systemic side effects.

Interestingly, the presence of steric stabilizers such as PVP K30 and K90 did not contribute to a benefit in particle stabilization efforts. As it is described in literature, PVP impacts on particle stabilization due to steric repulsion when adsorbing on the particle surface [159]. However, PVP polymers tend to adsorb on a cluster of particles rather than individual particles and thus increase the measured diameters [160]. Nevertheless, rapid sedimentation occurred in case of an aqueous PVP K-90 based imiquimod suspension. This polymer showed a negative effect on both, suspension stability but also average imiquimod particle size. Here, the presence of polysorbate 80 sufficiently stabilized imiquimod particles in case of both, an aqueous suspension but also the jojoba wax based emulsion gel.

6.2.3. Dissolved state SN formulation based on oleic acid

Since dissolved state imiquimod containing formulations including Aldara® 5% creme and “Med Shine Li Di” induced a potent immune response, a noteworthy aspect in formulation development was to evaluate the extent as to which a dissolved state imiquimod SN formulation generates a T-cell answer in C57BL/6 mice. In short, investigations on a freeze dried formulation using oleic acid in order to completely dissolve imiquimod thereby mimicking the basic aspect of Aldara® 5% creme and “Med Shine Li Di” resulted in the following:

i) Oleic acid based SN demonstrated an equivalent imiquimod liberation characteristic across a synthetic membrane when compared with Aldara® 5% creme (figure 39).
ii) This formulation failed to generate an *in vivo* effect (figure 40).

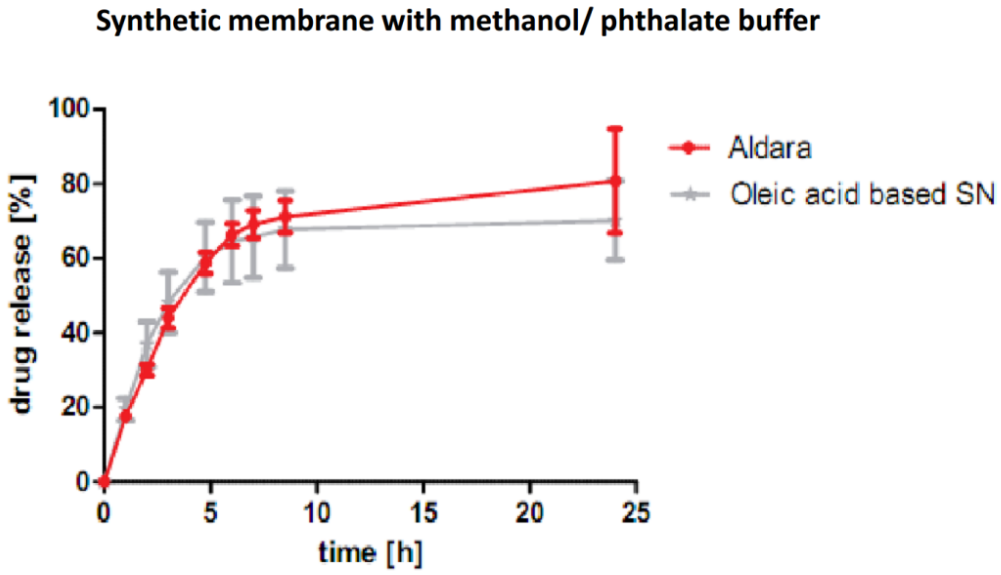

Figure 39: I*n vitro* imiquimod release in a simple Franz diffusion cell model across synthetic membranes. The acceptor phase consisted of a blend of phthalate buffer pH 3.6/ Methanol in a 7/3 ratio (n=4). Error bars described as standard deviation.

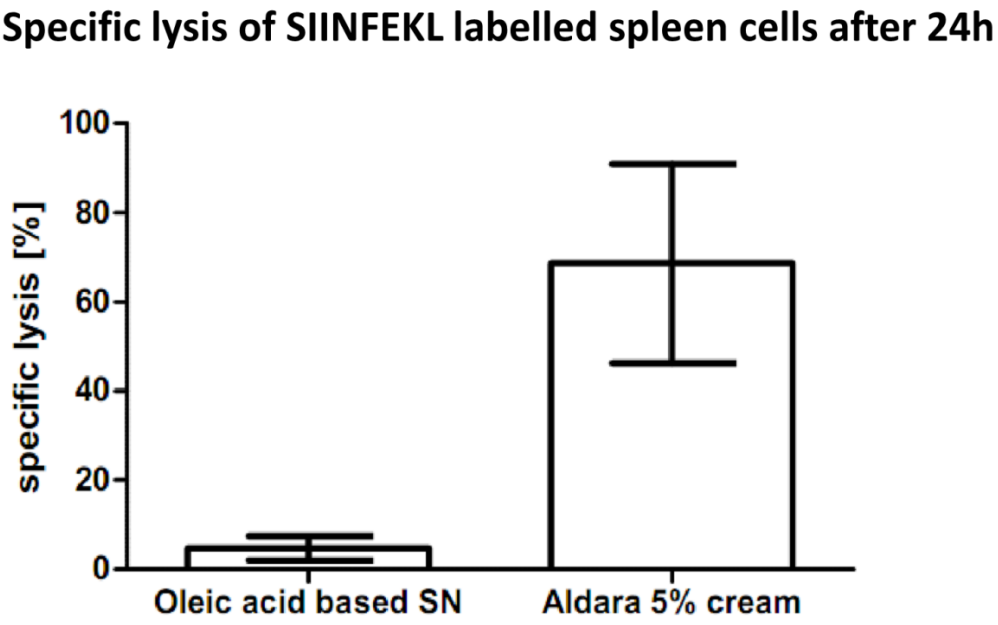

Figure 40: I*n vivo* cytotoxic T-cell induced lysis of i.v. applied labeled spleen cells in a C57BL/6 mouse model after 24 hours (n=4). Error bars described as standard deviation.

Besides lacking *in vivo* performance, oleic acid based SN caused serious adverse effects such as sore skin on the back of mice.

6.2.4. Oil related effects

Jojoba wax as lipophilic semi-solid formulation component is described to significantly decrease the rate of diclofenac penetration across the skin. Results obtained within this work confirmed this literature finding that is presumed to be associated with the three-dimensional structure of jojoba wax [161]. As a beneficial effect the use of jojoba wax in the emulsion gel was justified by

i) Reducing permeation rates across the skin in order to decrease systemic API exposure [162].
ii) A prolonged resistance time at the site of action. The viscosity of the emulsion gel was increased up to 25fold in comparison with inviscid Aldara® 5% creme to additionally improve the dermal residence time.

Stability issues particularly concerning unsaturated chemical compounds such as squalen, avocado oil, and oleic acid represent a challenge. This situation will be exacerbated on the basis that nano scale oil droplets with their large surface area promote oxidative processes. However, adding tocopherol as antioxidant, as demonstrated for squalen containing SN 6, stabilization efforts enabled the applicability of this SN formulation. As indicated by SN 1-4, MCT but also squalen demonstrated to adequately induce *in vivo* T-cell response. SIINFEKL was applied by the i.d. injection route in order to ensure a defined antigen access. Nevertheless, SN 5 and SN 6 have demonstrated the potential to enable SIINFEKL transport across the skin in combination with imiquimod, as it has been described by i*n vivo* generated effects.

In terms of squalen related effects, a noticeable impact occurred in case of squalen/tocopherol related SN 6. This SN formulation significantly augments *in vivo* performance when compared with both, SN 5 but also the innovators product. Interestingly, in case of the stability lacking SN 4 its boost of immune response occurred to a lower extent in comparison with SN 6, indicating the necessity of an adequate anti oxidative stabilization. Considering the influence of the pharmaceutical oil component, a noticeable effect was detectable with respect to both, pharmaceutical parameters but also cytotoxic T-cell answers. Permeation rates of all tested SN formulations were similar among each other except for jojoba wax. *In vitro* data on jojoba wax containing formulation confirmed a strong excipient related permeation reduction. I*n vivo* performance of jojoba wax based SN was slightly below SN 1 but also SN 4. Other than suggested by *in vitro* permeation data, avocado oil demonstrated lowest capacity to induce an imiquimod based cytotoxic T-cell answer (figure 29).

6.2.5. Isostearic acid versus squalen

Recently published work outlined an immunomodulatory effect induced by the vehicle (no imiquimod present) of Aldara® 5% creme. It has been shown that isostearic acid promotes inflammasome activation in cultured keratinocytes and thus may contribute to the observed effect of Aldara® 5% creme towards murine skin. As a result, Aldara®

5% creme activates at least two immune pathways independently. In consequence both, imiquimod and the nonmedicated vehicle cream are required for a full inflammatory response [163].

The concept of an additional immunostimulation in a TLR receptor independent manner was mainly accomplished by the use of squalen in case of SN 6. Mechanism of action in case of squalen was investigated inter alia towards vaccination adjuvant MF59. MF59 represents an oil in water adjuvant used for parenteral immunizations in combination with a seasonal influence vaccination. This squalen based immunopotentiator additionally contains polysorbate 80 and sorbitanoleate 85. Since MF 59 rapidly reaches the lymphatic tissue it seems to increase the uptake of antigen by the immune system. Hence MF59 is recommended for elderly patients owning a reduced immune response [164]. Recent results identified macrophages, monocytes and granulocytes as target cells for squalen containing MF59. Interestingly, the response pattern induced by MF59 differs greatly from the pro-inflammatory response induced by most TLR agonists, suggesting a TLR independent mechanism [143].

Both, isostearic acid but also squalen strongly impact on T-cell activation. However, a potential objection against an additional TLR independent dermal immune activation is presumed to intensify the potential for local side effects such as itching and erythema.

As described in the literature for hydrophilic drugs, a fourfold increase of permeation was generated by squalen compared to MCT [165]. This oil related influence but also penetration enhancers might be of particular interest in order to develop formulations containing more hydrophilic antigens or proteins. TRP-2 as a new tumor antigen which is recognized by cytotoxic T-cells derived from tumor reactive TIL (tumor infiltrating lymphocytes) line provides a possible example to further improve TCI against melanoma. Besides the attempt to create an immunization approach the SN but also the emulsion gel formulations may offer a possible treatment option against HPV induced genital- and perianal warts. Since this work mainly focused on imiquimod as immunostimulator little attention was put on SIINFEKL due to its model antigen character. In order to delve into further imiquimod containing SN formulations, both, the antigen residence at the site of action, but also its

physicochemical characterization as well as stabilization issues will be of particular interest.

6.2.6. Laurocapram related differences

In terms of laurocapram related skin penetration enhancements, Franz diffusion cell based comparison between SN 1 (without laurocapram) and SN 5 (with laurocapram) did not point out measurable differences regarding permeation enhancing effects for imiquimod. In line with this result, SN 6 demonstrated similar permeation results compared with SN 1 and SN 5. Independent of the presence of a penetration enhancer all SN formulations did not match the API permeation level of Aldara® 5% creme (figure 28). Studies on this issue demonstrated that the antiviral active cidofovir at simultaneous presence of laurocapram enabled a more effective local treatment and preventing option of cutaneous HSV-1 infections [166]. According to the results obtained within this work, laurocapram did not impact on *in vitro* permeation across ablated murine skin samples. One reason for the imperceptible *in vitro* effect of laurocapram can be substantiated by the circumstance that even if the SC barrier is perturbed, a substantial barrier to the drug permeation remains due to the following skin layers [167]. SN formulations generally did not match skin permeation of imiquimod as formulated in Aldara® 5% creme. To this end this might be interpreted as a chance to reduce systemic side effects and API burden to the patient.

In order to reveal further insights into the effect of laurocapram towards *in vivo* data, two emulsion gel formulations were compared with regard to cytotoxic T-cell activation. Both formulations were equally composed except for the presence of laurocapram in case of “emgel lauro”. Other than “emgel lauro”, “emgel” did not contain any further enhancing excipients. In consequence, a noticeable diminished *in vivo* performance was observed which was however not significant (figure 41).

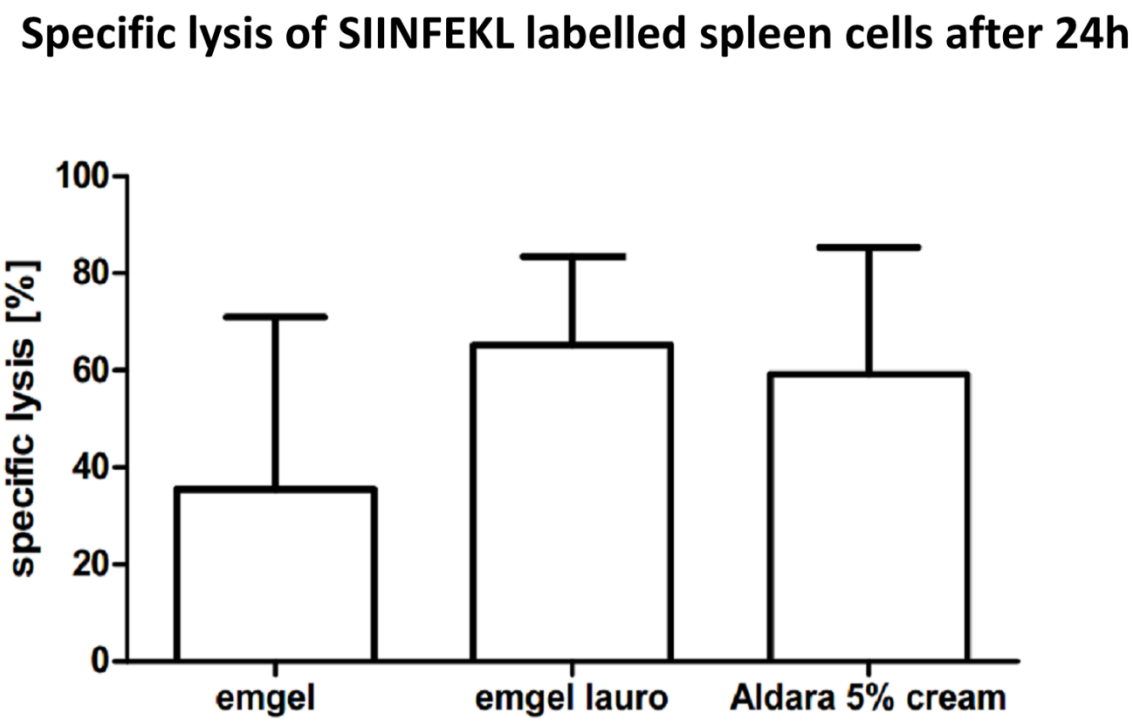

Figure 41: *In vivo* generated spleen cell lysis in order to estimate whether laurocapram impacts on cytotoxic T-cell activation. “Emgel” and “emgel lauro” are identically composed except for presence of laurocapram in case of the latter one (n=3). SIINFEKL was incorporated in officinal cremor basalis. Administration of the antigen was performed previous to the emgel administration in order to provide a defined amount of antigen at the site of action. Error bars described as standard deviation.

In spite of what may appear at first glance, utilizing a penetration enhancer contradicts to the attempt retarded emulsion gel formulation approach. To shed light on this apparent controversy, investigations dealing with jojoba wax formulations demonstrated a lack of efficacy by omitting laurocapram (details on preliminary formulations during the development of the emulsion gel with respective cytotoxic T-cell response see appendix figure 42. Moreover, figure 42 shows differences referring to i.d. and dermal administration of SIINFEKL.). Additionally, TCI based approaches using more hydrophilic antigens are assumed to benefit from penetration enhancers.

6.3. General considerations, open questions, and future perspectives

6.3.1. General aspects

In terms of tumor rejection data, a prolonged survival rate and additionally a noticeable remission of tumors emphasize a benefit of the emulsion gel formulation. Since this formulation induced a prolonged residence time at the skin site it may thus act as a promising approach to ameliorate imiquimod based TCI performance. As it was demonstrated by cytotoxic T-cell activation in C57BL/6 mice, omitting further irritant excipients such as isostearic acid may additionally demonstrate an advantage of a jojoba wax based imiquimod formulation. Another limitation of Aldara® 5% creme refers to its lacking stability which was mentioned by literature findings thus requiring the use of single dose sachez [135]. Regarding the compositions of Aldara® 5% creme in comparison with the emulsion gel, both formulations follow a simple design with a manageable number of excipients. Both formulations have in common that ethoxylated sorbitan fatty acid esters act as emulsifier which is in case of Aldara® 5% creme polysorbate 60 with additional cetyl- but also stearyl alcohol. Moreover, Aldara® 5% creme comprises purified water and xanthan gum as a viscosity enhancer. In order to improve shelf life, Aldara® 5% creme contains also preservatives such as PHB- esters. Except for the use of a HPH technique which is essential to create a stable emulsion gel formulation with incorporated imiquimod nanoparticles this concept comprises of even less excipients compared with Aldara® 5% creme. Key elements are the use of jojoba wax which essentially prolongs skin residence time combined with a penetration enhancer to overcome the SC barrier. Further excipients include purified water, Polysorbate 80, and a carbomer gel in order to adjust emulsion gel viscosity. Since it improves shelf life, preservatives such as commonly used methyl-4-hydroxybenzoat may additionally be added. In summary, the formulation concept of a jojoba wax based emulsion gel emphasizes an opportunity towards a stable but cost effective semi-solid formulation enabling the use of a multi use packaging.

Based on prolonged survival rates using the emulsion gel concept there is a clear interest as to which extent excipients such as squalen impact on tumor rejection data. Squalen not only augments the activity of vaccinations but has also shown its capacity to promote a prolonged duration of survival in mice after challenging with ascites sarcoma 180 cells [168].

It has been demonstrated within this work that pharmaceutical efforts can strongly contribute to the success of imiquimod based TCI. In particular in can be shown that

i) In contrast to commercially available products, particles in a submicron to nano scale range have demonstrated a high potential to enhance imiquimod based immune stimulation.
ii) An additional TLR independent immune-stimulation is desirable as shown by isostearic acid in case of Aldara® 5% creme but also squalen containing SN 6. On the other hand jojoba wax based emulsion gel demonstrated an at least equivalent effect compared with the innovators product.

It remains to be tested whether and to which extent dose – response relations occur particularly in case of squalen and laurocapram.

Within this work, SIINFKEL served as antigen for TCI experiments. It is an open question whether antigens, especially hydrophilic peptides and proteins of high molecular weight, traverse the SC barrier. It is assumed that an SN formulation concept as described within this work may offer advantages with respect to storage conditions for hydrolysis sensitive antigens due to its anhydrous character.

6.3.2. Significance of murine skin models towards *in vivo* generated cytotoxic T-cell activation

Choosing a convincing animal model in order to convey results to the situation in humans depends on multiple factors. The permeability of a variety of different animal skin samples has been studied for fast penetrating but also slow absorbing compounds. Moreover, physiological differences such as the thickness of SC, epidermis, and the whole skin but also the density of hair follicles were taken into account. Within that study, thickness of SC was found to be important, however, differences in permeability and SC thickness did not correlate 1:1. The authors emphasize that the animal model of choice is dependent on the respective compound [169].

Permeation data on human skin on the one hand would be desirable, however such a skin model is not the be-all and end-all. As it is described in literature, a human membrane is not produced as easily as an animal membrane and its properties vary from sample to sample due to differences in age, sex, race and health of the donor even if skin samples are removed from the same anatomic site [170]. Additionally, it is not available on demand and must be frozen for variable periods, a condition that induces some physicochemical alteration.

In terms of future perspective, skin sectioning for instance by tape stripping might allow conclusions as to which extent imiquimod permeates across the SC over a defined time period. Additionally, investigations on follicular API reservoirs offer promising insights into TCI efficiency but also further development efforts.

7. References

[1] P. Grasso, Essentials of pathology for toxicologists, CRC Press, 2004.

[2] A. Vollmar, I. Zündorf, T. Dingermann, Immunologie Grundlagen und Wirkstoffe, 2012.

[3] L.A. Hussain, T. Lehner; Comparative investigation of Langerhans' cells and potential receptors for HIV in oral, genitourinary and rectal epithelia. Immunology 85(3) (1995) 475-484.

[4] K. Takeda, S. Akira; Toll-like receptors. Current protocols in immunology / edited by John E. Coligan ... [et al Chapter 14 (2007) Unit 14 12.

[5] E.A. Grillot de Givry, Le musee des sorciers, mages et alchimistes, Librairie de France, 1929.

[6] M. Ditton, Die Bedeutung der Frauen bei der Entwicklung der Geburtshilfe. Ludwig-Maximilians Universität München, 1929.

[7] T.R. Forbes; Midwifery and witchcraft. Journal of the history of medicine and allied sciences 17 (1962) 264-283.

[8] M.R. Prausnitz, S. Mitragotri, R. Langer; Current status and future potential of transdermal drug delivery. Nature Reviews Drug Discovery 3(2) (2004) 115-124.

[9] E. Mutschler, Mutschler Arzneimittelwirkungen: Lehrbuch der Pharmakologie und Toxikologie, Wiss. Verl.-Ges., Stuttgart, 2008, 2008.

[10] Ādas vēzis, tā riska raktori un melanomas jutības gēns CDKN2A, http://www.anti-aging-skin-care.com/forever-young-how-it-works-diagram.html, 2004

[11] G.M. Glenn, R.T. Kenney, L.R. Ellingsworth, S.A. Frech, S.A. Hammond, J.P. Zoeteweij; Transcutaneous immunization and immunostimulant strategies: capitalizing on the immunocompetence of the skin. Expert review of vaccines 2(2) (2003) 253-267.

[12] J.D. Bos, M.M. Meinardi; The 500 Dalton rule for the skin penetration of chemical compounds and drugs. Experimental dermatology 9(3) (2000) 165-169.

[13] P. Langguth, G. Fricker, H. Wunderli-Allenspach, Biopharmazie, Wiley-VCH, Weinheim, 2004.

[14] M.L. Williams, P.M. Elias; From basket weave to barrier. Unifying concepts for the pathogenesis of the disorders of cornification. Archives of dermatology 129(5) (1993) 626-629.

[15] G.K. Menon; New insights into skin structure: scratching the surface. Adv Drug Deliv Rev 54 Suppl 1 (2002) S3-17.

[16] R. Voigt, A. Fahr, Pharmazeutische Technologie: für Studium und Beruf Dt. Apotheker-Verl., Stuttgart, 2010.

[17] H.E. Junginger, H.E. Bodde, F.H.N. De Haan; Visualization of drug transport across human skin and the influence of penetration enhancers. Drug Permeation Enhancement 62 (1994) 59-89.

[18] J. Hadgraft; Modulation of the Barrier Function of the Skin. Skin Pharmacology and Physiology 14(suppl 1)(Suppl. 1) (2001) 72-81.

[19] J. Bouwstra, G. Pilgram, G. Gooris, H. Koerten, M. Ponec; New aspects of the skin barrier organization. Skin pharmacology and applied skin physiology 14 Suppl 1 (2001) 52-62.

[20] J. Lademann, H. Richter, U.F. Schaefer, U. Blume-Peytavi, A. Teichmann, N. Otberg, W. Sterry; Hair follicles - a long-term reservoir for drug delivery. Skin Pharmacol Physiol 19(4) (2006) 232-236.

[21] H. Schaefer, T.E. Redelmeier, Skin barrier: principles of percutaneous absorption Karger, Basel {[u.a.], 1996.

[22] M. Ossadnik, H. Richter, A. Teichmann, S. Koch, U. Schäfer, R. Wepf, W. Sterry, J. Lademann; Investigation of differences in follicular penetration of particle- and nonparticle-containing emulsions by laser scanning microscopy. Laser Physics 16(5) (2006) 747-750.

[23] J. Lademann, H. Richter, A. Teichmann, N. Otberg, U. Blume-Peytavi, J. Luengo, B. Weiss, U.F. Schaefer, C.M. Lehr, R. Wepf, W. Sterry; Nanoparticles-an efficient carrier for drug delivery into the hair follicles. Eur J Pharm Biopharm 66(2) (2007) 159-164.

[24] A.C. Williams, B.W. Barry; Penetration enhancers. Advanced drug delivery reviews 56(5) (2004) 603-618.

[25] N. Buyuktimkin; Transdermal drug permeation enhancement. Transdermal and Topical Drug Delivery Systems (1997) 357-475.

[26] E. Touitou, N. Dayan, L. Bergelson, B. Godin, M. Eliaz; Ethosomes - novel vesicular carriers for enhanced delivery: characterization and skin penetration properties. J Control Release 65(3) (2000) 403-418.

[27] S. Patil, P. Singh, C. Szolar-Platzer, H. Maibach; Epidermal enzymes as penetration enhancers in transdermal drug delivery? Journal of pharmaceutical sciences 85(3) (1996) 249-252.

[28] H.E. Hofland, R. van der Geest, H.E. Bodde, H.E. Junginger, J.A. Bouwstra; Estradiol permeation from nonionic surfactant vesicles through human stratum corneum in vitro. Pharmaceutical research 11(5) (1994) 659-664.

[29] Y. Yokomizo, H. Sagitani; Effects of phospholipids on the in vitro percutaneous penetration of prednisolone and analysis of mechanism by using attenuated total reflectance-Fourier transform infrared spectroscopy. Journal of pharmaceutical sciences 85(11) (1996) 1220-1226.

[30] B.W. Barry., Dermatological formulations: Percutaneous absorption, 1984.

[31] B.W. Barry; Novel mechanisms and devices to enable successful transdermal drug delivery. European Journal of Pharmaceutical Sciences 14(2) (2001) 101-114.

[32] G.K. Menon, D.B. Bommannan, P.M. Elias; High-frequency sonophoresis: permeation pathways and structural basis for enhanced permeability. Skin Pharmacol 7(3) (1994) 130-139.

[33] B.W. Barry; Mode of action of penetration enhancers in human skin. Journal of Controlled Release 6(1) (1987) 85-97.

[34] R.L. Bronaugh, H.I. Maibach, Percutaneous Absorption; Drugs-Cosmetics-Mechanism-Methodology, 1985.

[35] A.N.C. Anigbogu, A.C. Williams, B.W. Barry, H.G.M. Edwards; Fourier transform raman spectroscopy of interactions between the penetration enhancer dimethyl sulfoxide and human stratum corneum. International Journal of Pharmaceutics 125(2) (1995) 265-282.

[36] M.B. Sulzberger, T.A. Cortese, L. Fishman, H.S. Wiley, P.S. Peyakovich; Some effects of DMSO on human skin in vivo. Annals of the New York Academy of Sciences 141(1) (1967) 437-450.

[37] A.M. Kligman; Topical Pharmacology and Toxicology of Dimethyl Sulfoxide. Part 1. Jama 193 (1965) 796-804.

References

[38] R.R. Stoughton, W.O. McClure; Azone: A New Non-Toxic Enhancer of Cutaneous Penetration. Drug Development and Industrial Pharmacy 9(4) (1983) 725-744.

[39] G. Allan; Azone® - Percutaneous penetration enhancers. CRC Press (1995) 129-136.

[40] I.B. Pathan, C.M. Setty; Chemical penetration enhancers for transdermal drug delivery systems. Tropical Journal of Pharmaceutical Research 8(2) (2009).

[41] A.J. Hoogstraate, J. Verhoef, J. Brussee, A.P. Ijzerman, F. Spies, H.E. Bodde; Kinetics, ultrastructural aspects and molecular modelling of transdermal peptide flux enhancement by N-alkylazacycloheptanones. International Journal of Pharmaceutics 76(1-2) (1991) 37-47.

[42] J.W. Wiechers, B.F. Drenth, J.H. Jonkman, R.A. de Zeeuw; Percutaneous absorption and elimination of the penetration enhancer Azone in humans. Pharmaceutical research 4(6) (1987) 519-523.

[43] C.A. Phillips, B.B. Michniak; Topical application of Azone analogs to hairless mouse skin: A histopathological study. International Journal of Pharmaceutics 125(1) (1995) 63-71.

[44] M. Lopez-Cervantes, E. Marquez-Mejia, J. Cazares-Delgadillo, D. Quintanar-Guerrero, A. Ganem-Quintanar, E. Angeles-Anguiano; Chemical enhancers for the absorption of substances through the skin: Laurocapram and its derivatives. Drug Dev Ind Pharm 32(3) (2006) 267-286.

[45] M.E. Lane; Skin penetration enhancers. Int J Pharm 447(1-2) (2013) 12-21.

[46] E.W. Smith, H.I. Maibach, Percutaneous penetration enhancers, CRC Press, 1995.

[47] T. Kurihara-Bergstrom, K. Knutson, L.J. DeNoble, C.Y. Goates; Percutaneous absorption enhancement of an ionic molecule by ethanol-water systems in human skin. Pharmaceutical research 7(7) (1990) 762-766.

[48] R.M. Watkinson, C. Herkenne, R.H. Guy, J. Hadgraft, G. Oliveira, M.E. Lane; Influence of ethanol on the solubility, ionization and permeation characteristics of ibuprofen in silicone and human skin. Skin Pharmacol Physiol 22(1) (2009) 15-21.

[49] M.E. Lane; The transdermal delivery of fentanyl. Eur J Pharm Biopharm 84(3) (2013) 449-455.

[50] A.C. Williams, B.W. Barry; Essential oils as novel human skin penetration enhancers. International Journal of Pharmaceutics 57(2) (1989) R7-R9.

[51] A. Williams, B. Barry; Terpenes and the Lipid-Protein-Partitioning Theory of Skin Penetration Enhancement. Pharmaceutical research 8(1) (1991) 17-24.

[52] E.L. Giudice, J.D. Campbell; Needle-free vaccine delivery. Adv Drug Deliv Rev 58(1) (2006) 68-89.

[53] B. Combadiere, B. Mahe; Particle-based vaccines for transcutaneous vaccination. Comp Immunol Microbiol Infect Dis 31(2-3) (2008) 293-315.

[54] L. Simonsen, A. Kane, J. Lloyd, M. Zaffran, M. Kane; In Focus-Unsafe injections in the developing world and transmission of bloodborne pathogens: A review. Bulletin of the World Health Organization 77(10) (1999) 789-800.

[55] B. Aylward, M. Kane, R. McNair-Scott, D.J. Hu, D.H. Hu; Model-based estimates of the risk of human immunodeficiency virus and hepatitis B virus transmission through unsafe injections. International journal of epidemiology 24(2) (1995) 446-452.

[56] B. Aylward, J. Lloyd, M. Zaffran, R. McNair-Scott, P. Evans; Reducing the risk of unsafe injections in immunization programmes: financial and operational implications of various injection technologies. Bulletin of the World Health Organization 73(4) (1995) 531-540.

[57] A. Kane, J. Lloyd, M. Zaffran, L. Simonsen, M. Kane; Transmission of hepatitis B, hepatitis C and human immunodeficiency viruses through unsafe injections in the developing world: model-based regional estimates. Bulletin of the World Health Organization 77(10) (1999) 801-807.

[58] L. Simonsen, A. Kane, J. Lloyd, M. Zaffran, M. Kane; Unsafe injections in the developing world and transmission of bloodborne pathogens: a review. Bulletin of the World Health Organization 77 (1999) 789-800.

[59] R. Koch-Institut, Impfkalender. Vol. 2013, http://www.rki.de/DE/Content/Kommissionen/STIKO/Empfehlungen/Aktuelles/Impfkalender.pdf?__blob=publicationFile, 2013

[60] R.M. Jacobson, A. Swan, A. Adegbenro, S.L. Ludington, P.C. Wollan, G.A. Poland; Making vaccines more acceptable--methods to prevent and minimize pain and other common adverse events associated with vaccines. Vaccine 19(17-19) (2001) 2418-2427.

[61] Y. Nir, A. Paz, E. Sabo, I. Potasman; Fear of injections in young adults: prevalence and associations. The American journal of tropical medicine and hygiene 68(3) (2003) 341-344.

[62] D.U. Ekwueme, B.G. Weniger, R.T. Chen; Model-based estimates of risks of disease transmission and economic costs of seven injection devices in sub-Saharan Africa. Bulletin of the World Health Organization 80(11) (2002) 859-870.

[63] Y. Roth, J.S. Chapnik, P. Cole; Feasibility of aerosol vaccination in humans. The Annals of otology, rhinology, and laryngology 112(3) (2003) 264-270.

[64] R.T. Kenney, S.A. Frech, L.R. Muenz, C.P. Villar, G.M. Glenn; Dose sparing with intradermal injection of influenza vaccine. The New England journal of medicine 351(22) (2004) 2295-2301.

[65] H. Micozkadioglu, A. Zumrutdal, D. Torun, S. Sezer, F.N. Ozdemir, M. Haberal; Low Dose Intradermal Vaccination Is Superior to High Dose Intramuscular Vaccination for Hepatitis B in Unresponsive Hemodialysis Patients. Clinical Studies 29(3) (2007) 285-288.

[66] S.S. Chiu, J.S. Peiris, K.H. Chan, W.H. Wong, Y.L. Lau; Immunogenicity and safety of intradermal influenza immunization at a reduced dose in healthy children. Pediatrics 119(6) (2007) 1076-1082.

[67] J. Lang, D.Q. Hoa, N.V. Gioi, N.C. Vien, C.V. Nguyen, N. Rouyrre, R. Forrat; Immunogenicity and safety of low-dose intradermal rabies vaccination given during an Expanded Programme on immunization session in Viet Nam: results of a comparative randomized trial. Transactions of the Royal Society of Tropical Medicine and Hygiene 93(2) (1999) 208-213.

[68] M.K. Sudarshan, S.N. Madhusudana, B.J. Mahendra, D.A. Narayana, M.A. Giri, K. Muhamuda, H.S. Ravish, G.M. Venkatesh; Boosting effect of purified chick embryo cell rabies vaccine using the intradermal route in persons previously immunized by the intramuscular route or vice versa. The National Medical Journal of India 19(4) (2006) 192.

[69] P. Auewarakul, U. Kositanont, P. Sornsathapornkul, P. Tothong, R. Kanyok, P. Thongcharoen; Antibody responses after dose-sparing intradermal influenza vaccination. Vaccine 25(4) (2007) 659-663.

[70] K.B. Lankarani, A.R. Taghavi, S. Agah, A. Karimi; Comparison of intradermal and intramuscular administration of hepatitis B vaccine in neonates. Indian J Gastroenterol 20(3) (2001) 94-96.

References

[71] H.S. Gill, D.D. Denson, B.A. Burris, M.R. Prausnitz; Effect of microneedle design on pain in human volunteers. The Clinical journal of pain 24(7) (2008) 585-594.

[72] F.J. Verbaan, S.M. Bal, D.J. van den Berg, W.H. Groenink, H. Verpoorten, R. Luttge, J.A. Bouwstra; Assembled microneedle arrays enhance the transport of compounds varying over a large range of molecular weight across human dermatomed skin. J Control Release 117(2) (2007) 238-245.

[73] M.S. Gerstel, V.A. Place, 1976, Drug delivery device, Patent US3964482 A

[74] S. Henry, D.V. McAllister, M.G. Allen, M.R. Prausnitz; Microfabricated microneedles: a novel approach to transdermal drug delivery. Journal of pharmaceutical sciences 87(8) (1998) 922-925.

[75] Z. Ding, F.J. Verbaan, M. Bivas-Benita, L. Bungener, A. Huckriede, D.J. van den Berg, G. Kersten, J.A. Bouwstra; Microneedle arrays for the transcutaneous immunization of diphtheria and influenza in BALB/c mice. J Control Release 136(1) (2009) 71-78.

[76] H.S. Gill, M.R. Prausnitz; Coating formulations for microneedles. Pharmaceutical research 24(7) (2007) 1369-1380.

[77] Q. Zhu, V.G. Zarnitsyn, L. Ye, Z. Wen, Y. Gao, L. Pan, I. Skountzou, H.S. Gill, M.R. Prausnitz, C. Yang, R.W. Compans; Immunization by vaccine-coated microneedle arrays protects against lethal influenza virus challenge. Proceedings of the National Academy of Sciences of the United States of America 106(19) (2009) 7968-7973.

[78] U.O. Hafeli, A. Mokhtari, D. Liepmann, B. Stoeber; In vivo evaluation of a microneedle-based miniature syringe for intradermal drug delivery. Biomedical microdevices 11(5) (2009) 943-950.

[79] J.A. Mikszta, P.E. Laurent; Cutaneous delivery of prophylactic and therapeutic vaccines: historical perspective and future outlook. Expert review of vaccines 7(9) (2008) 1329-1339.

[80] M.L. Crichton, A. Ansaldo, X. Chen, T.W. Prow, G.J.P. Fernando, M.A.F. Kendall; The effect of strain rate on the precision of penetration of short densely-packed microprojection array patches coated with vaccine. Biomaterials 31(16) (2010) 4562-4572.

[81] R.A. Hingson, H.S. Davis, M. Rosen; Historical development of jet injection and envisioned uses in mass immunization and mass therapy based upon two decades' experience. Mil. Med. 128 (1963) 516-524.

[82] L.A. Jackson, G. Austin, R.T. Chen, R. Stout, F. DeStefano, G.J. Gorse, F.K. Newman, O. Yu, B.G. Weniger; Safety and immunogenicity of varying dosages of trivalent inactivated influenza vaccine administered by needle-free jet injectors. Vaccine 19(32) (2001) 4703-4709.

[83] J. Canter, K. Mackey, L.S. Good, et al.; An outbreak of hepatitis b associated with jet injections in a weight reduction clinic. Archives of Internal Medicine 150(9) (1990) 1923-1927.

[84] S. Mitragotri; Immunization without needles. Nature Reviews Immunology 5(12) (2005) 905-916.

[85] G.M. Glenn, T. Scharton-Kersten, R. Vassell, G.R. Matyas, C.R. Alving; Transcutaneous immunization with bacterial ADP-ribosylating exotoxins as antigens and adjuvants. Infection and immunity 67(3) (1999) 1100-1106.

[86] D.P. Snider; The mucosal adjuvant activities of ADP-ribosylating bacterial enterotoxins. Critical reviews in immunology 15(3-4) (1995) 317-348.

[87] W. Dallas, S. Falkow; Amino acid sequence homology between cholera toxin and Escherichia coli heat-labile toxin. Nature publishing group(288) (1980) 499-501.

[88] D.G. Millar, T.R. Hirst, D.P. Snider; Escherichia coli Heat-Labile Enterotoxin B Subunit Is a More Potent Mucosal Adjuvant than Its Closely Related Homologue, the B Subunit of Cholera Toxin. Infection and immunity 69 (2001) 3476-3482.

[89] G.M. Glenn, T. Scharton-Kersten, R. Vassell, C.P. Mallett, T.L. Hale, C.R. Alving; Transcutaneous immunization with cholera toxin protects mice against lethal mucosal toxin challenge. J Immunol 161(7) (1998) 3211-3214.

[90] J. Yu, F. Cassels, T. Scharton-Kersten, S.A. Hammond, A. Hartman, E. Angov, B. Corthesy, C. Alving, G. Glenn; Transcutaneous immunization using colonization factor and heat-labile enterotoxin induces correlates of protective immunity for enterotoxigenic Escherichia coli. Infection and immunity 70(3) (2002) 1056-1068.

[91] S.A. Hammond, D. Walwender, C.R. Alving, G.M. Glenn; Transcutaneous immunization: T cell responses and boosting of existing immunity. Vaccine 19(17-19) (2001) 2701-2707.

[92] K. Fujihashi, T. Koga, F.W. van Ginkel, Y. Hagiwara, J.R. McGhee; A dilemma for mucosal vaccination: efficacy versus toxicity using enterotoxin-based adjuvants. Vaccine 20(19-20) (2002) 2431-2438.

[93] M.M. Levine, J.B. Kaper, R.E. Black, M.L. Clements; New knowledge on pathogenesis of bacterial enteric infections as applied to vaccine development. Microbiol Rev 47(4) (1983) 510-550.

[94] Z. Ding, S.M. Bal, S. Romeijn, G.F. Kersten, W. Jiskoot, J.A. Bouwstra; Transcutaneous immunization studies in mice using diphtheria toxoid-loaded vesicle formulations and a microneedle array. Pharmaceutical research 28(1) (2010) 145-158.

[95] S.P. Vyas, R.P. Singh, S. Jain, V. Mishra, S. Mahor, P. Singh, P.N. Gupta, A. Rawat, P. Dubey; Non-ionic surfactant based vesicles (niosomes) for non-invasive topical genetic immunization against hepatitis B. Int J Pharm 296(1-2) (2005) 80-86.

[96] G. Cevc, D. Gebauer, J. Stieber, A. Schätzlein, G. Blume; Ultraflexible vesicles, Transfersomes, have an extremely low pore penetration resistance and transport therapeutic amounts of insulin across the intact mammalian skin. Biochimica et Biophysica Acta (BBA) - Biomembranes 1368(2) (1998) 201-215.

[97] P.N. Gupta, V. Mishra, P. Singh, A. Rawat, P. Dubey, S. Mahor, S.P. Vyas; Tetanus toxoid-loaded transfersomes for topical immunization. The Journal of pharmacy and pharmacology 57(3) (2005) 295-301.

[98] P.N. Gupta, V. Mishra, A. Rawat, P. Dubey, S. Mahor, S. Jain, D.P. Chatterji, S.P. Vyas; Non-invasive vaccine delivery in transfersomes, niosomes and liposomes: a comparative study. Int J Pharm 293(1-2) (2005) 73-82.

[99] A. Saupe, T. Rades, Nanocarrier Technologies, Springer, 2006, pp. 41-50.

[100] M.A. Clark, M.A. Jepson, B.H. Hirst; Exploiting M cells for drug and vaccine delivery. Advanced Drug Delivery Reviews 50(1-2) (2001) 81-106.

[101] M. Friede, M.T. Aguado; Need for new vaccine formulations and potential of particulate antigen and DNA delivery systems. Advanced Drug Delivery Reviews 57 (2005) 325-331.

[102] A.O. Gamer, E. Leibold, B. van Ravenzwaay; The in vitro absorption of microfine zinc oxide and titanium dioxide through porcine skin. Toxicology in Vitro 20(3) (2006) 301-307.

[103] L.W. Zhang, W.W. Yu, V.L. Colvin, N.A. Monteiro-Riviere; Biological interactions of quantum dot nanoparticles in skin and in human epidermal keratinocytes. Toxicology and applied pharmacology 228(2) (2008) 200-211.

[104] N.A. Monteiro-Riviere, J.E. Riviere; Interaction of nanomaterials with skin: Aspects of absorption and biodistribution. Nanotoxicology 3(3) (2009) 188-193.

[105] T. Gratieri, U.F. Schaefer, L. Jing, M. Gao, K.H. Kostka, R.F. Lopez, M. Schneider; Penetration of quantum dot particles through human skin. Journal of biomedical nanotechnology 6(5) (2010) 586-595.

[106] R. Toll, U. Jacobi, H. Richter, J. Lademann, H. Schaefer, U. Blume-Peytavi; Penetration profile of microspheres in follicular targeting of terminal hair follicles. The Journal of investigative dermatology 123(1) (2004) 168-176.

[107] A. Patzelt, H. Richter, F. Knorr, U. Schafer, C.M. Lehr, L. Dahne, W. Sterry, J. Lademann; Selective follicular targeting by modification of the particle sizes. J Control Release 150(1) (2011) 45-48.

[108] H. Fan, Q. Lin, G.R. Morrissey, P.A. Khavari; Immunization via hair follicles by topical application of naked DNA to normal skin. Nature biotechnology 17(9) (1999) 870-872.

[109] L.W. Phipps; Some operating characteristics of a simple homogenizing poppet valve; pressure profiles and separation: zone of fat globule dispersion. Journal of Diary Research 41(03) (1974) 339-347.

[110] M. Siewert, J. Dressman, C. Brown, V. Shah, J.-M. Aiache, N. Aoyagi, D. Bashaw, C. Brown, W. Brown, D. Burgess, J. Crison, P. DeLuca, R. Djerki, J. Dressman, T. Foster, K. Gjellan, V. Gray, A. Hussain, T. Ingallinera, J. Klancke, J. Kraemer, H. Kristensen, K. Kumi, C. Leuner, J. Limberg, P. Loos, L. Margulis, P. Marroum, H. Moeller, B. Mueller, M. Mueller-Zsigmondy, N. Okafo, L. Ouderkirk, S. Parsi, S. Qureshi, J. Robinson, V. Shah, M. Siewert, R. Uppoor, R. Williams; FIP/AAPS guidelines to dissolution/in vitro release testing of novel/special dosage forms. AAPS PharmSciTech 4(1) (2003) 43-52.

[111] V.P. Shah, Jerome S. Elkins, Roger L. Williams.; Evaluation of the Test System Used for In Vitro Release of Drugs for Topical Dermatological Drug Products. Pharmaceutical development and technology 4.3 (1999) 377-385.

[112] EDC-07 Diffusions Zelle, Labswiss International AG, http://www.labswiss.com/produkte/electrolab/Diffusionsapparatur.php, 2013

[113] A. Dominik, D. Steinhilber, Instrumentelle Analytik für Pharmazeuten : Kurzlehrbuch, Original-Fragen und Kommentare zum GKP 1, Jungjohann bei Fischer, Ulm {[u.a.], 1996.

[114] R. Erni, M.D. Rossell, C. Kisielowski, U. Dahmen; Atomic-Resolution Imaging with a Sub-50-pm Electron Probe. Physical Review Letters 102(9) (2009) 096101.

[115] A.N. Martin, H. Leuenberger, Physikalische Pharmazie pharmazeutisch angewandte physikalisch-chemische Grundlagen Wiss. Verl.-Ges., Stuttgart, 2002.

[116] H. Hemmi, T. Kaisho, O. Takeuchi, S. Sato, H. Sanjo, K. Hoshino, T. Horiuchi, H. Tomizawa, K. Takeda, S. Akira; Small anti-viral compounds activate immune cells via the TLR7 MyD88-dependent signaling pathway. Nat Immunol 3(2) (2002) 196-200.

[117] L.L. Thomsen, P. Topley, M.G. Daly, S.J. Brett, J.P. Tite; Imiquimod and resiquimod in a mouse model: adjuvants for DNA vaccination by particle-mediated immunotherapeutic delivery. Vaccine 22(13-14) (2004) 1799-1809.

[118] T. Warger, G. Rechtsteiner, B. Schmid, P. Osterloh, H. Schild, M.P. Radsak; Transcutaneous immunization with imiquimod is amplified by CD40 ligation and results in sustained cytotoxic T-lymphocyte activation and tumor protection. Clin Rev Allergy Immunol 32(1) (2007) 57-66.

[119] P. Stein, G. Rechtsteiner, T. Warger, T. Bopp, T. Fuhr, S. Prufer, H.C. Probst, M. Stassen, P. Langguth, H. Schild, M.P. Radsak; UV exposure boosts transcutaneous immunization and improves tumor immunity: cytotoxic T-cell priming through the skin. The Journal of investigative dermatology 131(1) (2011) 211-219.

[120] Fachinformation Aldara 5% creme Sachez, MEDA Pharma GmbH & Co. KG, http://www.fachinfo.de/suche/fi/003976, 2010

[121] M. Schön, A.B. Bong, C. Drewniok, J. Herz, C.C. Geilen, J. Reifenberger, B. Benninghoff, H.B. Slade, H. Gollnick, M.P. Schon; Tumor-selective induction of apoptosis and the small-molecule immune response modifier imiquimod. Journal of the National Cancer Institute 95(15) (2003) 1138-1149.

[122] D. De Paula, C.A. Martins, M.V. Bentley; Development and validation of HPLC method for imiquimod determination in skin penetration studies. Biomed Chromatogr 22(12) (2008) 1416-1423.

[123] J.L. Chollet, M.J. Jozwiakowski, K.R. Phares, M.J. Reiter, P.J. Roddy, H.J. Schultz, Q.V. Ta, M.A. Tomai; Development of a topically active imiquimod formulation. Pharm Dev Technol 4(1) (1999) 35-43.

[124] L.I. Harrison, J.D. Stoesz, J.L. Battiste, R.J. Nelson, I.E. Zarraga; A pharmaceutical comparison of different commercially available imiquimod 5% cream products. The Journal of dermatological treatment 20(3) (2009) 1-5.

[125] J.W. Moore, H.H. Flanner; Mathematical comparison of dissolution profiles. Pharm. Tech 20 (1996) 64-74.

[126] J.E. Polli, G.S. Rekhi, L.L. Augsburger, V.P. Shah; Methods to compare dissolution profiles and a rationale for wide dissolution specifications for metoprolol tartrate tablets. Journal of pharmaceutical sciences 86(6) (1997) 690-700.

[127] P. Stein, Transkutane Immunisierung –Mechanismen und

Optimierungsstrategien. Fachbereich Biologie der Johannes Gutenberg-Universität Mainz, Vol. PhD, Johannes Gutenberg-Universität, Mainz, 2010, p. 112.

[128] G. Rechtsteiner, T. Warger, P. Osterloh, H. Schild, M.P. Radsak; Cutting edge: priming of CTL by transcutaneous peptide immunization with imiquimod. J Immunol 174(5) (2005) 2476-2480.

[129] K. Schroder, P.J. Hertzog, T. Ravasi, D.A. Hume, Interferon-gamma: an overview of signals, mechanisms and functions, 2004.

[130] A. Hanefeld, M.V. Schmidt, S. Geissler, P. Langguth, 2009, Lyophilized nanoemulsion, Patent US8211948 B2.

[131] J. Lee, S.-J. Lee, J.-Y. Choi, J.Y. Yoo, C.-H. Ahn; Amphiphilic amino acid copolymers as stabilizers for the preparation of nanocrystal dispersion. European Journal of Pharmaceutical Sciences 24(5) (2005) 441-449.

[132] T.L. Hill; A Different Approach to Nanothermodynamics. Nano Letters 1(5) (2001) 273-275.

[133] J. Lee, J.Y. Choi, C.H. Park; Characteristics of polymers enabling nano-comminution of water-insoluble drugs. Int J Pharm 355(1-2) (2008) 328-336.

[134] B. Van Eerdenbrugh, J. Vermant, J.A. Martens, L. Froyen, J. Van Humbeeck, P. Augustijns, G. Van den Mooter; A screening study of surface stabilization during the production of drug nanocrystals. Journal of pharmaceutical sciences 98(6) (2009) 2091-2103.

[135] G. Winckle, D.W. Osborne, 2009, Imiquimod formulation, Patent US20090182004 A1.

[136] L. van der Fits, S. Mourits, J.S. Voerman, M. Kant, L. Boon, J.D. Laman, F. Cornelissen, A.M. Mus, E. Florencia, E.P. Prens, E. Lubberts; Imiquimod-induced psoriasis-like skin inflammation in mice is mediated via the IL-23/IL-17 axis. J Immunol 182(9) (2009) 5836-5845.

[137] K. Gogoll, P. Stein, H. Wei, H. Schild, M. Radsak, P. Langguth; Comparative transcutaneous immunization with imiquimod-containing ointments and potential of in vitro methods to predict effects. Biopharm Drug Dispos 33(4) (2011) 218-228.

[138] T. Dingermann, K. Hiller, G. Schneider, I. Zündorf, Schneider Arzneidrogen, 2004.

[139] M.T. Hierro, M.C. Tomas, F. Fernandez-Martin, G. Santa-Maria; Determination of the triglyceride composition of avocado oil by high-performance liquid chromatography using a light-scattering detector. J Chromatogr 607(2) (1992) 329-338.

[140] T. Miwa; Structural determination and uses of jojoba oil. Journal of the American Oil Chemists' Society 61(2) (1984) 407-410.

[141] G.S. Kelly; Squalene and its potential clinical uses. Altern Med Rev 4(1) (1999) 29-36.

[142] L.P. Rastrelli, S.; Ippolito, F.; Vacca, G.; De Simone, F.; Rate of degradation of a-tocopherol, squalene, phenolics, and polyunsaturated fatty acids in olive oil during different storage conditions. J. Agricul. Food Chem 50 (2002) 5566-5570.

[143] A. Seubert, E. Monaci, M. Pizza, D.T. O'Hagan, A. Wack; The adjuvants aluminum hydroxide and MF59 induce monocyte and granulocyte chemoattractants and enhance monocyte differentiation toward dendritic cells. Journal of immunology (Baltimore, Md. : 1950) 180(8) (2008) 5402-5412.

[144] X. Ma, J. Taw, C.-M. Chiang; Control of drug crystallization in transdermal matrix system. International Journal of Pharmaceutics 142(1) (1996) 115-119.

[145] W. Weyenberg, P. Filev, D. Van den Plas, J. Vandervoort, K. De Smet, P. Sollie, A. Ludwig; Cytotoxicity of submicron emulsions and solid lipid nanoparticles for dermal application. International journal of pharmaceutics 337(1-2) (2007) 291-298.

[146] C.B. Lippold, H. Schneemann; The influence of vehicles on the local bioavailability of betamethasone-17-benzoate from solution- and suspension-type ointments. International Journal of Pharmaceutics 22 (1984) 31-43.

[147] U. Blume-Peytavi, L. Massoudy, A. Patzelt, J. Lademann, E. Dietz, U. Rasulev, N. Garcia Bartels; Follicular and percutaneous penetration pathways of topically applied minoxidil foam. Eur J Pharm Biopharm 76(3) 450-453.

[148] F. Knorr, J. Lademann, A. Patzelt, W. Sterry, U. Blume-Peytavi, A. Vogt; Follicular transport route-research progress and future perspectives. Eur J Pharm Biopharm 71(2) (2009) 173-180.

[149] J. Lademann, N. Otberg, H. Richter, H.J. Weigmann, U. Lindemann, H. Schaefer, W. Sterry; Investigation of follicular penetration of topically applied substances. Skin pharmacology and applied skin physiology 14 Suppl 1 (2001) 17-22.

[150] A. Rolland, N. Wagner, A. Chatelus, B. Shroot, H. Schaefer; Site-specific drug delivery to pilosebaceous structures using polymeric microspheres. Pharmaceutical research 10(12) (1993) 1738-1744.

[151] V.P. Shah, J. Elkins, S.-Y. Lam, J.P. Skelly; Determination of in vitro drug release from hydrocortisone creams. International Journal of Pharmaceutics 53(1) (1989) 53-59.

[152] B. Young, P.R. Wheater, Wheater's functional histology : a text and colour atlas, Churchill Livingstone, Elsevier, Philadelphia, Pa, 2000

[153] B.J. Aungst; Structure/effect studies of fatty acid isomers as skin penetration enhancers and skin irritants. Pharm Res 6(3) (1989) 244-247.

[154] Guide to similar grades of Sucrose Esters, Mitsubishi-Kagaku Foods Corporation, http://www.mfc.co.jp/english/productinfor.htm, 2002

[155] G. Csoka, S. Marton, R. Zelko, N. Otomo, I. Antal; Application of sucrose fatty acid esters in transdermal therapeutic systems. Eur J Pharm Biopharm 65(2) (2007) 233-237.

[156] U. Blume-Peytavi, L. Massoudy, A. Patzelt, J. Lademann, E. Dietz, U. Rasulev, N. Garcia Bartels; Follicular and percutaneous penetration pathways of topically applied minoxidil foam. Eur J Pharm Biopharm 76(3) (2010) 450-453.

[157] J. Lademann, F. Knorr, H. Richter, U. Blume-Peytavi, A. Vogt, C. Antoniou, W. Sterry, A. Patzelt; Hair follicles--an efficient storage and penetration pathway for topically applied substances. Summary of recent results obtained at the Center of Experimental and Applied Cutaneous Physiology, Charite -Universitatsmedizin Berlin, Germany. Skin Pharmacol Physiol 21(3) (2008) 150-155.

[158] J. Lademann, H. Richter, A. Teichmann, N. Otberg, U. Blume-Peytavi, J. Luengo, B. Weiss, U.F. Schaefer, C.M. Lehr, R. Wepf, W. Sterry; Nanoparticles--an efficient carrier for drug delivery into the hair follicles. Eur J Pharm Biopharm 66(2) (2007) 159-164.

[159] A.M. El Badawy, T.P. Luxton, R.G. Silva, K.G. Scheckel, M.T. Suidan, T.M. Tolaymat; Impact of environmental conditions (pH, ionic strength, and electrolyte type) on the surface charge and aggregation of silver nanoparticles suspensions. Environmental science & technology 44(4) 1260-1266.

[160] H.S. Shin, H.J. Yang, S.B. Kim, M.S. Lee; Mechanism of growth of colloidal silver nanoparticles stabilized by polyvinyl pyrrolidone in gamma-irradiated silver nitrate solution. J Colloid Interface Sci 274(1) (2004) 89-94.

[161] M. Shevachman, N. Garti, A. Shani, A.C. Sintov; Enhanced percutaneous permeability of diclofenac using a new U-type dilutable microemulsion. Drug development and industrial pharmacy 34(4) (2008) 403-412.

[162] P. Stein, K. Gogoll, S. Tenzer, H. Schild, S. Stevanovic, P. Langguth, M.P. Radsak; Efficacy of imiquimod-based transcutaneous immunization using a nano-dispersed emulsion gel formulation. PloS one 9(7) (2014) e102664.

[163] A. Walter, M. Schafer, V. Cecconi, C. Matter, M. Urosevic-Maiwald, B. Belloni, N. Schonewolf, R. Dummer, W. Bloch, S. Werner, H.D. Beer, A. Knuth, M. van den

Broek; Aldara activates TLR7-independent immune defence. Nature communications 4 (2013) 1560.

[164] H. Gießen; Hilfsstoffe für bessere Vakzinen. Pharmazeutische Zeitung 48(2007) (2007) 24-25.

[165] K. Takahashi, S. Tamagawa, T. Katagi, H. Yoshitomi, A. Kamada, J.H. Rytting, T. Nishihata, N. Mizuno; In vitro transport of sodium diclofenac across rat abdominal skin: effect of selection of oleaginous component and the addition of alcohols to the vehicle. Chemical & pharmaceutical bulletin 39(1) (1991) 154-158.

[166] M.I. Afouna, T.K. Fincher, A.A. Zaghloul, I.K. Reddy; Effect of Azone upon the in vivo antiviral efficacy of cidofovir or acyclovir topical formulations in treatment/prevention of cutaneous HSV-1 infections and its correlation with skin target site free drug concentration in hairless mice. International journal of pharmaceutics 253(1-2) (2003) 159-168.

[167] C.S. Asbill, B.B. Michniak; Percutaneous penetration enhancers: local versus transdermal activity. Pharmaceutical science & technology today 3(1) (2000) 36-41.

[168] T. Ohkuma, K. Otagiri, S. Tanaka, T. Ikekawa; Intensification of host's immunity by squalene in sarcoma 180 bearing ICR mice. Journal of pharmacobio-dynamics 6(2) (1983) 148-151.

[169] R.L. Bronaugh, R.F. Stewart, E.R. Congdon; Methods for in vitro percutaneous absorption studies. II. Animal models for human skin. Toxicology and applied pharmacology 62(3) (1982) 481-488.

[170] R.T. Tregear, Physical functions of skin, Academic Press, London ; New York, 1966.

8. Zusammenfassung/ Abstract

Ziel der hier vorliegenden Arbeit ist die Entwicklung einer dermalen Impfzubereitung, welche in der Lage ist, zytotoxische T-Zellen zu aktivieren, um somit eine Tumor-spezifische Immunantwort auszulösen. Verwendung findet hier der Wirkstoff Imiquimod, ein kleines Molekül, welches eine Immunstimulation über den Weg der Toll-like Rezeptor 7 Aktivierung generiert. Neben dem europäischen Originalpräparat Aldara® 5% Creme existieren weltweit weitere Cremezubereitungen auf der Basis von fünf Prozent Imiquimod. Um neue Einblicke in die transkutane Immunisierung zu erhalten, wurden fünf verschiedene Cremezubereitungen hinsichtlich ihrer pharmazeutischen Eigenschaften charakterisiert. Die ermittelten Freisetzungsdaten wurden mit der Immunreaktion in zuvor dermal immunisierten Mäusen verglichen. Die physikochemischen Eigenschaften wie die sehr geringe Wasserlöslichkeit in Verbindung mit den hier gewonnen Erkenntnissen, bildeten die Grundlage, neue Formulierungskonzepte auf Basis von Sumbikron- bzw. Nanopartikel basiertem Imiquimod zu entwickeln. Gegenstand dieser Formulierungskonzepte sind unter anderem die Verwendung von Saccharosefettsäureestern, welche gleichsam als Emulgatoren, wie auch als Kryoprotektoren in gefriergetrockneten Formulierungen Verwendung finden. Durch ihren Status als Lebensmittelzusatzstoff sind Saccharosefettsäureester für pharmazeutische Zwecke von besonderem Interesse. Die Verwendung dieser Saccharose basierten Fettsäureester als wasserfreier gefriergetrockneter streichfähiger Formulierungsansatz in Kombination mit diversen pharmazeutischen Ölkomponenten bilden die Basis eines neuartigen dermalen Formulierungsansatzes. Ein weiterer Formulierungsansatz besteht aus einem Emulsionsgel, dessen Basis Jojobawachs darstellt. Neben rheologischen und mikroskopischen Untersuchungen wurde mittels Franz'scher Diffusionszelle der Einfluss unterschiedlicher Akzeptorlösungen, synthetischer Membranen sowie der exzidierten Haut von Mäusen hinsichtlich der im C57BL/6 Mausmodell ermittelten Immunstimulation untersucht. Die Quantifizierung des Wirkstoffes erfolgte sowohl mittels UV-Vis-Spektroskopie wie auch durch eine hierfür entwickelte HPLC-Methode. Im Rahmen der Produktcharakterisierung wiesen die kommerziell erhältlichen Cremes deutliche pharmazeutische Unterschiede auf. Im Gegensatz zu den mit synthetischen Membranen erhaltenen Ergebnissen korrelierten die mit Maushaut erhaltenen Resultate mit *in vivo* generierten Effekten in C57BL/6 Mäusen.

Weiterhin wurde durch die Verwendung von Maushaut ersichtlich, dass sich die einzelnen Cremes hinsichtlich des Vorhandenseins von kristallinem bzw. gelöstem Wirkstoff unterschieden. Bei der Entwicklung dermaler Imiquimod-Formulierungen wurde deutlich, dass Wirkstoffpartikel im Submikron- sowie Nanobereich vorteilhafte Eigenschaften aufweisen. Im Gegensatz dazu steht das Originalpräparat, welches den Wirkstoff vollständig in der Grundlage gelöst enthält. Im Rahmen der gefriergetrockneten Präparate zeigte sich ein starker Einfluss unterschiedlicher Ölkomponenten sowohl auf die *in vitro* wie auch die *in vivo* Eigenschaften. Durch die Verwendung eines Squalen-/ Tocopherol- Gemisches wurde eine signifikant ($p \leq 0.05$) erhöhte T-Zell-Aktivierung in Mäusen induziert. Gemeinsamkeit der gefriergetrockneten Formulierungen ist die im Vergleich zum Originalpräparat deutlich verringerte Wirkstoffpermeation durch die Haut. Insbesondere bei Jojobawachs enthaltenden Formulierungen wurde dieser Effekt deutlich. Ein identischer Effekt bezüglich der stark verminderten Wirkstoffpermeation trat im Falle des Jojobawachs enthaltenden Emulsionsgels auf. Diese halbfeste Formulierung generierte eine geringfügig erhöhte T-Zell-Aktivierung in Mäusen bei einer gleichzeitig 6-fach verringerten Hautpermeation des Wirkstoffes. Im Verglich zu dem Originalpräparat induzierte das Emulsionsgel eine verbesserte Tumorabstoßung im Mausmodell. Die Ergebnisse dieser Arbeit machen deutlich, dass das Originalpräparat Aldara® 5% Creme nicht die optimale transkutane Immunisierungsplattform darstellt. Die hier beschriebenen Formulierungskonzepte eröffnen neue Möglichkeiten der verbesserten transkutanen Immunisierung bei einer gleichzeitigen Verringerung der systemischen Wirkstoffbelastung für den Patienten.

Aim of this work is the development of a dermally applicable immunization scheme in order to sufficiently facilitate a tumor specific response by activating cytotoxic T-cells. Since imiquimod activates immune cells via the Toll-like receptor 7 pathway, this small molecule serves as the basis for transcutaneous immunization development efforts, described here. Besides Aldara® 5% creme, several competitor formulations are available on the world market. Five semi-solid imiquimod containing creams were investigated with regard to pharmaceutical characteristics but also *in vivo* generated effects in C57BL/6 mice in order to gain further insights into the field of transcutaneous immunization. Data obtained within this comparative study but also physicochemical properties of imiquimod such as poor water solubility provided the basis of development efforts concerning submicron- to nanoparticular imiquimod based formulations. Since sucrose fatty esters offer miscellaneous properties such as emulsification by simultaneously acting as kryoprotectants, these food grade status excipients are particularly suited in terms of pharmaceutical purposes. As one innovative approach, sucrose fatty esters in combination with various pharmaceutical oils as a spreadable freeze dried anhydrous solid nanoemulsion are subject of formulation development efforts. In addition, attempts on formulation development focused on a jojoba wax based emulsion gel. Besides rheological but also microscopic formulation characterization, various setups in a Franz diffusion cell model such as synthetic membranes versus murine skin but also different acceptor solutions were tested and compared with *in vivo* generated effects in C57BL/6 mice. Imiquimod was detected quantitatively either by UV-Vis spectroscopy or a RP-HPLC method. Results obtained here, displayed broad disparities between multisource commercial products. Unlike synthetic membrane related setups, murine skin related Franz diffusion cell results correlated well with *in vivo* detected immune effects in C57BL/6 mice. Moreover, permeation data across murine skin proved to be a suitable tool in order to distinguish whether each cream sample contains the active either in a dissolved or suspended state. In the course of the development of dermal imiquimod formulations, active ingredient particles in a submicron- to nanoscale range were found to possess previously unexpected beneficial properties, a fact that stands in contrast to the innovators product containing the active in a completely dissolved state. In the context of freeze dried formulations it became apparent that the respective oil component substantially impacts on *in vitro* but also *in vivo* performance. Particularly, a squalen-/ tocopherol blend induced a significant augment

(p≤0.05) in terms of cytotoxic T-cell activation in a mouse model. All freeze dried formulations have in common, that imiquimod permeation across the skin was distinctly diminished in comparison with the innovators product, a circumstance that became particularly obvious in case of jojoba wax within the formulation. In line with the convincingly low permeation results of jojoba wax based freeze dried formulation were those of the emulsion gel formulation. This semi-solid formulation induced a slightly increased cytotoxic T-cell activation by a simultaneously sixfold reduced permeation rate across the skin. Despite noticeable *in vitro* differences, data on tumor rejection in a mouse model demonstrated an enhanced induction of anti tumor activity in comparison with the innovators product. Results obtained within this work indicated that Aldara 5% creme does not represent an ideal transcutaneous immunization platform. Formulation concepts described here provide new possibilities of improved transcutaneous immunization by a concomitantly reduced systemic exposure to the patient.

9. Publications

K. Gogoll, P. Stein, H. Wei, H. Schild, M. Radsak, P. Langguth, Comparative transcutaneous immunization with imiquimod-containing ointments and potential of in vitro methods to predict effects." *Biopharmaceutics & drug disposition* 33.4 (2012): 218-228.

P. Stein, K. Gogoll, S. Tenzer, H. Schild, S. Stevanovic, P. Langguth, M.P. Radsak; Efficacy of imiquimod-based transcutaneous immunization using a nano-dispersed emulsion gel formulation. PloS one 9(7) (2014) e102664

K. Gogoll, P. Stein, K.D. Lee, P. Arnold, T. Peters, H. Schild, M. Radsak, P. Langguth Solid Nanoemulsion as Antigen and Immunopotentiator Carrier For Transcutaneous Immunization.

Manuscript is currently in process for submission at “European Journal of Pharmaceutics and Biopharmaceutics”.

Conference contributions including poster presentations:

K. Gogoll, P. Stein, M. Radsak, H. Schild, P. Langguth, "*In vitro and in vivo comparison of Imiquimod containing ointments: Are products from China pharmaceutically equivalent*", Joint meeting of the Austrian and German Pharmaceutical Societies Innsbruck, Austria, 2011.

K. Gogoll, P. Stein, M. Radsak, H. Schild, P. Langguth, "*Imiquimod based nanoscale approach for transcutaneous immunization in comparison with commercially available formulations*", 8th World Meeting on Pharmaceutics, Biopharmaceutics and Pharmaceutical Technology, Istanbul, Turkey, 2012.

K. Gogoll, P. Stein, M. Radsak, H. Schild, P. Langguth, "*Imiquimod based nanoscale approach for transcutaneous immunization*", Skin & Formulation, 4th Symposium, Lyon, France, 2012.

10. Appendix

Table 8: Evaluation of imiquimod particles sizes detected by transmission electron micrographs.

SN particle sizes determined as Martin's diameter.

Measurement no.	SN 1	SN 2	SN 3	SN 4
1	0,260	0,194	0,313	0,269
2	0,252	0,194	0,301	0,297
3	0,328	0,268	0,343	0,392
4	0,377	0,348	0,386	0,41
5	0,339	0,288	0,353	0,412
6	0,400	0,395	0,482	0,446
7	0,222	0,194	0,277	0,46
8	0,338	0,277	0,349	0,46
9	0,375	0,340	0,374	0,47
10	0,400	0,384	0,458	0,507
11	0,323	0,265	0,340	0,517
12	0,377	0,349	0,401	0,518
13	0,339	0,296	0,356	0,584
14	0,349	0,323	0,370	0,603
15	0,346	0,313	0,362	0,632
16	0,309	0,231	0,327	0,633
17	0,293	0,231	0,326	0,641
18	0,390	0,359	0,410	0,651
19	0,396	0,359	0,435	0,675
20	0,347	0,313	0,367	0,689
21	0,396	0,371	0,436	0,714
22	0,400	0,383	0,449	0,723
23	0,261	0,213	0,313	0,747
24	0,367	0,338	0,370	0,771
25	0,220	0,185	0,262	0,775
26	0,264	0,229	0,326	0,88
27	0,338	0,287	0,350	0,91
28	0,164	0,177	0,229	0,919
29	0,319	0,250	0,328	0,929
30	0,164	0,158	0,217	0,947
31	0,377	0,347	0,381	1,024
32	0,397	0,371	0,446	1,024
33	0,348	0,314	0,369	1,255
34	0,400	0,398	0,482	
35	0,405	0,410	0,482	

Table 8 continues				
Measurement no.	**SN 1**	**SN 2**	**SN 3**	**SN 4**
36	0,405	0,419	0,495	
37	0,412	0,422	0,503	
38	0,412	0,431	0,506	
39	0,415	0,431	0,517	
40	0,418	0,443	0,517	
41	0,432	0,446	0,518	
42	0,435	0,463	0,519	
43	0,436	0,468	0,521	
44	0,444	0,470	0,531	
45	0,448	0,470	0,531	
46	0,448	0,471	0,531	
47	0,450	0,481	0,531	
48	0,450	0,491	0,532	
49	0,454	0,491	0,542	
50	0,461	0,499	0,542	
51	0,461	0,499	0,562	
52	0,473	0,499	0,572	
53	0,473	0,499	0,577	
54	0,474	0,500	0,578	
55	0,475	0,515	0,578	
56	0,483	0,529	0,600	
57	0,485	0,530	0,600	
58	0,485	0,551	0,612	
59	0,497	0,563	0,613	
60	0,500	0,566	0,615	
61	0,509	0,599	0,626	
62	0,527	0,599	0,627	
63	0,535	0,601	0,663	
64	0,535	0,614	0,675	
65	0,540	0,619	0,684	
66	0,548	0,623	0,685	
67	0,556	0,635	0,686	
68	0,560	0,636	0,687	
69	0,569	0,638	0,694	
70	0,570	0,647	0,708	
71	0,575	0,647	0,714	
72	0,582	0,659	0,735	
73	0,599	0,683	0,735	
74	0,606	0,699	0,737	
75	0,606	0,707	0,740	
76	0,607	0,721	0,749	
77	0,611	0,731	0,771	
78	0,624	0,747	0,796	

Table 8 continues				
Measurement no.	**SN 1**	**SN 2**	**SN 3**	**SN 4**
79	0,642	0,759	0,796	79
80	0,647	0,767	0,832	
81	0,671	0,779	0,836	
82	0,695	0,782	0,843	
83	0,705	0,783	0,843	
84	0,747	0,790	0,858	
85	0,795	0,802	0,863	
86	0,800	0,802	0,865	
87	0,814	0,839	0,867	
88	0,830	0,886	0,872	
89	0,840	0,952	0,890	
90	0,864	0,960	0,940	
91	0,864	1,006	0,953	
92	0,980	1,020	1,000	
93	0,982	1,073	1,014	
94	0,995	1,102	1,096	
95	1,005	1,152	1,154	
96	1,025	1,174	1,217	
97	1,042	1,290	1,334	
98	1,043	1,557	1,347	
99	1,163	1,569	1,443	
100	1,217	1,618	1,644	
standard deviation [nm]	68,000	71,000	63,000	209
average particle size [nm]	525,000	568,000	617,000	663,00
gaussian distribution	no	yes	yes	yes

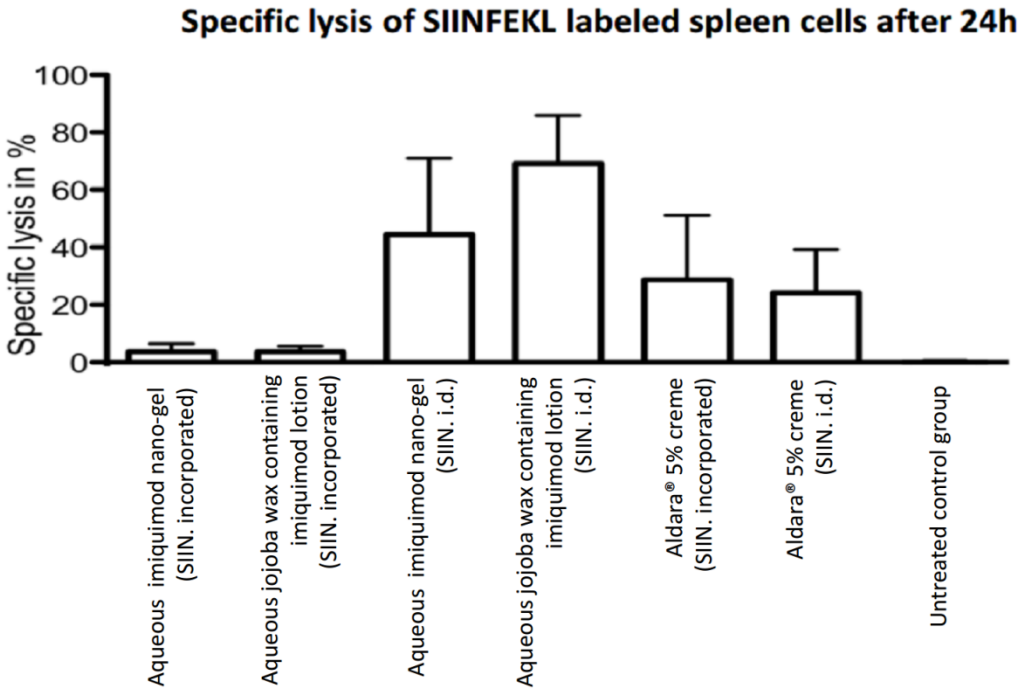

Figure 42: *In vivo* generated spleen cell lysis in order to emphasize the effect of i.d. and dermal administration of SIINFEKL. The "aqueous imiquimod nano-gel" as well as the "aqueous jojoba wax containing imiquimod lotion" were manufactured under a defined amount of planetary milling cycles but also HPH in the same manner as the emulsion gel. In contrast to the emulsion gel, the "aqueous jojoba wax containing imiquimod lotion" does not contain any gelling agents. Moreover, the aqueous formulations described here do not contain laurocapram. Since SIINFEKL is incorporated, the "aqueous imiquimod nano-gel" but also the "aqueous jojoba wax containing imiquimod lotion" formulation demonstrated lacking performance. Only when the antigen (SIINFEKL) is administered i.d. a sufficient immune response was detected following administration of imiquimod submicron particles dispersed in a hydrogel formulation. The i.d. administration of the antigen demonstrates the capacity of each nano particulate formulation to induce a CTL response. Compared with the "aqueous imiquimod nano-gel" the "jojoba wax containing imiquimod lotion" induced cytotoxic T-cell response is slightly increased. Error bars describe standard deviation (n=3).

In contrast hereto, the administration route of SIINEKL did not noticeably affect the performance of Aldara® 5% creme. This demonstrates an inferior concept of co-administrating antigen and immunopotentiator in a "ready to use" gel formulation. This also demonstrates the value of the solid nanoemulsion formulation as a ready to use formulation since both, antigen and immunopotentiator can be administered together.

Development of a HPLC method to detect imiquimod

In order to detect imiquimod in the acceptor medium of Franz diffusion cell investigations but also to extract the API from biological samples such as skin sections or by tape stripping it was required an analytical method. To this end, a HPLC method was developed to precisely detect even minute concentrations of imiquimod. Within this work, a 300 C8 5µm reversed phase RP 250*4.6mm column

was used. The mobile phase comprises double distilled water, trifluoric acid, and acetonitril (70: 0.0125: 30 V/V). This mobile phase ensured a pH value of 2.8 in order to avoid imiquimod precipitation in the column. Flow rate was 1.0ml/min generated by a Jasco PU-980 Intelligent HPLC pump. For quantitative API detection UV absorbance was determined by a Jasco UV-975 detector at 245nm wavelength. Imiquimod eluted after 5:30 minutes. Jasco-Borwin HSS-2000 software was used to analyze the revealed peaks. For method validation, imiquimod concentrations in a range of 35 – 1790ng/ml were measured on three consecutive days. Each day, the respective solutions were prepared freshly. These include the measurement of the concentrations described in table 9. 50µl of each test solution was injected into the instrument. The sequence of sample injection was increasing concentration/ decreasing concentration/ increasing concentration. Imiquimod solutions were freshly prepared each day. Therefore, 64,0mg imiquimod were dissolved with buffer solution in a 100,0ml volumetric flask up to the calibration mark. Then 1.0ml of this solution was transferred into a 50.0ml volumetric flask and dissolved with buffer solution up to the calibration mark. 3.50ml of the resulting solution were transferred into a 25.0ml volumetric flask and filled up to the calibration mark. The resulting stock solution contained 1.79µg/ml.

Table 9: Dilution series of imiquimod solutions in order to quantify the active via HPLC / UV detection

Konzentration [ng/ml]	Stock solution [µl][1,791µg/ml]	Buffer solution [ml]
1791	1	0
895,5	1	1
597	1	2
298,5	1	5
162,82	0,5	5
85,29	0,25	5
68,88	0,2	5
35,12	0,1	5

The following figures and tables show results of the validation procedure since they compare intra- and inter-day measurements. Moreover, correlation coefficients, but also p-values, upper and lower confidence intervals were calculated.

Appendix

Intra-day measurements day 1:

Table 10: Intra-day measurement of imiquimod mean peak areas detected at 245nm wavelength on day 1.

Concentration [ng/ml]	Day 1 peak area increasing conc.	Day 1 peak area decreasing conc.	Day 1 peak area increasing conc. b	Mean value peak area	Standard deviation	CV [%]
35,1	9526	9761,31	9845,6	9710,97	165,64	1,71
68,85	19907,97	20323,8	19904,78	20045,52	241,01	1,20
85,24	24979,11	25145,44	24166,51	24763,69	523,81	2,12
162,73	48444,02	50136,74	50123,72	49568,16	973,56	1,96
298,33	91760,72	92756,32	91645,82	92054,29	610,69	0,66
596,67	186939,16	186361,073	187652,92	186984,38	647,11	0,35
895	278065,86	277529,81	277671,7	277755,79	277,74	0,10
1790	554853,75	567234,46	562250,2	561446,14	6229,40	1,11

Figure 43: Graphical representations of measured peak area versus concentration including regression line and straight line equation of day 1 measurements.

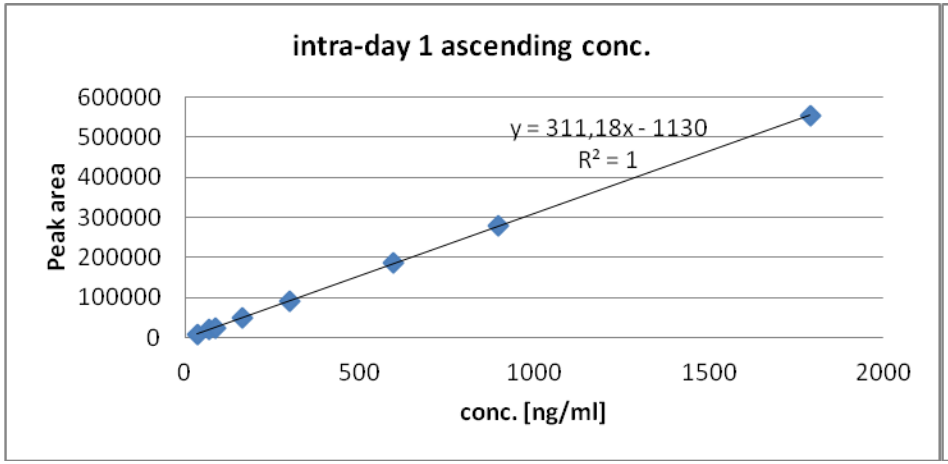

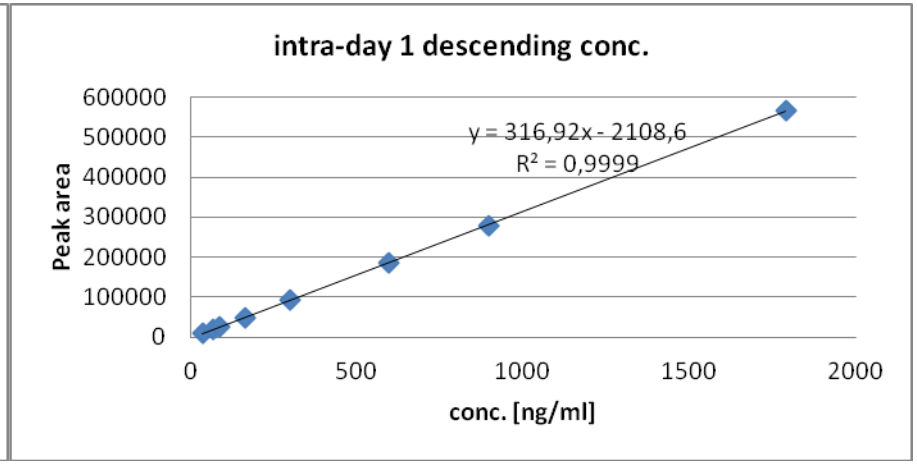

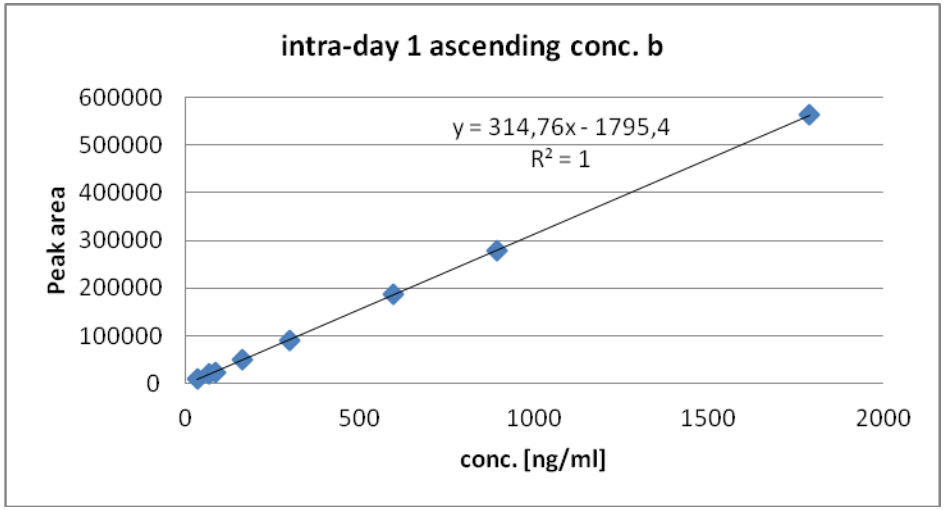

Table 11: Set concentration of each imiquimod solution and calculated real concentration after applying respective straight line equation from intraday 1 measurements.

Set concentration	Calculated concentration ascending	Calculated concentration descending	Calculated concentration ascending (b)
35,1	34,244	37,456	36,984
68,85	67,607	70,787	68,942
85,24	83,904	86,002	82,482
162,73	159,31	164,864	164,948
298,33	298,511	299,353	296,865
596,67	604,374	594,729	601,882
895	897,217	882,418	887,874
1790	1786,695	1796,602	1791,986

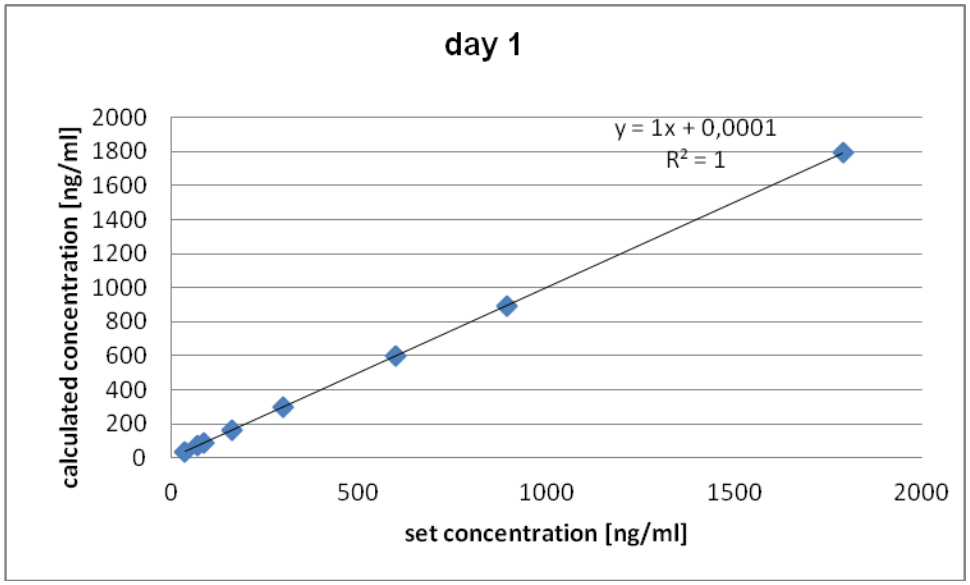

Figure 44: Set concentration of imiquimod vs. arithmetic mean of calculated imiquimod concentration day 1

Appendix

Table 12: Summary tables of regression analysis of intra-day detected set-concentration vs. calculated concentration on day 1. Tables calculate the correlation coefficient, but also p-values and upper and lower confidence interval.

Regressions-Statistik	
Multipler Korrelationskoeffizient	0,99998221
Bestimmtheitsmaß	0,99996442
Adjustiertes Bestimmtheitsmaß	0,99995849
Standardfehler	3,89402472
Beobachtungen	8

ANOVA

	Freiheitsgrade (df)	*Quadratsummen (SS)*	*Mittlere Quadratsumme (MS)*	*Prüfgröße (F)*	*F krit*
Regression	1	2557283,7	2557283,7	168648,12	1,4071E-14
Residue	6	90,980571	15,1634285		
Gesamt	7	2557374,68			

	Koeffizienten	*Standardfehler*	*t-Statistik*	*P-Wert*	*Untere 95%*	*Obere 95%*	*Untere 95,0%*	*Obere 95,0%*
Schnittpunkt	0,00015467	1,824207	8,4785E-05	0,9999351	-4,46351905	4,46382838	-4,46351905	4,46382838
X Variable 1	0,99998493	0,00243502	410,667894	1,4071E-14	0,99402665	1,00594322	0,99402665	1,00594322

Appendix

Regressions-Statistik	
Multipler Korrelationskoeffizient	0,99995678
Bestimmtheitsmaß	0,99991356
Adjustiertes Bestimmtheitsmaß	0,99989915
Standardfehler	6,07069313
Beobachtungen	8

ANOVA

	Freiheitsgrade (df)	*Quadratsummen (SS)*	*Mittlere Quadratsumme (MS)*	*Prüfgröße (F)*	*F krit*
Regression	1	2557738,77	2557738,77	69403,2211	2,0187E-13
Residue	6	221,11989	36,853315		
Gesamt	7	2557959,89			

	Koeffizienten	*Standardfehler*	*t-Statistik*	*P-Wert*	*Untere 95%*	*Obere 95%*	*Untere 95,0%*	*Obere 95,0%*
Schnittpunkt	5,2098E-05	2,84389589	1,8319E-05	0,99998598	-6,95871044	6,95881464	-6,95871044	6,95881464
X Variable 1	1,0000739	0,00379614	263,444911	2,0187E-13	0,99078508	1,00936272	0,99078508	1,00936272

Appendix

Regressions-Statistik	
Multipler Korrelationskoeffizient	0,99998043
Bestimmtheitsmaß	0,99996085
Adjustiertes Bestimmtheitsmaß	0,99995433
Standardfehler	4,08490575
Beobachtungen	8

ANOVA

	Freiheitsgrade (df)	*Quadratsummen (SS)*	*Mittlere Quadratsumme (MS)*	*Prüfgröße (F)*	*F krit*
Regression	1	2557415,02	2557415,02	153262,932	1,8748E-14
Residue	6	100,11873	16,686455		
Gesamt	7	2557515,14			

	Koeffizienten	*Standardfehler*	*t-Statistik*	*P-Wert*	*Untere 95%*	*Obere 95%*	*Untere 95,0%*	*Obere 95,0%*
Schnittpunkt	0,00016053	1,91362772	8,3889E-05	0,99993579	-4,68231781	4,68263888	-4,68231781	4,68263888
X Variable 1	1,00001061	0,00255438	391,4881	1,8748E-14	0,99376026	1,00626096	0,99376026	1,00626096

Appendix

Intra-day measurements day 2:

Table 13: Intra-day measurement of imiquimod mean peak areas detected at 245nm wavelength on day 2.

Concentration [ng/ml]	Day 2 peak area increasing conc.	Day 2 peak area decreasing conc.	Day 2 peak area increasing conc. b	Mean value peak area	Standard deviation	CV [%]
35,1	10199,05	10444,15	10279,25	10307,48	124,97	1,21
68,85	19741,92	20523,69	20750,82	20338,81	529,25	2,60
85,24	25202,87	25071,38	26200,4	25491,55	617,39	2,42
162,73	50052,25	49983,29	50543,88	50193,14	305,70	0,61
298,33	92546,62	91264,78	92637,76	92149,72	767,73	0,83
596,67	182306,82	184835,7	185832,98	184325,17	1817,67	0,99
895	276941,89	277671,7	279153,06	277922,22	1126,67	0,41
1790	560747,09	558271,5	562913,1	560643,90	2322,52	0,41

Figure 44: Graphical representations of measured peak area versus concentration including regression line and straight line equation of day 2 measurements.

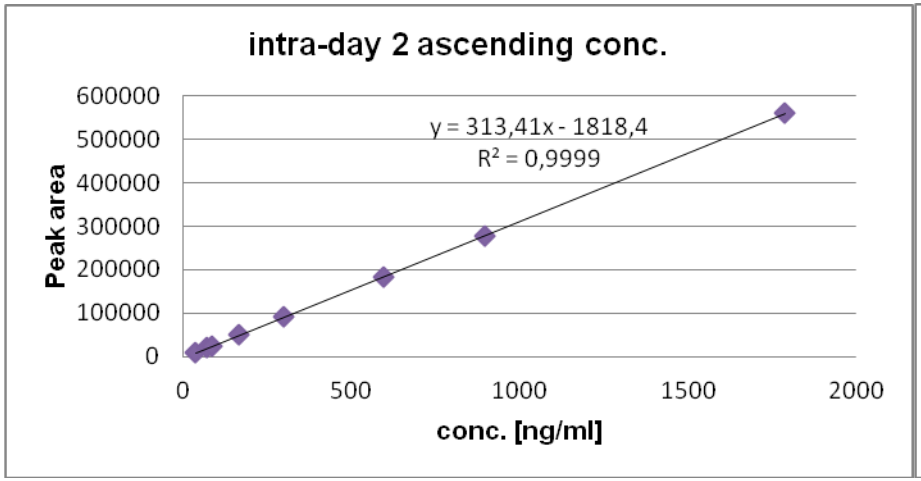

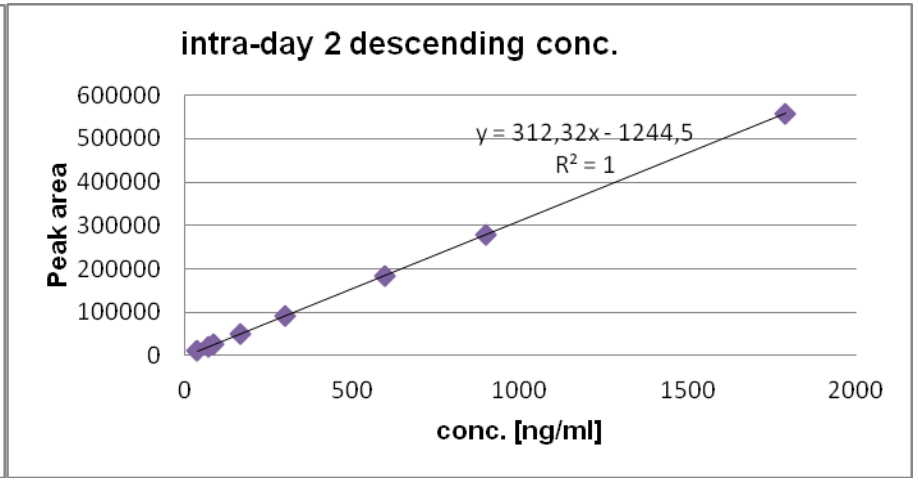

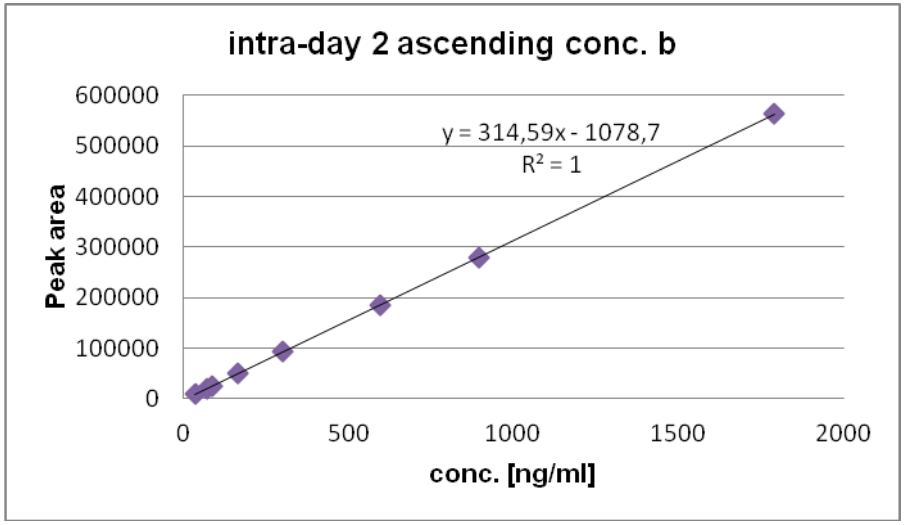

Table 14: Set concentration of each imiquimod solution and calculated real concentration after applying respective straight line equation from intra-day 2 measurements.

Set concentration	Calculated concentration ascending	Calculated concentration descending	Calculated concentration ascending (b)
35,1	38,344	37,425	36,104
68,85	68,793	69,698	69,39
162,73	165,504	164,023	164,095
298,33	301,091	296,2	297,9
596,67	587,49	595,8	594,144
895	889,443	893,046	890,784
1790	1794,983	1791,483	1792,784

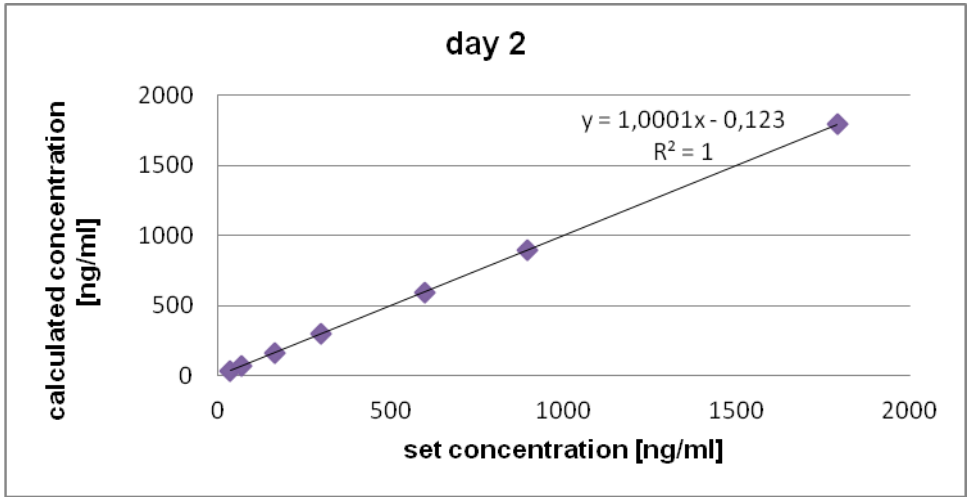

Figure 45: Set concentration of imiquimod vs. arithmetic mean of calculated imiquimod concentration day 2.

Appendix

Table 15: Summary table of regression analysis of intra-day detected set-concentration vs. calculated concentration on day 2. Tables calculate the correlation coefficient, but also p-values and upper and lower confidence interval.

Regressions-Statistik	
Multipler Korrelationskoeffizient	0,99996739
Bestimmtheitsmaß	0,99993479
Adjustiertes Bestimmtheitsmaß	0,99992392
Standardfehler	5,27227913
Beobachtungen	8

ANOVA

	Freiheitsgrade (df)	*Quadratsummen (SS)*	*Mittlere Quadratsumme (MS)*	*Prüfgröße (F)*	*F krit*
Regression	1	2557288,72	2557288,72	91998,9715	8,6672E-14
Residue	6	166,781563	27,7969272		
Gesamt	7	2557455,5			

	Koeffizienten	*Standardfehler*	*t-Statistik*	*P-Wert*	*Untere 95%*	*Obere 95%*	*Untere 95,0%*	*Obere 95,0%*
Schnittpunkt	4,7953E-05	2,46986837	1,9415E-05	0,99998514	6,04350222	6,04359813	6,04350222	6,04359813
X Variable 1	0,99998591	0,00329687	303,313322	8,6672E-14	0,99191875	1,00805308	0,99191875	1,00805308

Appendix

Regressions-Statistik	
Multipler Korrelationskoeffizient	0,99999608
Bestimmtheitsmaß	0,99999215
Adjustiertes Bestimmtheitsmaß	0,99999084
Standardfehler	1,82893737
Beobachtungen	8

ANOVA

	Freiheitsgrade (df)	*Quadratsummen (SS)*	*Mittlere Quadratsumme (MS)*	*Prüfgröße (F)*	*F krit*
Regression	1	2557382,95	2557382,95	764536,28	1,5104E-16
Residue	6	20,0700714	3,34501189		
Gesamt	7	2557403,02			

	Koeffizienten	*Standardfehler*	*t-Statistik*	*P-Wert*	*Untere 95%*	*Obere 95%*	*Untere 95,0%*	*Obere 95,0%*
Schnittpunkt	-0,00038233	0,85678972	-0,00044623	0,99965843	-2,09687124	2,09610659	-2,09687124	2,09610659
X Variable 1	1,00000434	0,00114368	874,377653	1,5104E-16	0,99720587	1,00280281	0,99720587	1,00280281

Appendix

Regressions-Statistik	
Multipler Korrelationskoeffizient	0,99999268
Bestimmtheitsmaß	0,99998537
Adjustiertes Bestimmtheitsmaß	0,99998293
Standardfehler	2,49744707
Beobachtungen	8

ANOVA

	Freiheitsgrade (df)	*Quadratsummen (SS)*	*Mittlere Quadratsumme (MS)*	*Prüfgröße (F)*	*F krit*
Regression	1	2557356,01	2557356,01	410013,922	9,7924E-16
Residue	6	37,4234513	6,23724188		
Gesamt	7	2557393,43			

	Koeffizienten	*Standardfehler*	*t-Statistik*	*P-Wert*	*Untere 95%*	*Obere 95%*	*Untere 95,0%*	*Obere 95,0%*
Schnittpunkt	-0,00029317	1,16996187	-0,00025058	0,99980819	-2,86308672	2,86250038	-2,86308672	2,86250038
X Variable 1	0,99999907	0,00156171	640,323295	9,7924E-16	0,9961777	1,00382044	0,9961777	1,00382044

Appendix

Intra-day measurements day 3:

Table 16: Intra-day measurement of imiquimod mean peak areas detected at 245nm wavelength on day 3

Concentration [ng/m]	Day 3 peak area increasing conc.	Day 3 peak area decreasing conc.	Day 3 peak area increasing conc. b	Mean value peak area	Standard deviation	CV [%]
35,1	10467,19	10398	9732,3	10199,16	405,79	3,98
68,85	20510,05	20568,48	20103,14	20393,89	253,49	1,24
85,24	25356,77	25863	25257,01	25492,26	324,92	1,27
162,73	50168,7	51043,19	49684,81	50298,90	688,49	1,37
298,33	91215,45	90530,32	92036,3	91260,69	754,01	0,83
596,67	183236,43	183789,68	183461,15	183495,75	278,24	0,15
895	275970,32	268037,07	271428,6	271812,00	3980,50	1,46
1790	554844,31	552909,91	554967,17	554240,46	1153,93	0,21

Figure 46: Graphical representation of measured peak area versus concentration including regression line and straight line equation of day 3 measurements.

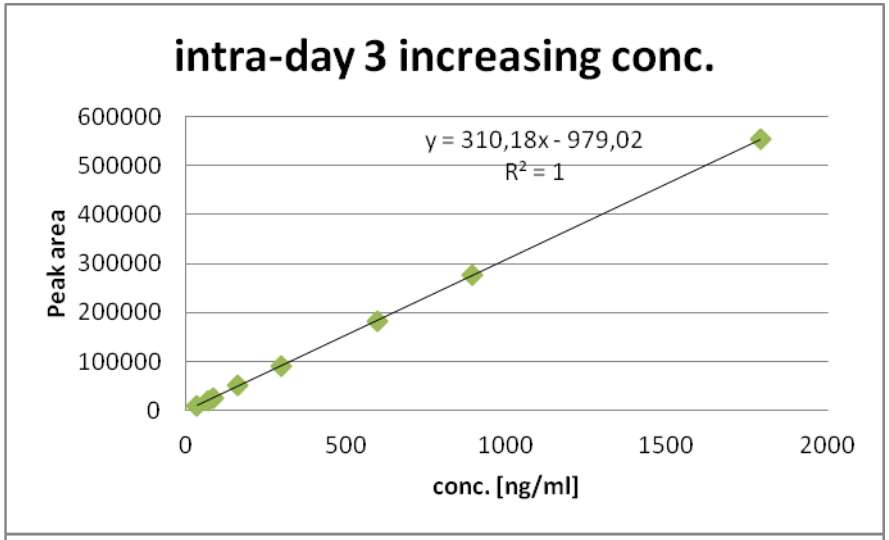

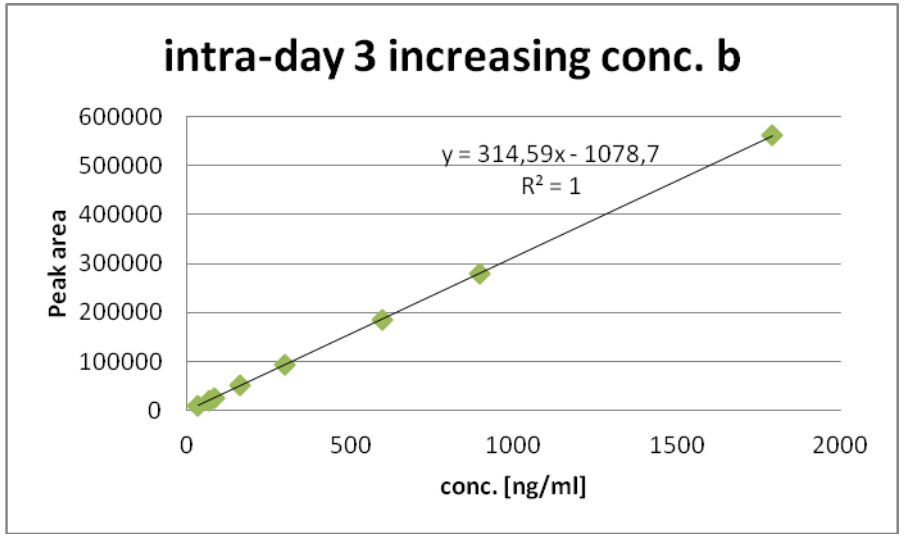

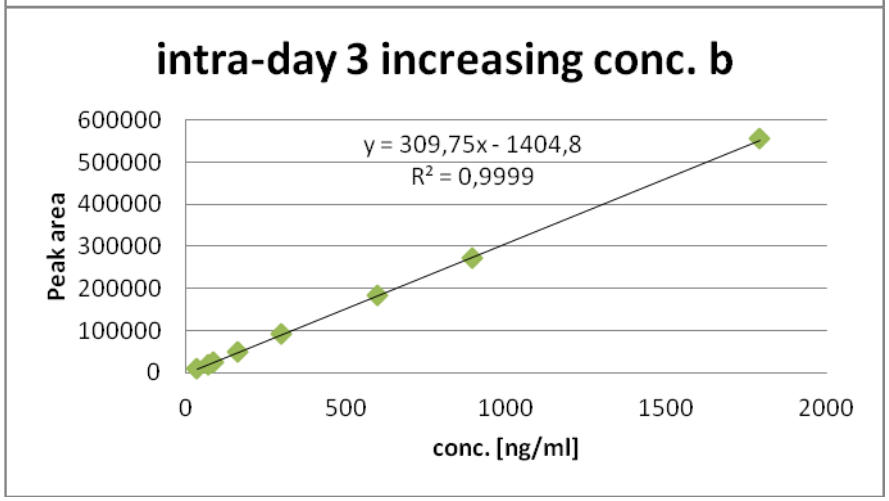

Table 17: Set concentration of each imiquimod solution and calculated real concentration after applying respective straight line equation from intra-day 3 measurements.

Set concentration	Calculated concentration ascending	Calculated concentration descending	Calculated concentration ascending (b)
35,1	36,902	36,712	35,955
68,85	69,279	69,751	69,436
85,24	84,905	86,95	86,075
162,73	164,897	168,749	164,938
298,33	297,229	297,025	301,666
596,67	593,899	599,982	596,823
895	892,867	873,664	880,818
1790	1791,938	1799,087	1796,197

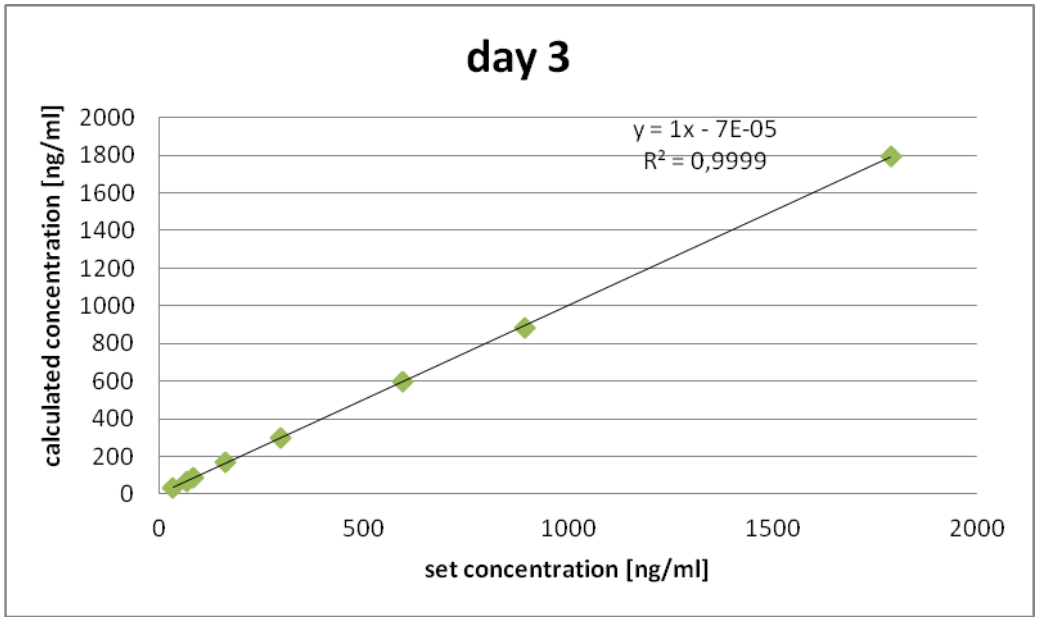

Figure 47: Set concentration of imiquimod vs. arithmetic mean of calculated imiquimod concentration day 1

Appendix

Table 18: Summary table of regression analysis of intra-day detected set-concentration vs. calculated concentration on day 3. Tables calculate the correlation coefficient, but also p-values and upper and lower confidence interval.

Regressions-Statistik	
Multipler Korrelationskoeffizient	0,99999503
Bestimmtheitsmaß	0,99999005
Adjustiertes Bestimmtheitsmaß	0,9999884
Standardfehler	2,05894506
Beobachtungen	8

ANOVA

	Freiheitsgrade (df)	*Quadratsummen (SS)*	*Mittlere Quadratsumme (MS)*	*Prüfgröße (F)*	*F krit*
Regression	1	2557354,73	2557354,73	603255,734	3,0746E-16
Residue	6	25,4355284	4,23925474		
Gesamt	7	2557380,16			

	Koeffizienten	*Standardfehler*	*t-Statistik*	*P-Wert*	*Untere 95%*	*Obere 95%*	*Untere 95,0%*	*Obere 95,0%*
Schnittpunkt	7,9554E-05	0,96453984	8,2478E-05	0,99993687	-2,36006441	2,36022351	-2,36006441	2,36022351
X Variable 1	0,99999882	0,0012875	776,695393	3,0746E-16	0,99684841	1,00314923	0,99684841	1,00314923

Appendix

Regressions-Statistik	
Multipler Korrelationskoeffizient	0,99988407
Bestimmtheitsmaß	0,99976816
Adjustiertes Bestimmtheitsmaß	0,99972952
Standardfehler	9,94177751
Beobachtungen	8

ANOVA

	Freiheitsgrade (df)	*Quadratsummen (SS)*	*Mittlere Quadratsumme (MS)*	*Prüfgröße (F)*	*F krit*
Regression	1	2557362,18	2557362,18	25874,0348	3,8945E-12
Residue	6	593,03364	98,83894		
Gesamt	7	2557955,21			

	Koeffizienten	*Standardfehler*	*t-Statistik*	*P-Wert*	*Untere 95%*	*Obere 95%*	*Untere 95,0%*	*Obere 95,0%*
Schnittpunkt	-0,00013601	4,65735618	-2,9204E-05	0,99997765	-11,396276	11,396004	-11,396276	11,396004
X Variable 1	1,00000028	0,00621682	160,854079	3,8945E-12	0,98478828	1,01521228	0,98478828	1,01521228

Regressions-Statistik	
Multipler Korrelationskoeffizient	0,99994969
Bestimmtheitsmaß	0,99989939
Adjustiertes Bestimmtheitsmaß	0,99988262
Standardfehler	6,54893262
Beobachtungen	8

ANOVA

	Freiheitsgrade (df)	*Quadratsummen (SS)*	*Mittlere Quadratsumme (MS)*	*Prüfgröße (F)*	*F krit*
Regression	1	2557346,75	2557346,75	59627,7709	3,183E-13
Residue	6	257,331111	42,8885185		
Gesamt	7	2557604,09			

	Koeffizienten	*Standardfehler*	*t-Statistik*	*P-Wert*	*Untere 95%*	*Obere 95%*	*Untere 95,0%*	*Obere 95,0%*
Schnittpunkt	-0,00015414	3,06793346	-5,0242E-05	0,99996154	-7,50711686	7,50680858	-7,50711686	7,50680858
X Variable 1	0,99999726	0,00409519	244,187983	3,183E-13	0,98997668	1,01001784	0,98997668	1,01001784

Appendix

Inter-day variability:

The following section describes inter-day variabilities regarding imiquimod based peak areas.

conc. [ng/mL]	Average mean peak area day 1	Average mean peak area day 2	Average mean peak area day 3	Average mean peak area	SD	CV [%]
35,1	9710,97	10307,48	10199,16	10072,54	317,78	3,15
68,85	20045,52	20338,81	20393,89	20259,41	187,27	0,92
85,24	24763,69	25491,55	25492,26	25249,17	420,44	1,67
162,73	49568,16	50193,14	50298,9	50020,07	394,92	0,79
298,33	92054,29	92149,72	91260,69	91821,57	488,07	0,53
596,67	186984,38	184325,17	183495,75	184935,1	1822,54	0,99
895	277755,79	277922,22	271812	275830	3480,69	1,26
1790	561446,14	560643,9	554240,46	558776,83	3949,04	0,71

Conc. [ng/mL]	Mean peak area ascending day 1	Mean peak area ascending day 2	Average mean peak area	SD	CV [%]
35,1	9526	10199,05	9862,525	475,91822	4,83
68,85	19907,97	19741,92	19824,945	117,41508	0,59
85,24	24979,11	25202,87	25090,99	158,22221	0,63
162,73	48444,02	50052,25	49248,135	1137,19034	2,31
298,33	91760,72	92546,62	92153,67	555,71522	0,60
596,67	186939,16	182306,82	184622,99	3275,55903	1,77
895	278065,86	276941,89	277503,875	794,76681	0,29
1790	554853,75	560747,09	557800,42	4167,22068	0,75

Appendix

Conc. [ng/mL]	Mean peak area descending day 1	Mean peak area descending day 2	Average mean peak area	SD	CV [%]
35,1	9761,31	10444,15	10102,73	482,84	4,78
68,85	20323,8	20523,69	20423,75	141,34	0,69
85,24	25145,44	25071,38	25108,41	52,37	0,21
162,73	50136,74	49983,29	50060,02	108,51	0,22
298,33	92756,32	91264,78	92010,55	1054,68	1,15
596,67	186361,073	184835,7	185598,39	1078,6	0,58
895	277529,81	277671,7	277600,76	100,33	0,04
1790	567234,46	558271,5	562752,98	6337,77	1,13

Conc. [ng/mL]	Mean peak area ascending (b) day 1	Mean peak area ascending (b) day 2	Average mean peak area	SD	CV [%]
35,1	9845,6	10279,25	10062,43	306,64	3,05
68,85	19904,78	20750,82	20327,8	598,24	2,94
85,24	24166,51	26200,4	25183,46	1438,18	5,71
162,73	50123,72	50543,88	50333,8	297,1	0,59
298,33	91645,82	92637,76	92141,79	701,41	0,76
596,67	187652,92	185832,98	186742,95	1286,89	0,69
895	277671,7	279153,06	278412,38	1047,48	0,38
1790	562250,2	562913,1	562581,65	468,74	0,08

conc. [ng/mL]	Mean peak area ascending day 2	Mean peak area ascending day 3	Average mean peak area	SD	CV [%]
35,1	10199,05	10467,19	10333,12	189,6	1,83
68,85	19741,92	20510,05	20125,99	543,15	2,70
85,24	25202,87	25356,77	25279,82	108,82	0,43
162,73	50052,25	50168,7	50110,48	82,34	0,16
298,33	92546,62	91215,45	91881,04	941,28	1,02
596,67	182306,82	183236,43	182771,63	657,33	0,36
895	276941,89	275970,32	276456,11	687	0,25
1790	560747,09	554844,31	557795,7	4173,9	0,75

Appendix

conc. [ng/mL]	Mean peak area descending day 2	Mean peak area descending day 3	Average mean peak area	SD	CV [%]
35,1	10444,15	10398	10421,08	32,63	0,31
68,85	20523,69	20568,48	20546,09	31,67	0,15
85,24	25071,38	25863	25467,19	559,76	2,20
162,73	49983,29	51043,19	50513,24	749,46	1,48
298,33	91264,78	90530,32	90897,55	519,34	0,57
596,67	184835,7	183789,68	184312,69	739,65	0,40
895	277671,7	268037,07	272854,39	6812,71	2,50
1790	558271,5	552909,91	555590,71	3791,22	0,68

conc. [ng/mL]	Mean peak area ascending (b) day 2	Mean peak area ascending (b) day 3	Average mean peak area	SD	CV [%]
35,1	10279,25	9732,3	10005,78	386,75	3,87
68,85	20750,82	20103,14	20426,98	457,98	2,24
85,24	26200,4	25257,01	25728,71	667,08	2,59
162,73	50543,88	49684,81	50114,35	607,45	1,21
298,33	92637,76	92036,3	92337,03	425,3	0,46
596,67	185832,98	183461,15	184647,07	1677,14	0,91
895	279153,06	271428,6	275290,83	5462,02	1,98
1790	562913,1	554967,17	558940,14	5618,62	1,01

conc. [ng/mL]	Mean peak area ascending day 1	Mean peak area ascending day 3	Average mean peak area	SD	CV [%]
35,1	9526	10467,19	9996,6	665,52	6,66
68,85	19907,97	20510,05	20209,01	425,73	2,11
85,24	24979,11	25356,77	25167,94	267,05	1,06
162,73	48444,02	50168,7	49306,36	1219,53	2,47
298,33	91760,72	91215,45	91488,09	385,56	0,42
596,67	186939,16	183236,43	185087,8	2618,23	1,41
895	278065,86	275970,32	277018,09	1481,77	0,53
1790	554853,75	554844,31	554849,03	6,68	0,00

Appendix

conc. [ng/mL]	Mean peak area descending day 1	Mean peak area descending day 3	Average mean peak area	SD	CV [%]
35,1	9761,31	10398	10079,66	450,208	4,47
68,85	20323,8	20568,48	20446,14	173,015	0,85
85,24	25145,44	25863	25504,22	507,392	1,99
162,73	50136,74	51043,19	50589,97	640,957	1,27
298,33	92756,32	90530,32	91643,32	1574,02	1,72
596,67	186361,073	183789,68	185075,38	1818,249	0,98
895	277529,81	268037,07	272783,44	6712,381	2,46
1790	567234,46	552909,91	560072,19	10128,986	1,81

Conc. [ng/mL]	Mean peak area ascending (b) day 1	Mean peak area ascending (b) day 3	Average mean peak area	SD	CV [%]
35,1	9845,6	9732,3	9788,95	80,12	0,82
68,85	19904,78	20103,14	20003,96	140,26	0,70
85,24	24166,51	25257,01	24711,76	771,1	3,12
162,73	50123,72	49684,81	49904,27	310,36	0,62
298,33	91645,82	92036,3	91841,06	276,11	0,30
596,67	187652,92	183461,15	185557,04	2964,03	1,60
895	277671,7	271428,6	274550,15	4414,54	1,61
1790	562250,2	554967,17	558608,69	5149,88	0,92